Investigating the role of translational accuracy in ageing in *Caenorhabditis elegans*

Abigail King

Genetics MRes

School of Biosciences
Dr Jennifer Tullet
Dr Tobias von der Haar

2018

University of Kent

Declaration

I declare that this thesis, which I submit to the University of Kent in consideration for the award of a higher degree, Genetics Research Masters, is my own personal effort.

No part of this thesis has been submitted in support of an application for any degree or qualification to the University of Kent or any other university or institute of learning.

I took reasonable care to ensure that the work is original, and, to the best of my knowledge, does not breach copyright law, and has not been taken from other sources except where such work has been cited and acknowledged within the text.

Acknowledgements

Isaiah 41:10 "Fear not, for I am with you; be not dismayed, for I am your God; I will strengthen you, I will help you, I will uphold you with My righteous right hand."

All the glory belongs to God. He gave me the strength to get through the sleepless nights, the courage to start this course, the knowledge to complete experiments and the determination to complete everything whilst working full-time teaching other potential scientists.

I would like to thank both of my supervisors Dr. Tobias von der Haar and Dr. Jennifer Tullet for their insight and expertise regarding this project and their patience with me as I completed this alongside achieving my QTS.

I'm grateful to Dan, Nikolas, Jack, Ana and Max for their friendship and all their help and advice in and around the *C. elegans* lab and especially Isabel for her kindness and guidance in writing this thesis.

Thanks to Connor and Mike for support throughout this programme their help with my protein work and to Kevin for his incognizant guidance in penning this thesis.

My work colleagues at Brompton Academy, Lauren, Kayley, Chris, Andy, Jamie, Pete, Steve, Georgia and my teaching mentor, Juliet have been so understanding and helpful.

I also want to thank Lin Riches for being an angel, providing advice and comfort every single step of the way.

~

Special thanks go to Laura, Niken, may her gorgeous soul rest in peace, and Chloe for being true gems, always with an encouraging word at hand when things were getting a bit hard and putting a smile on my face. I have so much gratitude towards Christene and Christena who took me in when I had nowhere to go allowing me to focus and actually finish writing.

~

I have unending gratitude towards my fabulous sister, Miriam, my sweet plantain, Samuel, my unashamed twin, Shelly Ann and my finest bebs Martha and Norma for supporting me, praying for me and being there for me throughout the two years of completing this degree.

~

Most importantly, would like to thank my phenomenal parents, Julius and Arit who were always there for me, who always believed in me and always supported me – driving me to be the best version of myself and who I dedicate this thesis to.

Abbreviations

ApE	A plasmid editor
APS	Ammonium persulphate
BLAST	Basic Local Alignment Search Tool
BIS	Bis-acrylamide
C. elegans	*Caenorhabditis elegans*
Cas9	CrispR associated protein 9
CDS	Coding sequence
CGCH	Caenorhabditis elegans Genetics Centre Hermaphrodite
CGCM	Caenorhabditis elegans Genetics Centre Male
CrispR	Clustered Regularly Interspaced Short Palindromic Repeats
DTT	Dithiothreitol
E. coli	*Escherichia coli*
E-value	Expectation value
eIF1, eIF 2 etc.	eukaryotic initiation factor 1 etc.
F1, F2 etc.	first filial generation, second filial generation etc.
kDa	kilodaltons
L1, L2 etc.	Larval stage 1, larval stage 2 etc.
LB	Lysogeny broth
MALDI-TOF	Matrix-assisted laser desorption ionization time-of-flight
Met-tRNAiMet	methionyl-initiator tRNA
MS/MS	Tandem mass spectrometry
m/z	Mass to charge ratio
NF H_20	Nucleotide free water
NGM	Nematode growth media
nt	nucleotide bases
NTC	Nourseothricin sulphate
OD	Optical density – measure of absorbance

PCR	Polymerase chain reaction
rps-2	ribosomal protein S2
S. pombe	*Schizosaccharomyces pombe*
S. cerevisiae	*Saccharomyces cerevisiae*
SD	Standard deviation
SDS PAGE	Sodium dodecyl sulphate polyacrylamide gel electrophoresis
TAE	Tris base, acetic acid, EDTA mix
TEMED	Tetramethylethylenediamine $(CH_3)_2NCH_2CH_2N(CH_3)_2$
Tm	Primer melting temperature
tRNA	Transfer ribonucleic acid
40S, 60S, 18S	Sedimentation coefficient

Keywords: accuracy, translation, mutation, lifespan, protein, spectrometry

Abstract

Life is dependent on several processes taking place simultaneously within an organism. One of these fundamental mechanisms include the production of fully functioning proteins. Making proteins consists of two general steps to decode genetic information - transcription and translation. Rigorous regulation of translation is essential in the assembly of accurate proteins, where many factors can directly affect the efficiency of this stage. The integrity of translational machinery, in particular, the ribosome, contributes to its functionality. One of approximately thirty-three constituent proteins, *rps-2*, combines to form the eukaryotic 40S small ribosomal subunit and is hypothesised to be responsible for the stability of the entire subunit. Approximately 98 interactions are made between *rps-2* and other proteins and binding ligands suggesting its unspecified role may be vital in the cohesion of the subunit.

Modification of the *rps-2* gene, to produce a loss in translation within *Saccharomyces cerevisiae* has displayed a significant effect on viability. This observation led to the commencement of this project, to further investigate *rps-2* within a higher order organism, *Caenorhabditis elegans*. We looked into how the mutagenesis of *rps-2* within translation affects the accuracy of the process and any apparent changes made to the stability of the ribosome structure. We also took into account the effect the A494G, C495T point mutations had on ageing, manifested through lifespan assays, and found no significant difference between our mutant strain COP872 and wildtype. Majority of the project involved verifying the mutation and conducting experiments that would contribute to the understanding of how translation is affected, since this remains unknown. Methodology to identify this mutation were devised through the use of genotyping polymerase chain reactions. Results from the brood size assays and lifespan assays completed were deemed as inconclusive since the statistical results of these tests were insignificant.

MALDI-TOF mass spectrometry and quantitative protein assays did not produce clear results to extract a sufficient amount of information to provide an exhaustive conclusion.
This indicates there is still capacity to explore and find definitive conclusions to the impact *rps-2* has on translation, ageing and in particular the integrity of the ribosome. It also provides an avenue to discuss further experimentation such as developmental time assays.

Chapter 1

Introduction

1.1 *C. elegans*

1.1.1 A model organism

To depict the origins, function and character of any life form, we customarily begin with investigating the genes of an organism. Understanding signalling pathways can reveal the function and activity of conserved genes and therefore proteins found within these organisms. To further understand the effect of mutations within the nervous system of eukaryotic organisms, biologist Sydney Brenner used the nematode worm, *Caenorhabditis elegans* as a model system (Brenner, 1974).

Caenorhabditis elegans, C. elegans, is a non-parasitic soil nematode worm that possesses multifarious attributes, each contributing to its ideal use as a non-human species to understand genetic phenomena. *C. elegans* grows to a full length of approximately 1 mm in favourable conditions, allowing its anatomic features to be observed clearly through a low-power dissecting microscope. The transparent, collagenous, extracellular cuticle facilitates manipulation and microscopic observation on the roundworm's ventral side. When present, eggs can be distinctly detected within the uterus, indicating the presence of an adult worm (McCulloch et al., 2003). The nematode exists primarily in a hermaphrodite form, but being an androdioecious species, males do arise at a frequency of <0.2%, as a result of a chromosomal "irregularity" referred to as X chromosome nondisjunction that takes place during gametogenesis (Zarkower, 2006). The production of reproductive cells, sperm and egg within the spermatheca and uterus respectively, is the root of its self-fertilising ability (Pechenick, 2005). Due to the uncommon generation of males in a CGCM or CGCH background a population of male nematodes can be fashioned through a number of in vitro processes, the most common of these is 'heat shocking' (Sulston et al, 1988). This involves incubating developed worms at a high temperature for a few hours to increase the rate of nondisjunction (Felix et al., 2011).

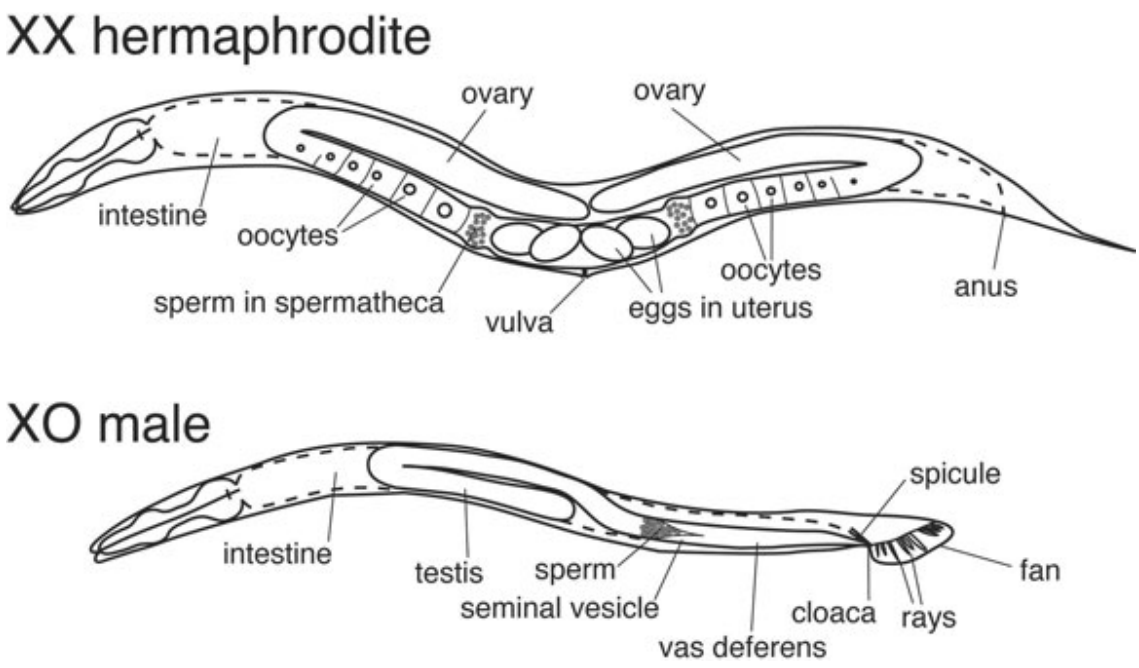

Figure 1 Comparing anatomical structures between both sexes of *C. elegans.* A labelled diagrammatic representation of the physical attributes seen within a hermaphrodite and male nematode. Variations are evident, features such as the overall size and presence of a fantail are used to differentiate between sexes when observed through a dissecting microscope (Zarkower, 2006).

The naturally occurring hermaphroditic nature of the nematodes removes the obstacle of finding a mate and proves advantageous when generating an isogenic offspring, which is beneficial to genetic investigations since these worms retain variations that have been caused by homozygous mutations. This is imperative when creating new genetic mutant combinations for single mutants *in vitro.* The production of variants may cause another physical trait to manifest with the organism being investigated; this will introduce multiple independent variables resulting in erroneous conclusions being formed.

Being the first multicellular organism to have its genome sequenced, the identification of homologous genes has been pivotal when hypothesising findings in complex mammalian models (Felix et al., 2011). Gene homologues in *C. elegans* have been conserved within approximately 70% of human genes (Lai et al., 2005), this characteristic provides the opportunity to methodically knockout a single gene to determine its role (Felix et al., 2011). With a generation time of 3.5 days, genetic changes can be incorporated efficiently into the genome (Corsi, 2006), for research purposes this is optimal to get results efficiently.

These self-fertile adults survive for up to three weeks (in ideal conditions) and cultivate large numbers of offspring, on average producing between 200 - 1000 eggs. As a food source the roundworms live and grow in the laboratory by consuming an *E. coli* strain - OP50 through

pharyngeal pumping, this strain can easily be cultured within in the laboratory environment and stored in an incubator (Altun et al., 2011; Corsi et al. 2015). Living temperatures in an incubator span from 12°C to 25°C, where an increase in 10°C doubles the rate of growth. *C. elegans* become sterile at temperatures exceeding 25°C and are not kept at temperatures higher than this for experimental purposes.

The genetic compatibility and capability of *C. elegans*, its reproductive mechanisms and simple laboratory maintenance are known characteristics that support the role of *C. elegans* as a model to aid the progression of knowledge in the mechanisms of higher order organisms (Fields et al., 2005), which forms the reasoning behind its use as a higher order mammalian model.

1.1.2 Life Cycle and lifespan of *C. elegans*

As aforementioned, the lifespan of *C. elegans* is an aspect that contributes to the value of it as a model organism. In optimal conditions, that includes favourable temperatures, an ample food supply and sufficient space to move, grow and access food, roundworms complete a life cycle in approximately 72 h at 20^{o}C (Cassada et al., 1975).
From an egg, *C. elegans* advances through four stages of larval development, each separated by a molt. Namely, these stages are referred to as L1—L4 and subsequently worms can go on to live for a further 14-21 days, as an adult, continuing to grow in size and produce eggs of its own (Fig. 2) (Riddle et al., 1997).

Upon fertilisation of the egg within the uterus, a protective layer of impermeable membrane coats the egg. This feature is convenient during the bleaching process of worms to eradicate contamination, this is discussed in succeeding chapters (outlined in 'Methods'- Chp. 2.1.4). After going through stages of proliferation, gastrulation and morphogenesis, the embryo begins to exhibit muscle movement indicative of movement in a coordinated fashion (Von Ehrenstein et al., 1980). At 14 h and approximately 600 cells, the L1 larvae breaks through the egg and development continues.

During unfavourable conditions – for example, starvation, overcrowding or an increase in environmental temperature, *C. elegans* experiences a specialized third larval stage known as dauer diapause (L2d) (Cassada et al., 1975). Starvation can be caused by the lack of bacteria to consume, resulting in worms consuming their fat supply. Whilst in this arrested

stage, dauer nematodes remain stagnant in growth and motility is reduced as they explore the environment in search of food sources. Dauer conditions can be induced in the laboratory to increase the longevity of *C. elegans* for the duration of experiments. Survival in this stage can last between one and six months (depending on the temperature of incubation). The introduction of favourable conditions, will return the nematode to its normal life cycle, growing into a healthy organism (Cassada et al., 1975; Schaler et al., 2005; Fienlenbach et al., 2008; Wolkow et al., 2015). The rates of development are modified depending on the temperature of incubation. It takes approximately 90 h for a healthy egg to reach the adult stage at 15°C, development time is reduced by half when incubated at 25°C (Porta-de-la-Riva et al., 2012). For experimentation purposes, this provides a greater depth of research - additional conditions can be constructed to analyse multiple effects. For example, the completion of the Nourseothricin drug trial, outlined in this study, observed how different temperatures affected potency (ibid).

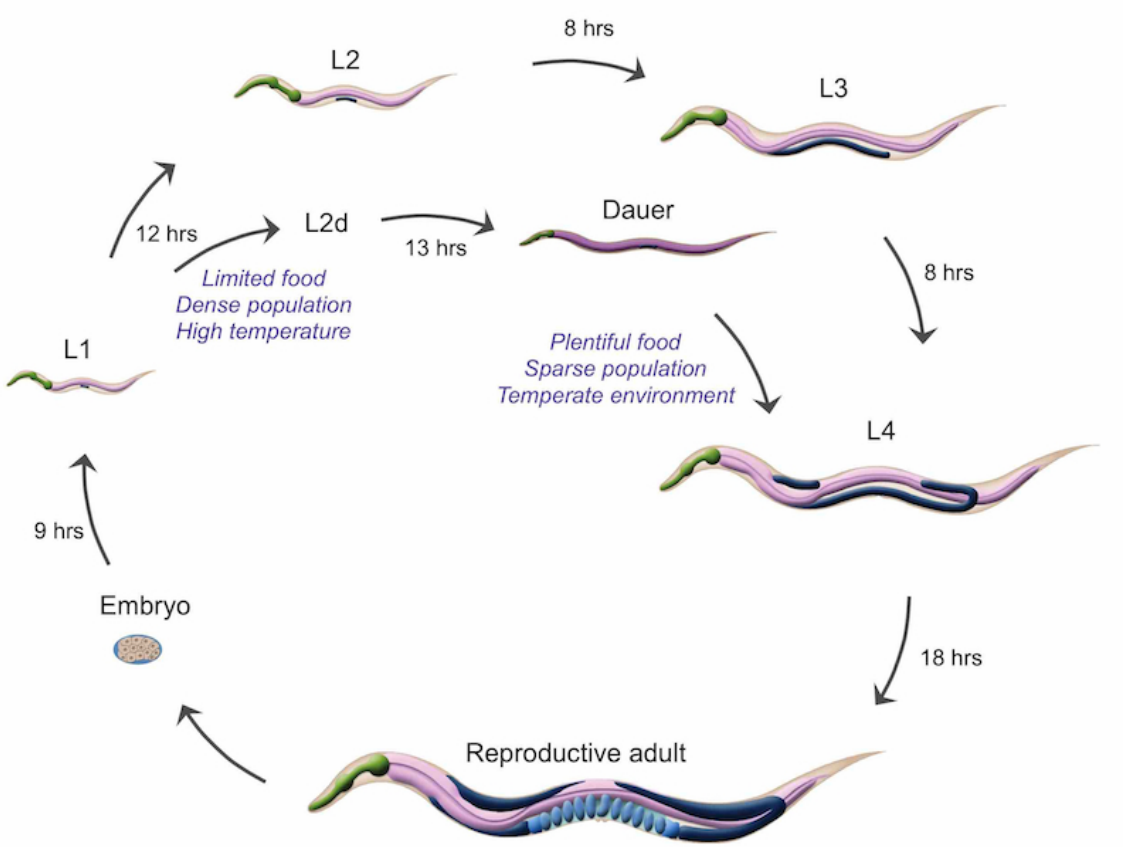

Figure 2 Schema depicting the life cycle of *C. elegans* outlining changes that occur between each stage. At 22 °C, nematodes progress through four stages of development. Incubation for approximately 9 h allows an embryo to develop into an L1 hatchling, environmental conditions within the next 12 h have a direct effect on progress through this cycle. As outlined limited food, overpopulation and elevated temperature can drive the worm into dauer instead of an L2. Movement into L3 sees an increase in length from ~370µm at L2 to ~500µm (double the length of an L1, ~250µm). The ovaries at L3 stage mature in preparation for reproduction and the vulva is also visible at this stage. L4 nematodes have fully developed ovaries. Eggs can be seen in a fully formed reproductive adult. Source: WormAtlas

Aging can be construed as the build-up of damage in cells (Rodríguez-Rodero, et al., 2011). This damage may be a result of changes in the genome therefore aging can be manipulated by mutations. Reducing insulin signalling through *daf-2* mutations have been recognised to cause a lifespan extension (Kenyon et al., 1993). These studies have shown the mean lifespan of an L4 nematode at 20^{o}C increased by a 2.3-fold compared to wild-type. The implementation of other experiments that monitor changes in lifespan can produce a data set that shows how temperature affects survival. An isogenic population has the potential to produce different lifespan outcomes and the lifespan distribution observed can be informative about a potential ageing mechanism (Henderson et al., 2018). As stated earlier, many factors can affect lifespan be it a genetic, physical or chemical manifestation. A point mutation on the *age-1* gene, involved in the insulin signalling pathway, has been recorded to double the lifespan (Friedman et al., 1988).

Wild-type nematodes from variant lines have previously been explored and when analysed comparably, it was observed they have different life expectancies where the CGCH is 'short lived' and the JW strain is even shorter lived compared to the N2 CGCM strain (Gems et al., 2000).

1.2 Translation of an mRNA transcript

1.2.1 Overview of the mechanism

Proteins, in one form or another, contribute to the constituents of almost all living things. The formation of proteins begins with transcription and is followed by translation. As stated, transcription precedes translation, and is referred to as the making or 'writing' of the mRNA molecule that with be decoded or 'read' during translation.

During transcription, an mRNA transcript is made containing a sequence of codons that can interact with an anticodon found on the periphery of the aminoacyl-tRNA. This association takes place during translation resulting in the linking of amino acids to an incipient polypeptide chain.

1.2.2 Machinery involved in translation

Translation relies on the cooperative activity of ribonucleoproteins that collectively form two unsymmetrical distinct subunits of the ribosome. Ribonucleoproteins in a ribosome have a high RNA to protein ratio, where the mass of RNA molecules provides a larger contribution to the ribosome compared to the proteins.

Pertaining to mammalian ribosomes, the large ribosomal unit (60S) of the cytoplasmic organelle has approximately 49 ribonucleoproteins and 3 rRNA molecules and operates in combination with the smaller (40S) unit in the nucleolus before being compartmentalised in the cytosol. The 40S unit contains an mRNA-binding site, one 18S ribosomal RNA and 33 ribonucleoproteins (Wilson et al., 2012). Investigating the activity of the integral proteins that each subunit is comprised of, will reveal its effect on the process of translation - by inspecting each respective protein and its associated gene.

Translation is comprised of three distinct stages; initiation, elongation and termination. Initiation is the first step of translation where all relevant molecules are prepared to bind to both subunits of the ribosome. Known to be the slowest of the three, this stage can be divided into four sequential phases that culminate in the transportation of a ternary complex; methionyl-initiator tRNA (Met-tRNAiMet), GTP and eukaryotic initiation factor 2 (eIF2) (Fig. 3). A ribosome can span over 35 bases on an mRNA molecule at a time. The molecule can interact with the mRNA binding site in the small ribosomal subunit and bind in a ‘lock and key’ orientation with the assistance of two rapidly associating tRNA molecules (Frank et al., 1998).

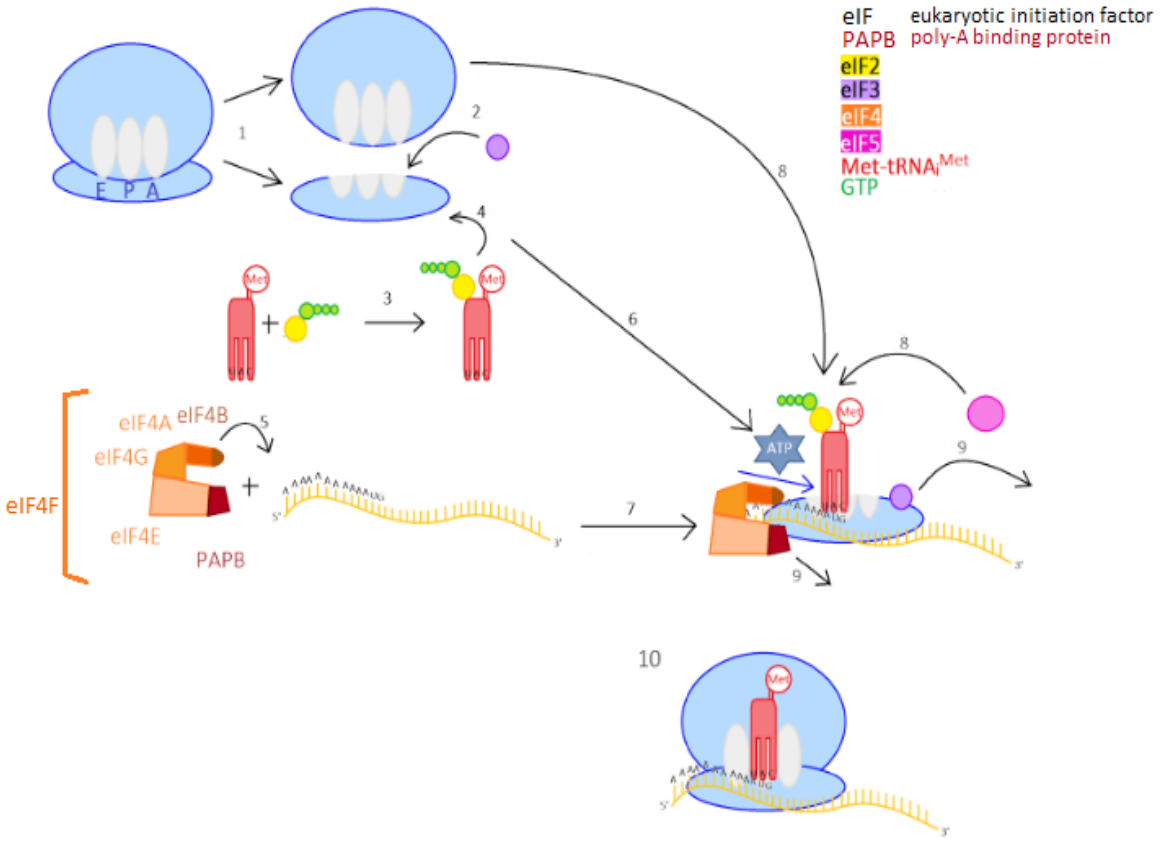

Figure 3 The mechanism of initiation during translation* Initially the eukaryotic ribosome dissociates into 40S and 60S subunits (1), the three tRNA-binding sites are seen here, labelled 'A', 'P' and 'E' for for aminoacyl-site, peptidyl-site and exit site, respectively. eIF3 binds to 40S subunit to prevent from re-association (2). eIF2 is a GTPase that recognizes an initiator tRNA and forms a ternary complex – eIF2, GTP and Met-tRNAiMet (3), the ternary complex binds to the 40S subunit and activates it (4) eIF4F recognizes the 5' poly A tail cap on mRNA [eIF4F consists of eIF4E, eIF4G, eIF4A –eIF4B – an auxiliary factor that promotes the unwinding of the secondary structure in the UTR and PABP – poly-A binding protein are also part of this subunit] (5) once eIF4F binds to the mRNA it guides the activated 40S subunit (with ternary complex) to the 5'-end of mRNA too – known as cap dependent initiation (6). Scanning takes place where the mRNA-bound 40S subunit travels along the 5'-untranslated end (in the 5'- 3' direction) until it recognizes the first AUG codon that serves as the start codon for the translation process (7). This process requires energy (ATP) and additional initiation factors. When the activated 40S subunit has reached the start codon, the 60S subunit binds to the 40S subunit with the aid of eIF5 that hydrolyses the eIF2-bound GTP (8). This releases all eIF from the ribosome positions the tRNA (9) at the ribosome P site – labelled in (1). The resulting ribosome interactions with mRNA are shown in (10) (Villa & Fraser, 2014).
*A few factors (eIF1, 1A, 5A, 5B) have been omitted for clarity of the initiation stage

Initiation results in the placement of a methionyl-initiator tRNA molecule in the P-site of the ribosome, where the tRNA anticodon is paired to the start codon on the mRNA molecule, usually AUG in eukaryotes which begins the elongation phase (More et al., 2002, Ramakrishnan, 2002). An aminoacyl-tRNA (schema seen in Fig. 4(a)) will bind to the codon adjacent to the start codon in the 5'→ 3' direction (because of its matching anticodon and the assistance of elongation factors and GTP). Correct codon matching results in a conformational change that stabilises the binding.

This allows the peptidyl component of the Met-tRNAiMet tRNA to be transferred to the N-terminus of the aminoacyl-tRNA that is in the A-site. Peptide bond formation happens spontaneously and the hydrolysis of GTP provides energy for the tRNA to reposition the aminoacyl-tRNA with the nascent peptide chain from the A-site to the P-site, shifting the now deacylated Met-tRNAiMet to the E-site, ready to leave the ribosomal complex. This process repeats itself as the peptide chain 'elongates' until a stop codon is reached (Rodnina et al., 2007, Schmeing et al., 2009). The binding of an eRF1 molecule, eukaryotic release factor, to the ribosome and the simultaneous reading of a stop codon (either UAG, UAA, and UGA) at the A site instigates the termination step. The peptide chain is released from the tRNA molecule and into the cytosol. With the aid of recycling factors, the mRNA, deacylated tRNA and ribosome subunits dissociated from each other ready to reassemble with a new mRNA molecule to restart the process of translation. The systematic regulation of these stages within a eukaryotic cell is central for accuracy of translation however due to a large number of factors and processes, translation is subject to error. (Green et al., 1997)

1.2.3 Translational accuracy in eukaryotic organisms

Translation must be precise as it determines the structure and ultimately the function of the nascent protein. The steps of translation are regulated thoroughly and the despite the number of conditions that have to be met, the fidelity of translation is upheld. The action of a preinitiation complex (PIC) binding at the 5' cap and scanning the mRNA for the AUG start codon is one form of quality control that regulates the selection of a start codon. (Pestova et al., 2007). The ribosome acts a "quality control" centre being able to regulate protein interactions. When bound to a ribosome, the presence of NAC, the nascent polypeptide-associated complex aids the fine tuning of protein synthesis by linking translation factors and ribosomes with the folding of nascent polypeptides. Under stress conditions, NAC will dissociate from the ribosome, decreasing translation and ensuring misfolded proteins are resolubilised in the cytoplasm. (Kirstein-Miles et al., 2013). Sleep patterns within humans have also been seen to affect transcription and therefore translation of the genes responsible for regulating ribosome biogenesis, this is done by "altering" the expression of initiation factors. (Jouffe et al., 2013). eIF1 (Fig. 3) promotes continual scanning of the mRNA when a non-AUG codon occupies the P-site ensuring protein synthesis does not begin in the wrong place, at the wrong triplet. Mutations in eIF1 have resulted in initiation at a near-cognate codon that still results in errors(Pestova et al., 2002).

Initiation involves recognition of the start codon. If this is inaccurate, the wrong start site can be chosen resulting in N-terminally extended or shortened proteins, or the wrong abundance of protein expression. Elongation involves the actual synthesis of the body of the polypeptide. Errors during this phase can affect the functioning of the protein being made. Termination involves the release of the polypeptide when a stop codon has been reached. Anomalies here may cause C-terminal extension and therefore misfolding in tertiary structures. Regulation of protein synthesis primarily occurs during initiation, subsequently, the precision of this stage directly relates to translation accuracy. Despite the fact inaccuracies can cause problems, the intricate process of initiation is not without exemption to errors. Low-level errors occur that potentially affect the function of the protein resulting in selection over generations (Drummond et al., 2009). Irregular substitutions of amino acids have been detected to contribute to the loss of function within a protein (Guo et al. 2004). As a result of this process being well controlled, the estimated frequency of errors developing during translation in wild-type eukaryotes is usually very low (Bidou et al. 2010).

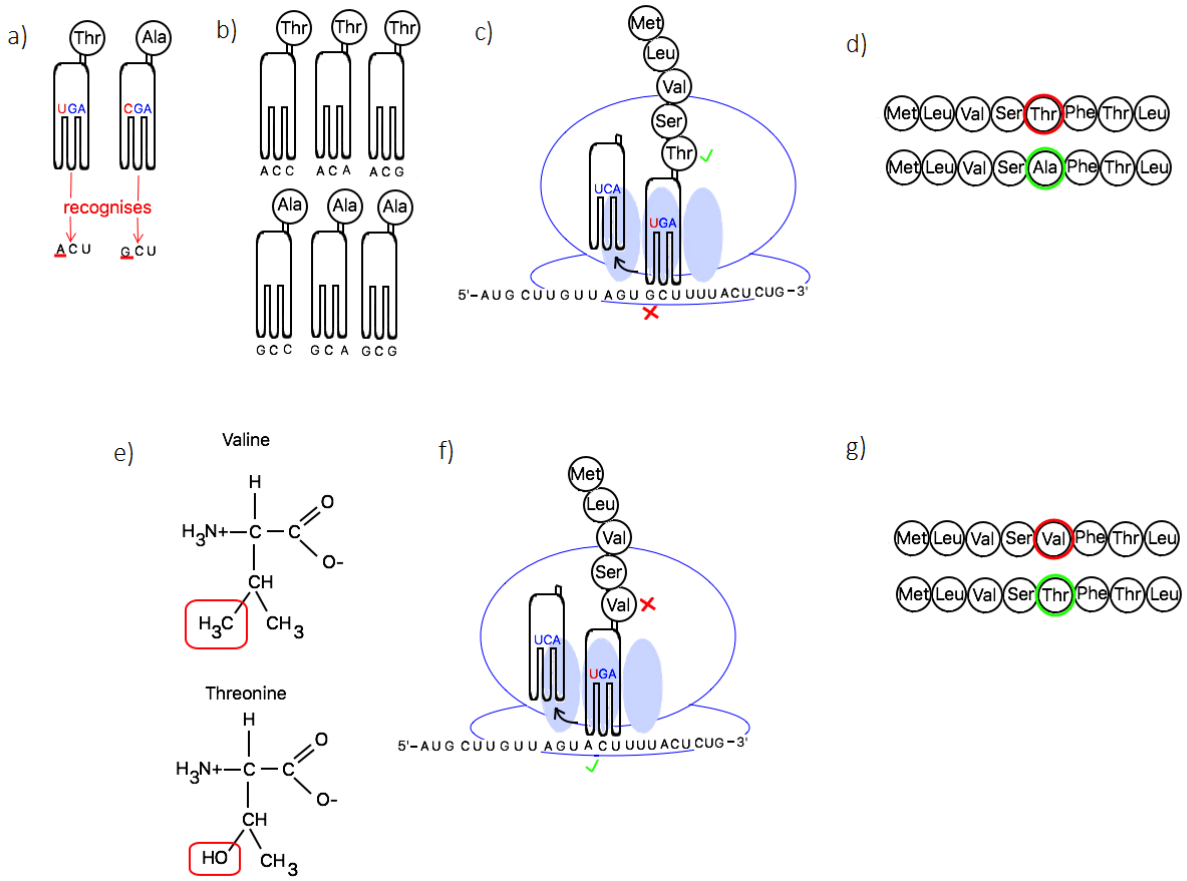

Figure 4 Types of translational errors that are most prevalent (a) The amino acid tRNA bound with threonine is seen to recognise the codon ACU on an mRNA molecule (anticodon: UGA) as the tRNA bound with alanine recognises GCU (anticodon: CGA) there is only one base pair difference between the tRNA molecules (b) other tRNA molecules are able to code for the same amino acid; ACC, ACA, ACG all code for threonine and GCC, GCA and GCG code for alanine (c) a mismatch has occurred where the tRNA that has entered the P-site was not a match to the mRNA molecule yet still incorporated the relative amino acid to the nascent polypeptide chain resulting in the incorrect primary structure (d), threonine instead of alanine. Another cause for inaccuracies is the incorrect catalysis of the tRNA molecule by tRNA synthetase. Valine and threonine seem to be very similar in structure bar the difference in hydroxyl and methyl group (e). This leads to the correct "reading" of mRNA (f) but the subsequent incorrect incorporation to the polypeptide chain. Therefore, valine is integrated instead of threonine (g).

Translational errors can be caused by three different mechanisms; frame shifting, stop codon read-through or amino acid misincorporations.

Frame shifting arises when the reading frame is not maintained, and the ribosome is not shifted forward by exactly three nucleotides. This may be caused by insertions and deletions to the genetic sequence. Frame shifting commences if the positioning of the anticodon loop of the tRNA is not exact in relation to the codons on the mRNA molecule. The addition of a ribosomal mutation can initiate ribosomal frame shifting, resulting in the production of multiple varied polypeptides arising from a single mRNA molecule.

ATA GGT ACC TCT GGG TAG AGC GTC GAT
ATA GGT AC**a** CTC TGG GTA GAG CGT CGA T

The remainder of the protein after the inserted mutation (seen in bold) causes a frame shift that can result in a 'garbled' protein since all the amino acids produced will be incorrect – creating a global catastrophe. The possibility a protein may have only local errors can still have a significant effect on binding residues. Stop codon read-through arises when the ribosome accepts a tRNA molecule on a stop codon, where translation should stop. The integrity of translation is also regulated by the stabalisation of the anticodon:codon pairing of tRNA and mRNA found in the elongation stage. (Ramakrishnan, 2002). An incorrect pairing is one of the main causes of amino acid misincorporation. Amino acid misincorporation can also be caused by misreading, when the wrong tRNA is accepted due to mistakes made by the similarities within the genetic code and misacylation - when a tRNA delivers the wrong amino acid to the polypeptide chain (Fig. 4(c)). The aminoacyl tRNA can carry an amino acid that does not match to the anticodon it codes for, inserting the incorrect amino acid despite "reading" the sequence accurately. Stop codon read-through takes place when stop codons are recognised as a sense codon by near-cognate tRNAs (that can pair with two of three bases that make up the stop codon), rather than being identified as a termination codon by class 1 release factors (Frolova et al., 1994).

It has been stated that the appearance of the likes of errors mentioned above are subject to bringing about very consequential effects within a cell. Orgel states in the 'error catastrophe' theory, proposed in 1963, that the stochastic appearance of transcriptional and translational errors will ultimately lead to the breakdown of the cell, since proteins involved in these processes are responsible for successive pathways. Dysfunctional molecules will begin to be produced and a steady rate. The error catastrophe engages the idea that 'errors' continually being made and building up within a cell leads to a catastrophic level of error resulting in cellular death (Orgel, 1970). The lack of evidence supporting this theory has resulted in it not being widely accepted, however studies such as those conducted in this project, form a platform to implement these ideas. Our gene of interest encodes one of the components of the 40S subunits, therefore, observing a build-up of errors this may have been the case within the nematodes we investigated.

Translational errors have been associated with neurodegenerative disorders such as autosomal myelination defects displayed as Charcot-Marie-Tooth disease type 2N. This is seen with mutations to aminoacyl-tRNA synthetases (Meyer-Schuman et al., 2017).

However, there are also studies showing that this is not always the case, sense to sense tRNA mutations in pathogen Candida albicans generated the ability to display different morphologies as a consequence of generating phenotypic diversity (Gomes et al., 2007). For this reason, monitoring the effect of a mutation within translation may produce unfamiliar results providing provides an avenue for research.

To decipher the functions of proteins within the ribosome such as *rps-2*, experimental measures can be implemented. Monitoring the effects of induced mutations within genes responsible for ribosomal proteins can identify the role of these molecules in signalling pathways and reactions. The effect of these mutations on ribosomal function and structure can be determined and compared to non-mutated (wild type) variants.

1.2.4 Role of translation in ageing

Many processes come to a recession as organisms age, however, the efficiency of protein synthesis must not deteriorate. As discussed earlier (Chp. 1.2.3) the ageing process may have a concordance with the accumulation of errors in protein synthesis.

Ageing is usually seen as a progressive decline in cellular function ultimately resulting in mortality but the putative idea had been ousted since evidence supporting the target of rapamycin (TOR) and insulin/IGF-1 (IIS) pathways has been brought to light. Systematic mutagenesis that resulted in the extension of life within *C. elegans*, were a construct of the IIS pathway. The IIS pathway forms an organised system that includes the use of mTOR kinases in a TOR pathway. The TOR pathway is involved in 'sensing' the same amino acids that are created during translation (Gems et al., 2013). This provides a direct link between translation and increasing lifespan. It is well known that within *C. elegans* reducing protein synthesis can increase lifespan (Charmpilas et al., 2015). Previous studies have shown that an increase in translational errors can notably decrease the viability of mutants. This is supported by investigations into *rps-2* with *S. cerevisiae* (budding yeast). A 72% reduced growth rate, lower biomass and longer lag phase has been seen in *rps-2* mutants. A faster-aging phenotype has been observed within yeast cells where the presence of an error-inducing drug, paromomycin, did not affect the growth of cells but did shorten the life span by over 60% (Haar, et al., 2017). These findings now need to be established in a multicellular eukaryote such as *C. elegans*.

1.3 Small ribosomal protein 2 (*rps-2*)

1.3.1. Function and structure

The eukaryotic ribosome is constructed of two unequal subunits that are named according to sedimentation coefficients, a smaller unit (40S) and a larger subunit (60S). Residing in the cytoplasm, the 40S ribosomal subunit is made up of 33 constituent ribosomal proteins (Ben-Shem et al., 2011), one of which is RPS2 (33kDa). Belonging to the S5P family of ribosomal proteins, it is found in the cytoplasm - the site of translation (NCBI).

The roles of many ribosomal proteins are still ambiguous, however, studies into *Saccharomyces cerevisiae* has pinpointed the role of *rps-2* in ribosomal assembly, specifically exporting 20S pre-rRNA from the nucleolus to the cytoplasm for cleavage into 18S rRNA (Ferreira-Cerca et al., 2005). Mutations to the *S. cerevisiae* orthologue of *rps-2* have been linked to an increase in stop codon read-through translational errors as well as reduced viability (Stroustrup, et al., 2017). The RPS2 *C. elegans* orthologue is *rps-2*, it contains 3 exons (1045bp) and it is found on chromosome 4 (Kenmochi et al., 1998, Wang et al., 2009).

Given the results describing the effect *rps-2* has on the lifespan of *S. cerevisiae*, exploration of this gene in a whole organism context is a logical next step. *rps-2* is an excellent gene to study further since not much has been documented about its function, this provides a constructive avenue for development and research.

1.3.2. Role of *rps-2* in ageing

A definitive role has not been dictated for *rps-2,* within the process of ageing and translation. By understanding *rps-2* encodes a ribosomal protein*,* we can suggest its function is necessary. Cellular energy and resources are being used to synthesize *rps-2,* its conservation *alone* amongst eukaryotes and higher mammalian organisms prove its importance. Projects such as this provide steppingstones to engaging with the purpose of *rps-2*.

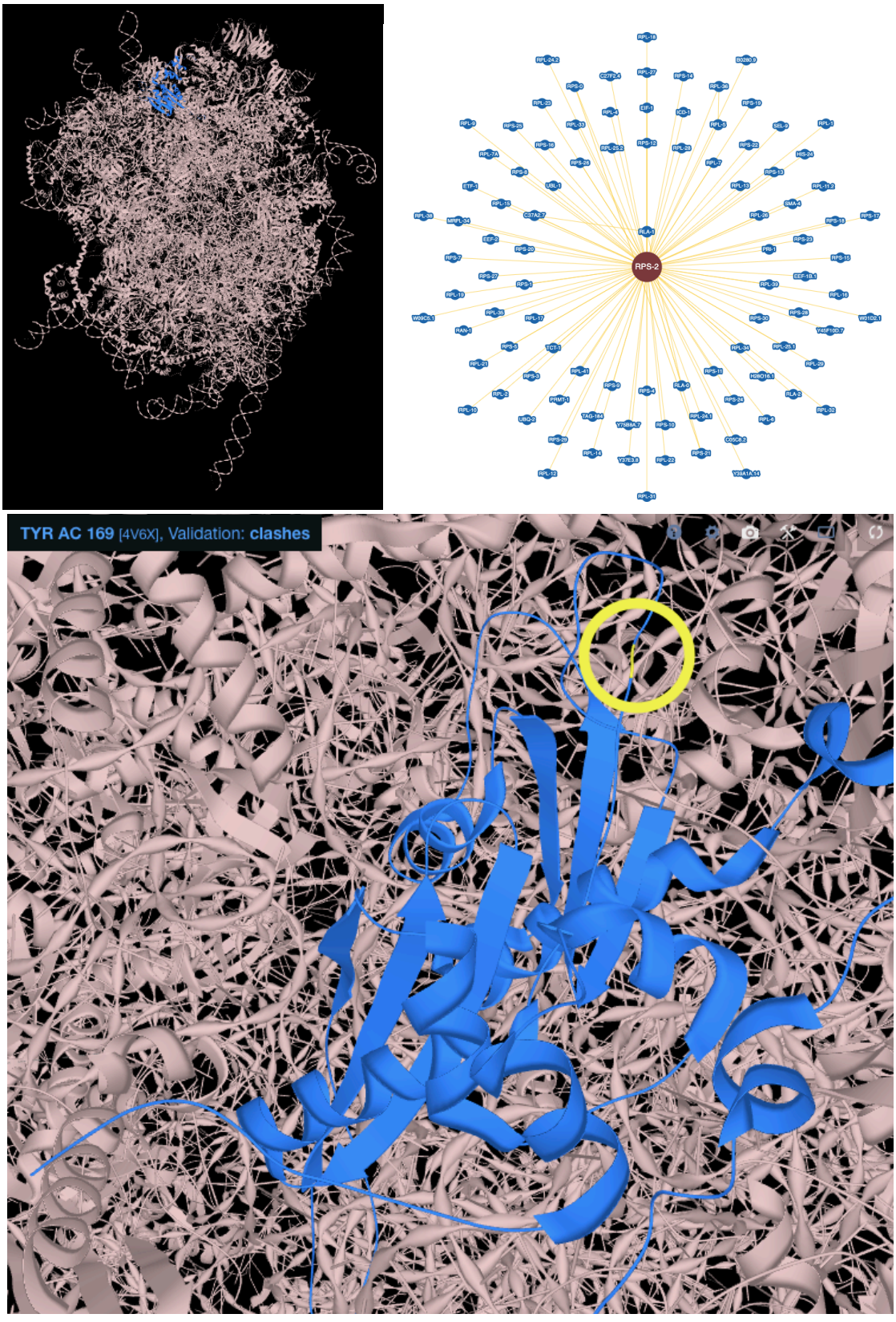

Figure 5 Crystal structure of the human 40S small ribosomal subunit (*rps-2*) in a ribbon arrangement the (brown) (top left) and of *rps-2* has been pinpointed in (blue) from Protein Data Bank in Europe Knowledge Base (PDBe-KB). [Uniprot**:** P15880] Circle/highlight in yellow represents the tyrosine residue (TYR) of interest subjected to mutation. It has been seen to have 98 interactions with ligands and other binding proteins (top right)

1.4 Aims of study

The global topic of ageing is beyond the research completed here. The focus of the following experimentation was to establish the relationship between the ability to accurately synthesise fundamental proteins and lifespan in a whole model organism - *C. elegans.* To do this we tested how modifying residues in RPS2 affected the lifespan of a worm whilst monitoring other markers of health. In the literature, *rps-2* mutants will be referred, as allelic, to as COP872/*rps-2* -/-.

This can be addressed by focussing on the following specific aims:

1: Generate genetic tools to study *rps-2* and its role in translational accuracy in worms
We outcrossed the mutant strains with the wild type strains, and then amplified *rps-2* via PCR which was followed by the purification and sequencing of the PCR product which corroborated the presence of the mutant in the gene pool.

2: Use *rps-2* mutants to determine the role of *rps-2* in lifespan and health in worms
Physiological changes to the nematodes and their behaviour in the presence of the mutation was a main factor to focus on. Positive error inducing drug Nourseothricin sulphate (NTC) was be trialled to mimic the action of the *rps-2* mutation before beginning further analysis. Quantitative assays were initiated to expose the global effect of the mutation on the organism. Fecundity of nematodes was investigated during brood size assays and comparisons of both wild type strains with mutant strains survival rate were displayed through lifespan assays.

3: Measure translational accuracy in wild type compared to *rps-2* mutant nematodes
Biochemical investigations precisely show the direct effect the mutation has on protein structure. Yolk proteins extracted from SDS-PAGE gels and analysed using MALDI-TOF spectrometry revealed the effect of any translational errors made during synthesis on the protein tertiary structure.

This project provided evidence to determine the significance of the *rps-2* mutation. Understanding the localised and global effects of mutations within *rps-2* will allow future advancements in its contribution to the progression of ageing.

Chapter 2

Methods and Materials

2.1 Nematode handling and maintenance

2.1.1 Strains and growth conditions

The mutant strains used are a result of outcrossing strains acquired from the CGC, Caenorhabditis Genetics Centre, (N2 wild-type background) and the mutation COP background from Knudra Transgenics™. 5 strains were obtained, COP872, COP873, COP874, COP875 and COP876. These were grown at 15 ^{o}C and 20 ^{o}C.

Strain	Genotype
COP872, COP873, COP875	*rps-2 -/-*
COP874, COP876	*rps-2 +/+*

2.1.2 NGM agar plates

NGM agar plates were made to sustain *C. elegans* nematodes for all experimentation. A 1.6L solution containing 0.3% (w/v) NaCl, 1.7% (w/v) Agar, 0.25% (w/v) Bactopeptone and distilled H_2O 1.6L was autoclaved. When cooled to 55 ^{o}C, buffering salts; 2.5% (w/v) KH_2PO_4 (pH 6), 0.1% (w/v) $MgSO_4$ (1M), 0.1% (w/v) $CaCl_2$ (1M) and 0.1% (w/v) Cholesterol (at 5 mg/ml in EtOH) were added to the bottle and aliquoted into 15ml petri dishes under the sterile conditions of a fume hood.

2.1.3 OP50 cultures

The most common procedure uses live OP50 *E. coli*, which is defective in the synthesis of uracil and cannot overgrow into a thick layer that would obscure the worms (Porta-de-la-Riva, 2012). 2.5 g LB broth is added to 100ml of distilled H_2O and autoclaved. Once cooled a streak of OP50 from a stock plate was incubated overnight in the media at 37 ^{o}C. 200µl of the OP50 is aliquoted onto the NGM plates as food for the nematodes.

2.1.4 Bleach drop

1 ml solution is made from 7 parts bleach: 8 parts 4M NaOH. Gravid, adult worms that are contaminated by fungus can be placed in bleach drop and since their eggs are impermeable and will not be affected by surrounding bleach solutions.

2.2 Bioinformatic methods

2.2.1 BLAST

In silico sequence alignments obtained via NCBI Basic Local Alignment Search Tool (BLAST) carried out on *C. elegans rps-2* used, with a genomic position IV: 7925298.7926391 to identify the missense mutation.

Accessed at: https://www.ncbi.nlm.nih.gov/BLAST/

2.2.2 ApE

A plasmid editing software used to map out primers constructed to sequence and genotype sections of *rps-2*. This is then used to identify the presence of the mutation in the laboratory setting when completing a PCR reaction.

Accessed at: http://jorgensen.biology.utah.edu/wayned/ape/

2.3 Biomolecular construction

2.3.1 CrispR

Knudra Transgenics™ generated all COP strains (COP872/3/4/5/6) using a type 2 CrispR-based genome engineering strategy known as PCR Discovery, a technique used to make precise, targeted edits to the genome. Out of the three major techniques Knudra Transgenics™ uses, PCR Discovery was the optimal method as the genome edit induced is a point mutation (Hopkins, 2016), another technique is the pointMUTATION™ CRISPR knock-in (KI) project is designed to change an amino acid or small region in a gene.

CrispR is clustered, regularly interspaced, short palindromic repeats of genomic information. These were originally found within bacteria and used as a means to store information harvested from invading bacteriophages. Storing the DNA from an invading host will ensure upon return the phage will be cleaved and destroyed. A recombinant Cas9 protein is combined with a chimera known as sgRNA (sub genomic/single guide RNA) to make a site-specific nuclease to cleave DNA. SgRNA consists of crRNA (CRISPR RNA – spacer segment/ variable region containing targeting sequence) and tracrRNA (trans-activating crRNA - as a constant region to hold crRNA in place), this recognises specific sequences that form targets for cleaving.

PAM (protospacer adjacent motif) sites are used to differentiate between inserted DNA its own CrispR array. It is a sequence ~2-6 bp in length found after the protospacer sequence in the "inserted" DNA sequence. The PAM sequence 5'-TGG-3' was recognised adjacent to the mutation indicating the position of the Cas9 directed cleavage.

Accessed at: https://www.addgene.org/crispr/guide/

The presence of a PAM sequence after the target sequence is required for the binding of Cas9 (Mali et al., 2013; Doudna et al., 2014). The presence of a PAM sequence also accelerates the search process of the mutation by Cas-9, which helps to validate this process.

Accessed at: https://www.synthego.com/guide/how-to-use-crispr/pam-sequence.

2.3.2 Worm lysis for sequencing and genotyping

For sequencing, 10 adult worms were picked with a platinum pick into 5µl of lysis buffer (50mM KCL, 10mM Tris (pH 8.3), 2.5mM $MgCl_2$, 0.45% NP40, 0.45% Tween20, 0.01% Gelatin and 0.1mg/ml of proteinase K. Lysis was carried out in a Bio-Rad T100 thermal cycler at 70 ^{o}C for 60 minutes followed by 95 ^{o}C for 15 minutes. The number of worms lysed can be increased to attain a higher yield of DNA if the bands produced after gel electrophoresis are not prominent.

2.3.3 DNA Sequencing

Primer mix

100µM stock of primer can be made from custom primers (see Appendix). Specific sequencing primers (Forward: 5' → 3' - TGC CGG ACA ACG TAC CCG CTT CAA G; Reverse: 5' → 3': GGA TCC CTT AGC GGC GGT GTA GC) were constructed to specifically establish the exact sequence of the mutation. 10µM has to be used to create a primer mix, so the stock is diluted accordingly. 10µl of 10µM forward primer, 10µl of 10µM backward primer is then aliquoted from the stock and mixed gently vortexed with 80µl NF H_2O and is ready to use as a primer mix.

For every sample required, 10µl GoTaq DNA Polymerase (from Promega), 3µl of primer mix and 2µl NF H_2O is pipetted into an Eppendorf that already contains 5µl worm lysate. This is the master mix that was gently vortexed before it was placed in a Bio-Rad T100 Thermal cycler for DNA amplification to take place. Following this, it was loaded onto a 1% agarose gel (made with 1 drop of Ethidium Bromide per 0.6g of agarose salt) for gel electrophoresis at the subsequent temperatures; Step 1 - 95 ^{o}C, 120s; Denaturing step 2 - 95 ^{o}C, 45s; Primer annealing Step 3 - 55^{o}C, 45s; Elongation Step 4 - 72 ^{o}C, 45s; Replication Step 5 - Step 2 repeated 30 times; Step 6 - 72^{o}C, 10 mins. It can be stored at between 4-12 ^{o}C.

Sequencing reactions result in the production of 334bp bands including primers.
1% TAE buffer is used to run the gel at 120V for between 20-30 minutes. After observing the presence of the mutation by running a 1% agarose gel in running buffer (10 x 30.3g Tris, 144g Glycine, 15g SDS in 1L. Diluted 100ml with 900ml Milli-Q H_20) the band is excised with a sharp scalpel and purified using the Thermo Fisher Gene JET PCR Purification Kit.

Purification

All reagents used were provided in the GeneJET PCR Purification Kit. A 1:1 volume of Binding Buffer was added to a completed PCR mixture (e.g. for every 100 µL of reaction mixture, add 100 µL of Binding Buffer) and mixed thoroughly. The DNA fragment to be sequenced was ≤500 bp, therefore a 1:2 volume of 100% isopropanol was added and mixed (e.g., 100 µL of isopropanol should be added to 100 µL of PCR mixture combined with 100 µL of Binding Buffer). The sample was placed in the GeneJET purification column and was centrifuged for up to 1 minute and the flow through was discarded. This was repeated until the entire solution had been added to the column membrane. Wash buffer was added to the column and this process was repeated. The GeneJET purification column was then transferred to a clean 1.5 mL microcentrifuge tube and elution buffer was added to the column and centrifuged. The GeneJET purification column was discarded and the concentration of the purified cDNA in the microcentrifuge tube was checked using a nanodrop. With a concentration of 20-80ng/µl, ~50µl of the purified cDNA fragment is sequenced by GATC Biotech (see Appendix).

2.3.4 Genotyping PCR

Custom desalted genotyping primers (Forward: 5' → 3' - CAG AGC CGG ACG CGG AGG AG; Reverse: 5' → 3' - GAG TCC GAT CTT GTT ACC CCA GT) detecting the GT point mutations in *rps-2* sequence, result in the production of 426bp bands including primers. This was easily identified when run on a 1% agarose gel in 1x TAE buffer at 120V and observing both the presence and the strength of the band produced. PCR reactions were carried out in a Bio-Rad T100 Thermal cycler. GreenTaq DNA polymerase from Promega was used in all reactions. Per sample, the reaction mix was as follows: 10µl GreenTaq, 3µl primer mix, 2µl H2O and 5µl DNA lysate (see Appendix).

Step 1 - 95 °C, 120s; Denaturing step 2 - 95 °C, 45s; Primer annealing Step 3 - 71°C, 45s; Elongation Step 4 - 72 °C, 45s; Replication Step 5 - Step 2 repeated 30 times; Step 6 - 72°C, 10 mins. It can be stored at between 4-12 °C.

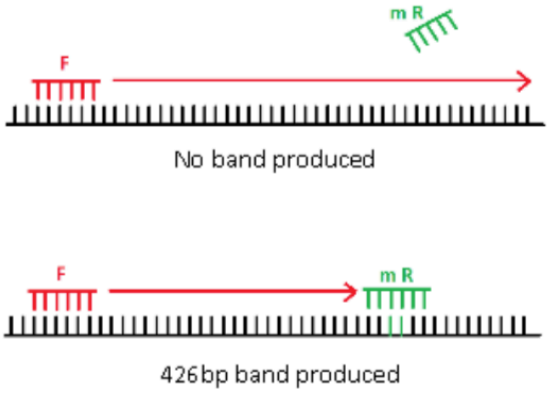

Figure 6 Representation of customised primers (Fig 24) Top: Mutant reverse primer will not anneal to a strain without the mutation. No band is produced during PCR. Bottom: In the presence of the mutation (green bases) the mutant reverse can anneal and produce a 426bp band. This is a quicker method to differentiate between mutant and non-mutant strains compared to sequencing. F = forward primer, mR = mutant reverse

2.3.5 Outcrossing the wild type (N2) strain with the COP872 mutant

3 plates of 10 *rps-2* L4 hermaphrodite worms were incubated at 30 °C and heat-shocked for 5 h to generate an increased number of males within the progeny. Male cultures can be maintained by adding males to hermaphrodites (2:1) on a seeded NGM plate. Progeny produced was heterozygous for the gene of interest, *rps-2*. Mating was perceived to have been successful if approximately a 1:1 ratio of males

to hermaphrodites was observed in the F1 offspring. From the resultant progeny, 5 hermaphrodites (L3-L4 stage) than the males in the offspring were selected and cloned out to fresh NGM plates before being genotyped to confirm that they were heterozygous for the mutation. The offspring of the worms were then screened by genotyping for *rps-2*. 12 hermaphrodites showing were cloned out to individual plates and then genotyped for the mutation (see Fig.26]

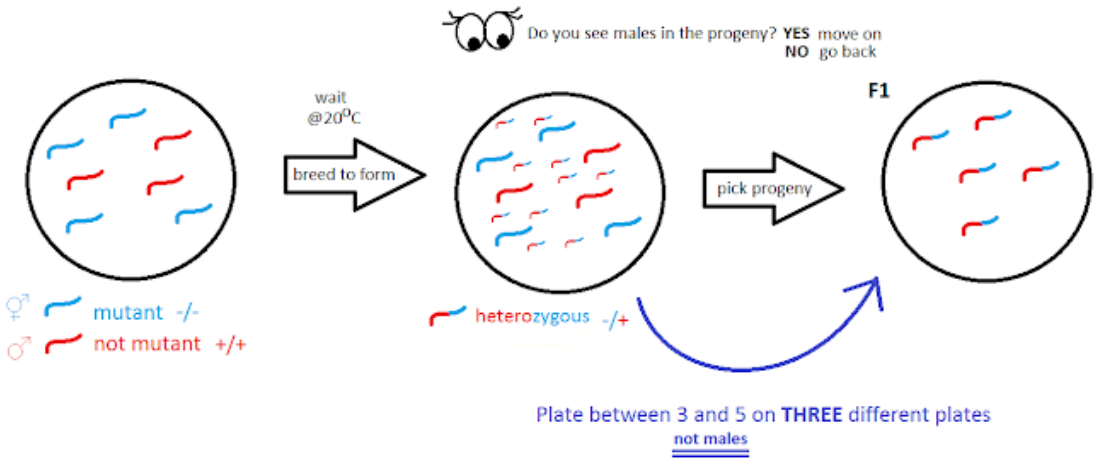

Figure 7 The initial stages of outcrossing 3 L4 hermaphrodites from the *rps-2* mutant strain were crossed with 3 males from the wild type strain and incubated at 20°C to form a mixed progeny containing only heterozygous mutants. This is the F0 cross. If the majority of the progeny population are males the initial cross has been successful, and outcrossing can continue. 3-5 hermaphrodites were picked from the progeny onto 3 plates [total of ~15 worms spread over 3 plates] and incubated at 20 °C for 24 h. This is the F1 cross.

F0 cross:

		♂ CGCM male	
		rps-2 +	rps-2 +
♀ COP2 hermaphrodite	rps-2 -	rps-2 -/+	
	rps-2 -		

F1 cross:

		♂ COP2 hermaphrodite	
		rps-2 +	rps-2 -
♀ COP2 hermaphrodite	rps-2 +	rps-2 +/+	rps-2 +/-
	rps-2 -	rps-2 +/-	rps-2 -/-

Figure 8 Punnett squares of F0 and F1 crosses. The first cross (top) resulted in a heterozygous population (*rps-2 -/+)* and the second cross (bottom) resulted in a population of non-mutants, heterozygous nematodes and homozygous worms in a 1:2:1 ratio. (25% *rps-2 +/+*, 50% *rps-2 +/-* heterozygous, 25% *rps-2 -/-*).

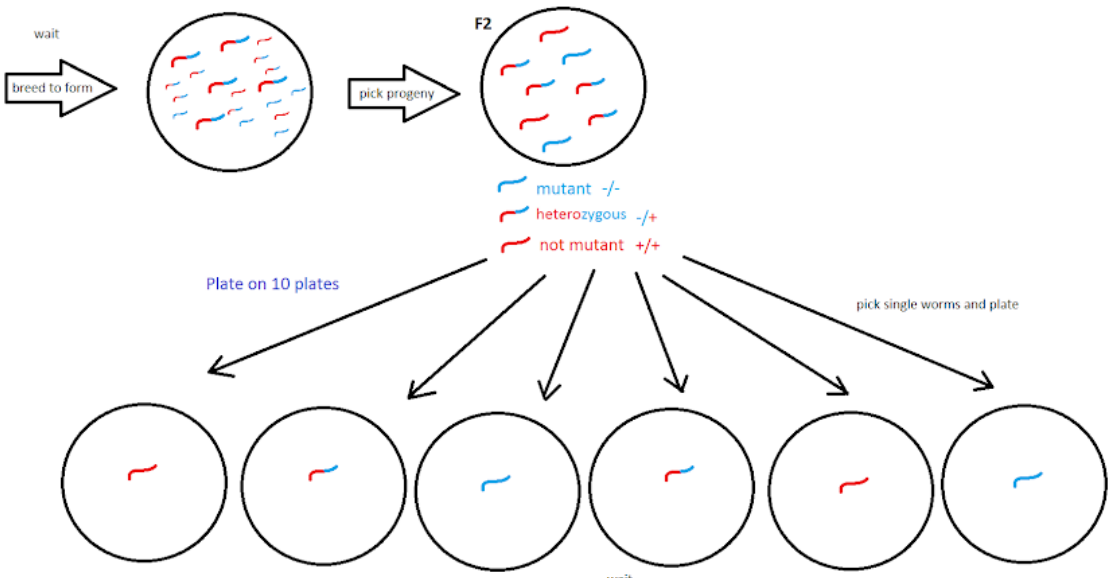

Figure 9 Next stages of outcrossing. A mixed progeny is formed from the F1 cross with a population of homozygous mutants, heterozygous mutants and non- mutants. The mixed progeny then has to be cloned out. One hermaphrodite worm from the mixed progeny was placed on individual seeded plate. This is repeated 10 times on 10 empty plates.

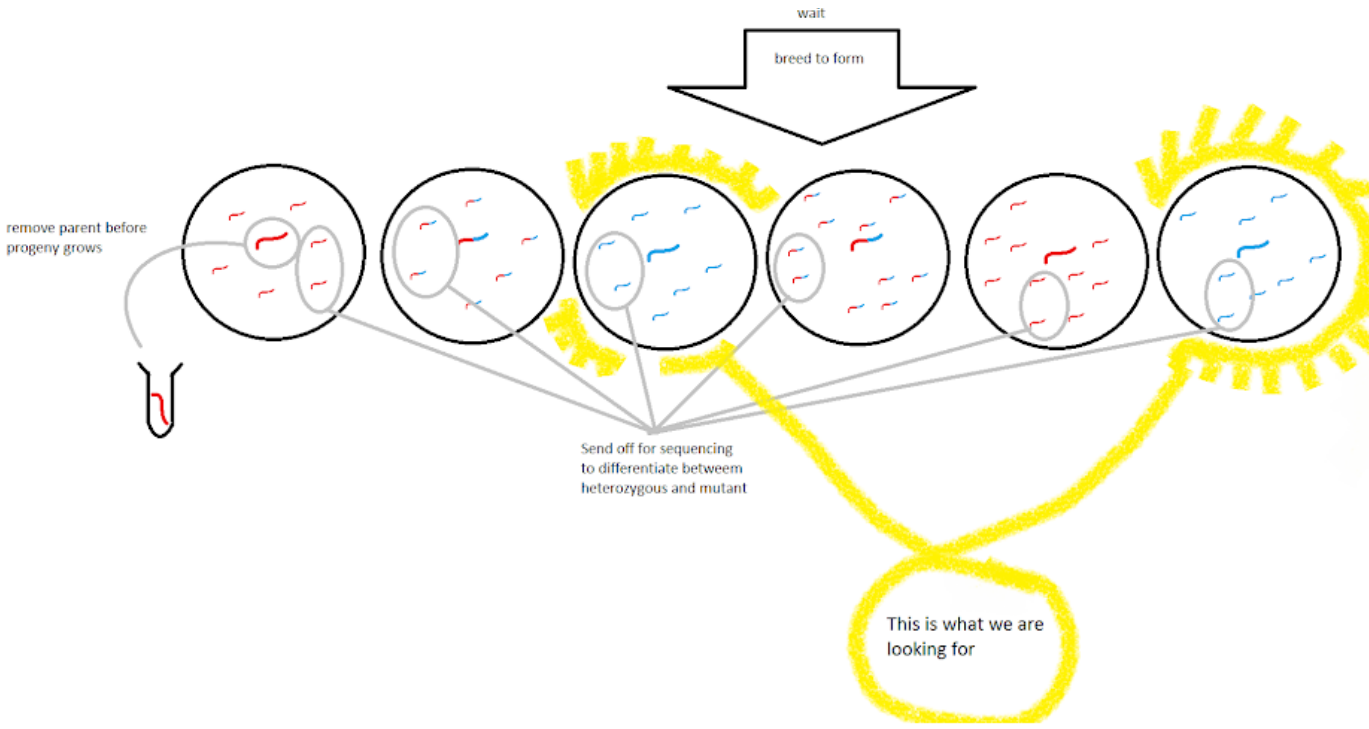

Figure 10 Cloning staged of outcross. As soon as progeny has formed on these plates from the self-fertilising parent, the parent worm was removed and sent off for sequencing or used in a single worm PCR reaction with customised primers (Fig. 24).

2.4 *C. elegans* physiological assays

2.4.1 NTC treatment optimisation assay

Nourseothricin sulphate (NTC) is the drug used for this assay since it has been known to induce miscoding in an mRNA molecule and subsequently inhibit protein synthesis. This drug assay is used to imitate the action of a mutation. To find the optimum concentration to use, a range of concentrations are trialled.

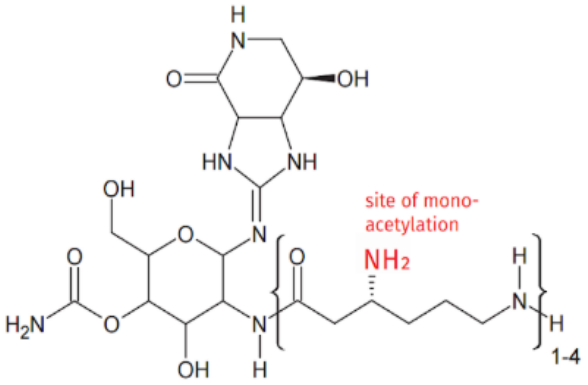

Figure 11 Structure of Nourseothricin sulphate (NTC) from Sigma Life Science DATA Sheet

Each well contained different concentrations of NTC (Fig. 12), 2µl of 0P50 and 95.5 µl of S -media and is left to incubate at 20°C for 24 h allowing the OP50 to grow to ensure food is not a limiting factor. 10 L4 worms worms are then picked into each well and scored after 24 h and again after 48 h.

50 µg/ml	/10 alive	/10 alive	/10 alive	
25 µg/ml	/10 alive	/10 alive	/10 alive	
12.5 µg/ml	/10 alive	/10 alive	/10 alive	
0 µg/ml	/10 alive	/10 alive	/10 alive	

Figure 12 Diagrammatic representation of a 96-well plate to find the optimum NTC concentration. The first row will contain 50µg/ml, the second 25 µg/ml, the third row 12.5 µg/ml and the last 0µg/ml.

2.4.2 Yolk protein quantification assay

Strains are aged to produce yolk protein necessary to be analysed during mass spectrometry. A plate was synchronised and held ~20-50 adult worms. 20µl of M9 buffer is placed a cut Eppendorf lid and an adult worm added. This was spun down for 15 minutes at 20°C, Laemelli buffer was added in a 1:1 ratio. It is boiled at 95 °C

for 5 mins and loaded onto a 7.5% SDS gel and run at 110V with the protein ladder. These are 'Day 1' worms. After 72 hours, another 20 worms are harvested ensuring they were not starving to ensure food availability is not a limiting factor for protein production. This was counted as 'Day 4' worms. This repeated to collect 'Day 7' and 'Day 10' worms.

2.4.3 Lifespan assay

The lifespan of *C. elegans* can be monitored through the use of lifespan assays. The assay compares lifespan differences between worms with the *rps-2* mutation and wildtype worms. 5 Floxuridine (FuDR) treated plates are prepared for each strain. FuDR inhibits DNA synthesis and consequently prevents a synchronous population from reproducing. All plates are incubated at 20°C. After 24 h, 20 L4 worms are added to each plate. The total number of worms investigated can then be taken as a percentage upon counting. Incubate for 48 h and count the adults, this is 'Day 1' adults. Incubate for a further 48 h and count the worms, this is 'Day 3'. Incubation is repeated for another 48h and then counted; this is 'Day 5'. After this, worms are incubated and counted every 24 h (Days 6, 7, 8 etc.). The following diagram outlines these steps (Fig.13).

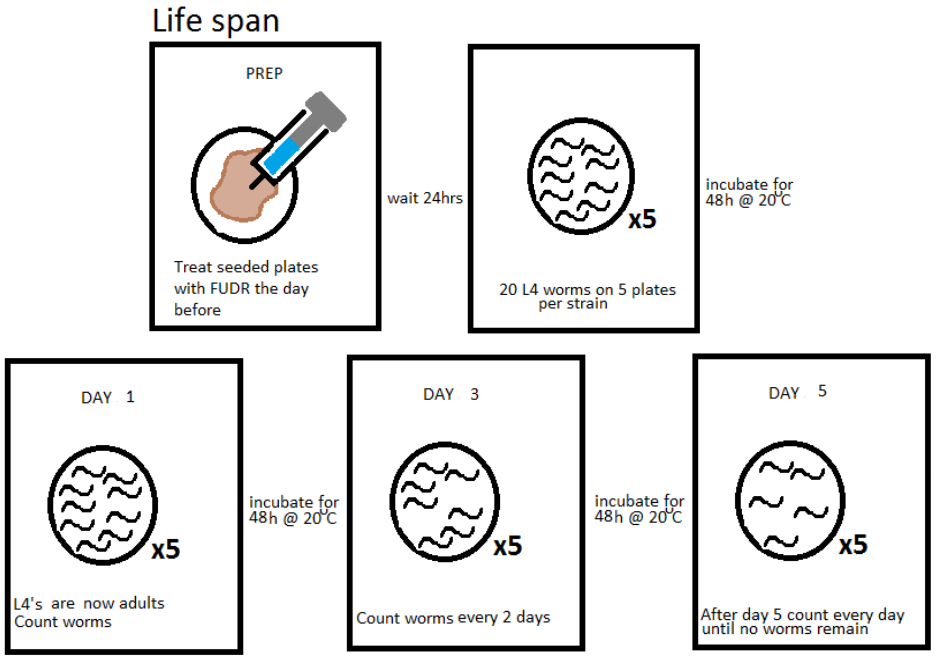

Figure 13 Life span assay. Seeded plates are treated with FuDR and left for 24 h. 20 L4 worms are picked onto each plate. Repeated five times and left to incubate for 48 h at 20°C. Worms are now day 1 adults and are counted. Plates are incubated again at 20°C for a further 48 h. Plates are counted at regular intervals and dead and alive worms scored.

2.4.4 Brood size assay

To decipher the number of progeny a worm can produce a brood assay is conducted. The brood sizes of wild-type worms are compared with that with the *rps-2* mutation. 1 hermaphrodite L4 worm from each investigated strain is placed on an individual 15ml plate. This is repeated on 10 plates. Incubate plates at 20 °C. On 'Day 2' move the worm from the original plate to a newly seeded plate and label it accordingly. Repeat incubation. On 'Day 3' the worm is moved again to a newly labelled plate and the progeny on the first plate "'Day 1'" is counted and disposed of. This is repeated until no larvae are found, dead worms are also acknowledged.

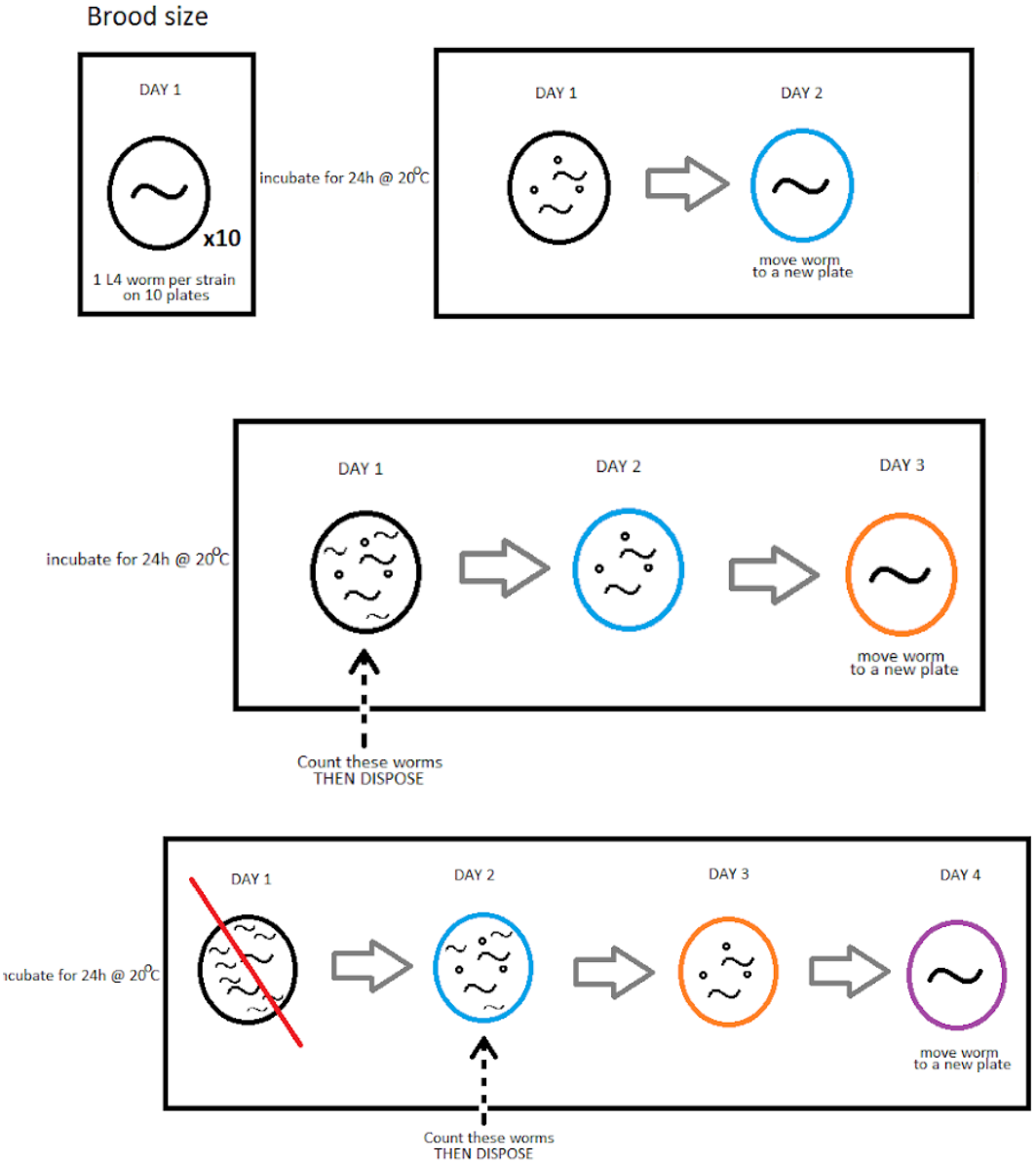

Figure 14 Brood size assay. 1 L4 worm per strain is plated on 1 plate, this is repeated 10 times and put to incubate for 24 h at 20°C. After 24 h, Day 1, the worm is moved to another seeded plate and all plates are put to incubate at 20°C for another 24 h. On Day 2 this is repeated. On Day 3 the progeny on the plate from day 1 (that should be at the L1 stage) is counted. The worm is moved again. This process continues until no more progeny is found on the plate. This usually takes between 5 and 7 days.

2.5 Biochemical techniques

2.5.1 SDS PAGE gels

High molecular weight (HMW) cast gels are made from separating gels and stacking gels (see Appendix for gel casting recipe).

The tape at the bottom of the cassette was present before the gel was cast and cassette was set in a suitable rack in a vertical position. Immediately after the separating gel solution has been prepared and mixed, the cassette is filled to a ~2 mm above the horizontal line located about 2 cm from the top edge of the U-shaped plate.

Air bubbles must not be trapped at the bottom of the cassette. Using a transfer pipette, the separating gel was overlaid with degassed water until the cassette is filled. The separating gel must polymerize for about 1 hour. The interface will become more distinct as the gel polymerizes. The stacking gel solution was prepared, mixed well. The overlay solution is completely poured out and the cassette is filled within a couple of millimetres of the top with the stacking gel solution. The comb is completely inserted into the gel by starting at one end and rocking it down until both ends are in place. The stacking gel is polymerised for up to an hour and can be kept in a 37 ^{o}C incubator whilst doing so.

HMW gels can run at 200V enveloped in ice for 24 h. SDS PAGE gels are run at 180V for ~30 mins and stained with Coomassie. For myosin extraction, SDS PAGE gel is run on ice at 110V overnight and stained with Coomassie (Stock solution: 12g brilliant blue R-250, 300ml methanol and 60ml acetic acid; Working staining solution: 500ml methanol, 30ml Coomassie stock solution, 400ml distilled H2O, 100ml acetic acid). Gels were removed from the plastic cassette and soaked in fixing solution for 30 minutes in a plastic container. Fixing solution (500ml methanol, 100ml acetic acid, 400ml distilled H_2O) was poured out and gels were soaked 40 minutes in Coomassie staining solution. Coomassie solution was replaced with destaining solution (450ml methanol, 100ml acetic acid and 450ml distilled H_2O) and gels were soaked for 20 minutes. Destaining solution was poured out and replaced before allowing gels to destain overnight.

2.5.2 Myosin extraction

C. elegans protein extraction was performed on ice unless specifically mentioned otherwise. 5 L4 stage worms from each desired strain were placed on three large plates (60ml; x4 Peptone, seeded with 2/4ml OP50), this ensures a large number amount of healthy worms are harvested and plates were populated but not starved. It was then incubated at 20^{o}C. Worms were washed off with 2 ml of M9 buffer (49.3mM $Na_2HPO_4.2H_2O$, 22mM K_2HPO_4, 85.5mM NaCl, 2.07mM $MgSO_4.7H_2O$ in 1L diH2O) into a 15ml falcon tube and allowed to settle until a visible worm pellet has formed at the bottom of the tube. M9 is commonly used as bacterial media for maintenance of *E. coli* strains such as OP50 the food source of *C. elegans* [ThermoFisher]. The supernatant was then removed and 5 ml of fresh M9 was added to the falcon tube. This step is repeated 3 times to remove excess media and OP50. After the last wash, the worm pellet was placed on ice and 100µl of chilled cell lytic buffer with added DTTs and protease inhibitors were added to the pellet (50mM).

Myosin extraction buffer (also known as Guba buffer; 0.3 M KCl, 100 mM KH_2PO_4, 50 mM K_2HPO_4 make up to 1L (pH6.6)) was added to sample, 50µl for pieces 3-5 mg and 75 µl for 5-8 mg and vortex with care. Placed on ice, it was mixed every 10 mins for 30 minutes. Spun at ~6000 rpm for 2 mins at 4^{o}C. The supernatants are pipetted into the new labelled tube (combine any tubes) and topped with 1 ml water. Myosin may be visible as a white precipitate. Then centrifuged for 4 mins at 13000 rpm at 4^{o}C. The supernatant was transferred to a new tube (pellet was kept for SDS PAGE – also keep some supernatant and run on gel). For a very concentrated myosin sample add 100 µl -250 µl 3M KCl to the pellet and flick tube until pellet goes into solution and spin again 4mins 13000 rpm. All water is removed with a pipette and discarded. 250µl of MOPS buffer (250mls (pH7) 500mM KCl, 20 mM MOPS, 5 mM $MgCl_2$) was added to the pellet.

2.5.3 Tryptic Digest of myosin protein samples

Digesting a protein prepares the protein sample for mass spectrometry and further proteomic analysis after the protein has been run on a gel and stained, e.g. SDS PAGE gels stained with Coomassie Blue. The digest is broken into the following stages: protein excision, reduction and alkylation, in-gel digestion, extraction of peptides. A 100mM NH_4HCO_3 (ammonium bicarbonate) stock was freshly prepared.

Protein Excision

The whole 7.5% protein/HMW gel was washed with water twice for 10 minutes each time. (If the gel is Coomassie-stained: wash twice for 5mins in destain (100mM NH_4HCO_3, 50% Methanol)). The band/spot with excised with a clean scalpel, cutting as close to the edge of band/spot as possible to minimise background interference. The band was cut into small squares (~1mm^3) then transferred to microcentrifuge tube (Eppendorf), the supernatant was discarded by pipetting.

Reduction and Alkylation

The excised gel pieces are washed with 100µl NH_4HCO_3: acetonitrile solution (50mM NH_4HCO_3: acetonitrile (1:1)) for 15 min (on shaker). The water bath was preheated now at 56°C for later stages. The samples were spun down for 15 s in a centrifuge and any liquid was removed by pipetting. These stages were repeated.

100µl acetonitrile was added for 15 min, until the gel pieces had become shrunken (white appearance and stuck together) then spun down and liquid was removed. An equal proportion of DTT solution (10mM DTT in 50mM NH_4HCO_3) was added to cover the gel (~50µl) for 30 mins at 56°C, swelling the gel pieces - ensuring not too much DTT is added to dilute the sample). Once again the sample was spun down and any liquid was removed. Acetonitrile was added for approximately 15 mins to shrink the gel pieces until they appeared small and white (be observant this may happen sooner). Any additional liquid was removed and add equal proportions of Iodoacetamide solution (55mM Iodoacetamide in 50mM NH_4HCO_3) was used to cover the gel (~50µl) for 15 mins at room temperature in the dark – covered in foil. Using a centrifuge, the samples were spun down again and washed with 100µl 50mM NH_4HCO_3 for 15 mins. A final spin and removal of supernatant was conducted and the wash was repeated.

In-gel digestion

Gel pieces were rehydrated in 20µl digestion buffer (trypsin) (25mm NH_4HCO_3 10% acetonitrile, make up w/ dH_2O +10ng/µl trypsin) for 30 min at 4°C. After 15 min, the samples were checked and more digestion buffer and trypsin were added if all the liquid has been absorbed by the gel pieces. Remaining liquid was Removed with a pipette. 10µl Digestion Buffer (no trypsin) (25mm NH_4HCO_3 10% acetonitrile) was added to cover gel pieces and keep wet during digestion. If necessary, add digestion buffer to cover pieces, however, the volume must be kept to a minimum to avoid diluting the final sample. This was then left covered at room temperature overnight in a rack.

Extraction of Peptides

5µl acetonitrile was added and the samples were sonicated for 15 mins in an ultrasound water bath. Sample was spun down and the supernatant collected in 0.5ml microcentrifuge tubes. 10µl extraction solution (50% acetonitrile, 5% formic acid, 45% dH_2O) was added and sonicated for 15 mins. After being spun down, supernatant was collected and samples were pooled. The gel pieces were retained until the supernatant has been analysed by mass spectrometry. Samples were stored at -80°C.

2.5.4 MALDI-TOF of myosin protein samples

Mass spectrometry is used to aid the analysis of the isolated myosin protein extracted from the nematodes that have incorporated the *rps-2* mutation by measuring the mass to charge ratio. The gel pieces are treated with DTT to reduce disulphides treated with chloroacetamide to alkylate the cysteines (by adding an alkyl group C_nH_{2n+1}).

The peptides generated were extracted and prepared for analysis by MALDI-TOF mass spec. Peptide mixtures were analysed by ultra-performanceY nanoLC (ACQUITY M Class, Waters) paired with an IMS mass spectrometer (SYNAPT G2-Si, Waters) fitted with a NanoLockSpray source (Waters). Samples were loaded via a Symmetry C18 5 µm, 180 µm x 20 mm trap column and separated through a HSS T3 C18 1.8 µm, 75 µm x 150 mm analytical column. Peptides were eluted using a 3 % to 40 % acetonitrile 0.1 % formic acid gradient over 40 min at a flow rate of 300 nL/min.

MALDI creates ions using a matrix that can absorb energy from a laser. It ensures a minimal amount of fragmentation occurs. The mixed sample was combined with the applicable matrix (HSS T3). The mass spectrometer was operated in positive ion mode with a capillary voltage of 3.25 kV, cone voltage of 30 V and a source offset of 80 V.

A pulsed laser penetrates the sample which causes desorption and ablation of the matrix and sample. The last step involves the protonation or deprotonation of the analyte before being accelerated into the mass spectrometer. TOF (Time of Flight) mass spectrometry materialises as different sized ions are formed on a sample slide. Lighter ions with a small m/z value and ions with a higher charge have a higher velocity through the drift space until they reach the detector. (Aparna C.H., 2015). Mass spectra would have been collected, over 50–2000 m/z, alternating between low (4 eV) and elevated (15–45 eV) collision energies at a scan speed of 0.5 s. ConSurf server was the computational analysis used (Ashkenazy et al., 2016).

Chapter 3

Results:

Verification of the *rps-2* mutant

In this project, we were interested in investigating the role of the small ribosomal protein, *rps-2,* in the accuracy of translation. We began by identifying the relevant gene of interest and establishing its ability to receive two missense point mutations A494G, C495T. Once multiple mutant strains had been validated through the use of genotyping PCR (as specified in the 'Methods' - Chp. 2.3.3-2.3.4), strain COP872 was chosen to represent the *rps-2* mutant and COP876 was picked to represent the non-mutant control stain. These strains were then outcrossed three times to ensure the backgrounds of the strain from Knudra and the in-house strain are the same.

3.1 Identification of the *rps-2* gene in *C. elegans* and the generation of mutant strains

To explore *rps-2* in our model nematode, the gene must be conserved within humans. This is important to ensure findings can be reproduced in the future within a human genome. It has been recognised that missense mutations affiliated with inherited human diseases are prevalent at highly conserved genomic regions, this has been seen in the likes of rodents studies (Huang et al., 2004). Conclusions drawn from these experiments can contribute to identifying age-related illnesses inherent to the pathway of translation.

We began by confirming if the mRNA sequence stored in the Tullet lab from *C. elegans* accurately contained the *rps-2* gene of interest. To do so, the generated sequence was run through the Basic Local Alignment Search Tool (BLAST) software. With the ability to search through a biological database to find similar sequences, BLAST confirmed the mRNA we retained was *rps-2*.

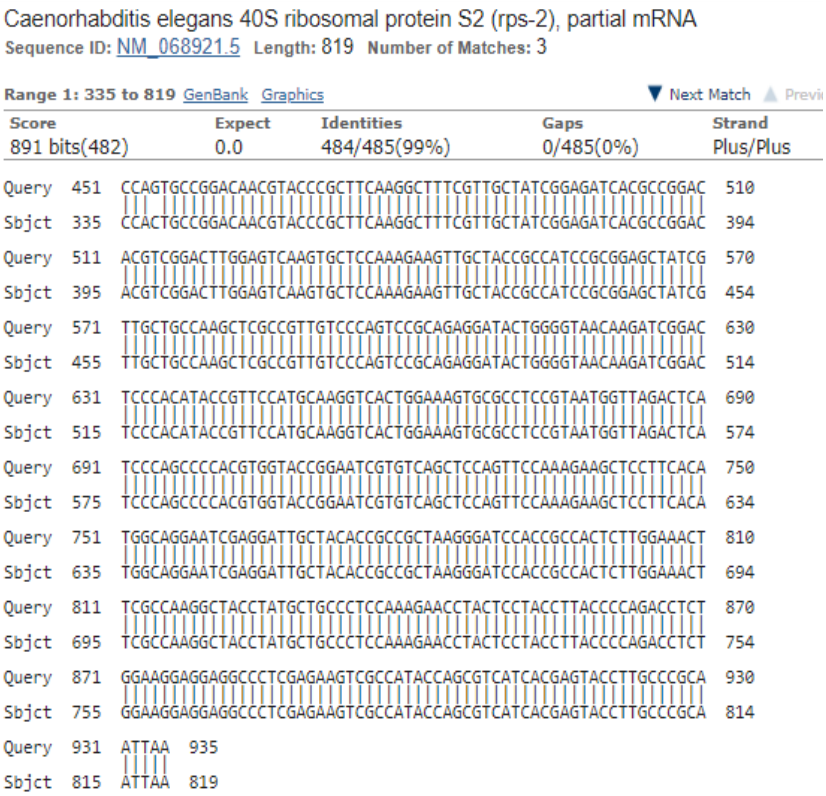

Figure 15 BLAST search that identifies the bases pertaining to the small ribosomal protein. This proved to be a correct match to Caenorhabditis elegans 40S ribosomal protein (*rps-2*). The alignments showed 819 nucleotides conceptually coding for 272 amino acids. The sequence possessed an E-value of 0.0, significantly validating the sequence for with research. 'Query' – the input nucleotides sequences; 'Sbject' – the nucleotides sequences in the database.

From the mRNA obtained and 819 nucleotides found (Fig. 15), the bases needed to be pinpointed using WormBase, an online biological database, to the correct exons of *rps-2*.

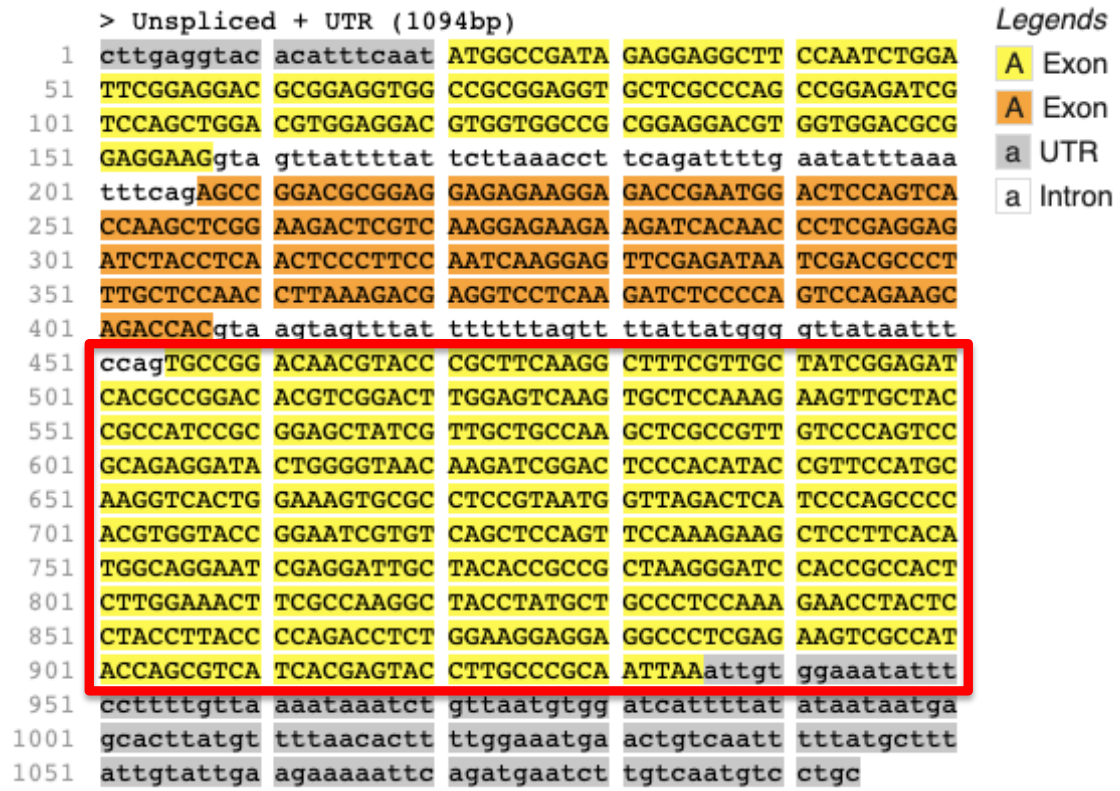

Figure 16 WormBase unspliced 1094bp sequence that displays all exons and introns and UTRs (untranslated regions) of *rps-2*. This was compared to the sequence from BLAST that disclosed the mRNA obtained in the lab corresponds to the third exon of *rps-2* only (boxed in red).

3.2 Verification of the Pam-1 site mutation found adjacent to *rps-2* mutant

Knudra Transgenics, a genome engineering company specialises in custom-built transgenic model organisms for research and drug discovery. The construction of a missense mutation relies on the process of CrispR carried out by the Knudra lab. The operation requires the presence of a protospacer adjacent motif (Pam-1) site that the Cas9 enzyme can recognise located in close proximity to the base to be mutated.

To check the presence of a suitable Pam-1 site, the *rps-2* sequence from BLAST was analysed with ApE (A plasmid editor) software. A restriction site that could be used for annealing when constructing primers were also inspected. This is necessary to confirm if Knudra can complete the procedure accurately. It is understood that the Pam-1 site does not increase the contingence the mutation however the lack of a Pam-1 site in close proximity to the mutation may result in the CrispR method to being viable. This verification step proved important since it indicated the capability of inserting a mutation through CrispR (as specified in the 'Methods' - Chp. 2.3.1).

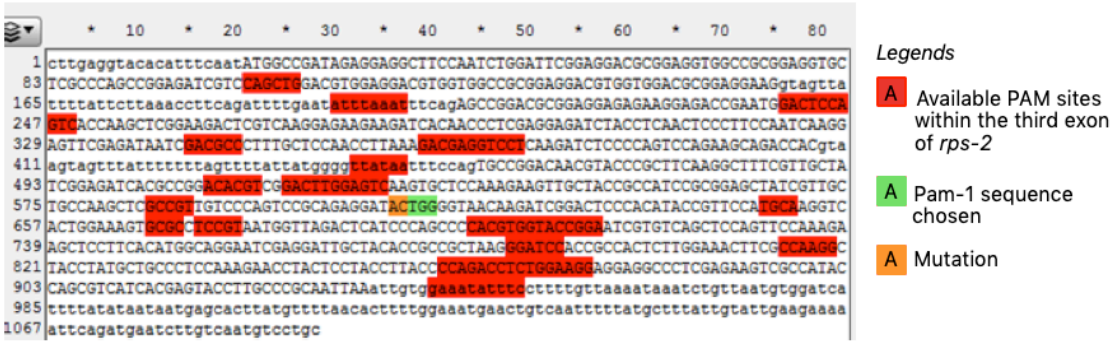

Figure 17 ApE, a plasmid editor, is used to display the sequences. The mutation is highlighted in orange followed by the CRISPR/Cas9 specific Pam-1 sequence 5'-NGG-3' (https://www.addgene.org/crispr/guide/), here it is 5'-TGG-3' in green. The location of the Pam-1 site adjacent to the mutation increases the confidence that the mutation is present in the given strains from Knudra. Restriction sites of unique enzymes are highlighted in red to display possible target for primers surrounding the mutation ('Methods' - Chp. 2.3.1).

3.3 Using BLAST to evidence the position of the *rps-2* mutation

Knudra provided five mutated strains of *C. elegans* via CrispR (outlined in 'Methods' - Chp. 2.3.1)), named COP872, COP873, COP874, COP875 and COP876. The mutation chosen to incorporate into *C. elegans* was a tyrosine (Y) to cysteine (C) residue, found in the third exon of *rps-2*. This is the same Y143C mutant observed in SUP38-5 variant during *Rps-2* protein studies with previous *S. cerevisiae* studies (Haar, T.V.D. et al., 2017). The genes are conserved in both organisms.

To verify the strains, all five strains were sequenced with GATC Biotech (see Method 2.3.3). The process of sequencing confirmed the work that has been completed externally by Knudra. After running PCR protocols, the PCR products were cut out of the 1% agarose gels and purified using Thermo Fisher's Purification Kit (see Appendix). When the sequencing information returned, three of the five strains created by Knudra possessed the mutation; COP872, COP873 and COP875 (Fig. 18).

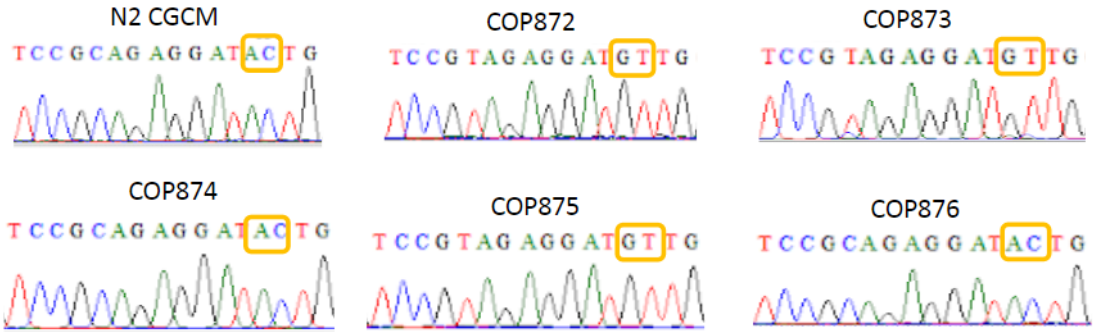

Figure 18 GATC Biotech sequencing chromatogram Wild type worms (N2) and the five strains retrieved from Knudra, COP872, COP873, COP874, COP85 and COP876. Clear peaks are colour coded according to the bases and are shown with limited background noise. Mutations can be seen in COP872, COP73 and COP875, circled in yellow.

The sequences provided from GATC BioTech were analysed with BLAST to observe how the whole *rps-2* gene compares to the human genome we are already familiar with. Sequences were placed in the BLAST database. Findings validated this by also showing missense mutations in three of the five sequences, however, BLAST also revealed a sense mutation in COP875.

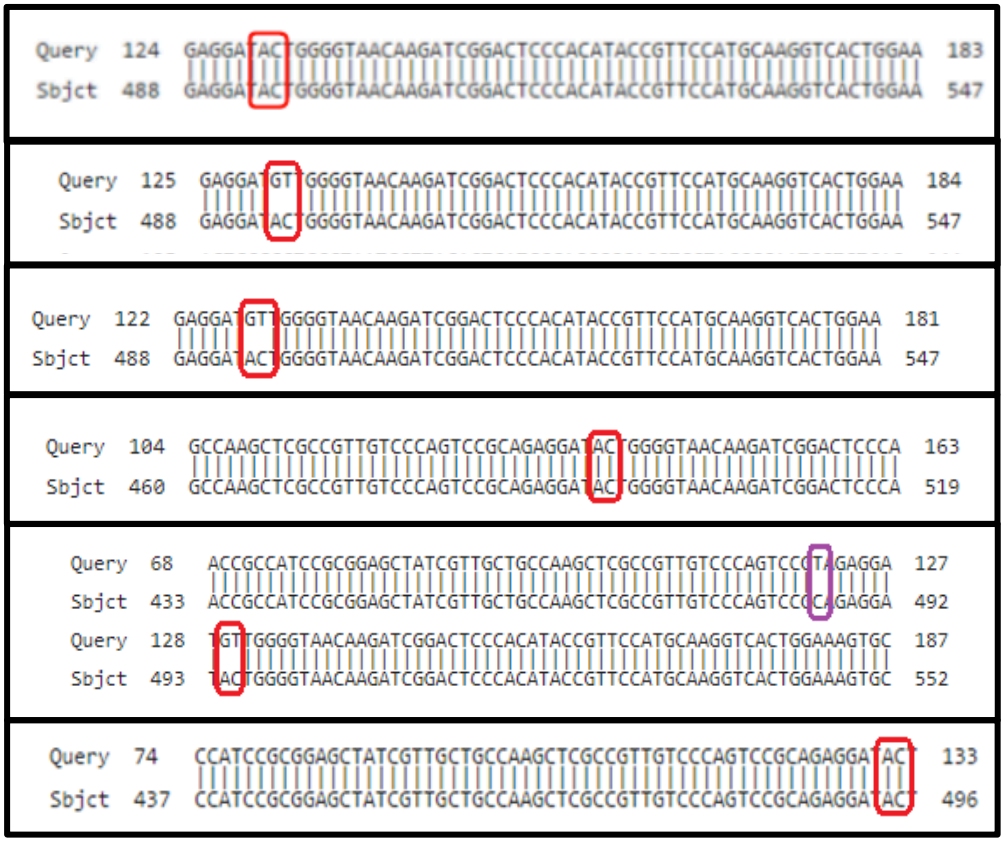

Figure 19 BLAST Sequence alignments (top – wild-type N2, second – COP872, third – COP873, fourth – COP874, fifth – COP875, bottom – COP876). Red square highlights where the bases are in *rps-2*. COP872, COP873, COP875 have mutated bases seen with a missense point mutation A494G, C495T in the query sequence. N2, COP874 and COP876 have AC bases, no change to the nucleotide sequence. An additional sense mutation, C486T, was found highlighted in purple in COP875. (see Appendix for full alignment and E-values).

The resulting effect of these missense mutations is the formation of a thiol containing cysteine residue in place of an aromatic tyrosine amino acid. This can be seen in the nucleotide to protein BLAST.

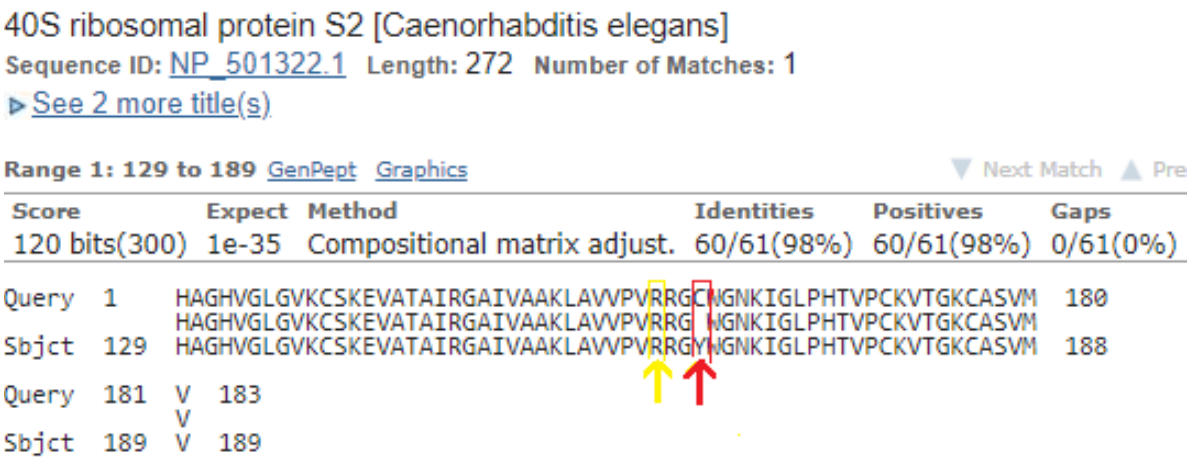

CAC	H	GTC	V	ACC	T	GCT	A	GTC	V	AAG	K	CCA	P	GCC	A
GCC	A	AAG	K	GCC	A	GCC	A	CGT	R	ATC	I	TGC	C	TCC	S
GGA	G	TGC	C	ATC	I	AAG	K	AGA	R	GGA	G	AAG	L	GTA	V
CAC	H	TCC	S	CGC	R	CTC	L	GGA	G	CTC	L	GTC	V	ATG	M
GTC	V	AAA	K	GGA	G	GCC	A	TGT	C	CCA	P	ACT	T		
GGA	G	GAA	G	GCT	A	GTT	V	TGG	W	CAT	H	GGA	G		
CTT	L	GTT	V	ATC	I	GTC	V	GGT	G	ACC	T	AAG	L		
GGA	G	GCT	A	GTT	V	CCA	P	AAC	N	GTT	V	TGC	C		

Figure 20

Top: BLAST Sequence alignment of amino acid residues with the mutation from the third exon. Bottom: Reading from up to down. The degenerate nature of the amino acid code has revealed the silent mutation, C486T, found in COP875 has no effect on the protein sequence (labelled in yellow). The missense mutations, A494G, C495T, resulted in the mutation Y165C. [UniProt]

```
        10          20          30          40          50
MADRGGFQSG FGGRGGGRGG ARPAGDRPAG RGGRGGRGGR GGRGGRAGRG
        60          70          80          90         100
GEKETEWTPV TKLGRLVKEK KITTLEEIYL NSLPIKEFEI IDALCSNLKD
       110         120         130         140         150
EVLKISPVQK QTTAGQRTRF KAFVAIGDHA GHVGLGVKCS KEVATAIRGA
       160         170         180         190         200
IVAAKLAVVP VRRGYWGNKI GLPHTVPCKV TGKCASVMVR LIPAPRGTGI
       210         220         230         240         250
VSAPVPKKLL HMAGIEDCYT AAKGSTATLG NFAKATYAAL QRTYSYLTPD
       260         270
LWKEEALEKS PYQRHHEYLA RN
```

```
        10          20          30          40          50
MADDAGAAGG PGGPGGPGMG NRGGFRGGFG SGIRGRGRGR GRGRGRGRGA
        60          70          80          90         100
RGGKAEDKEW MPVTKLGRLV KDMKIKSLEE IYLFSLPIKE SEIIDFFLGA
       110         120         130         140         150
SLKDEVLKIM PVQKQTRAGQ RTRFKAFVAI GDYNGHVGLG VKCSKEVATA
       160         170         180         190         200
IRGAIILAKL SIVPVRRGYW GNKIGKPHTV PCKVTGRCGS VLVRLIPAPR
       210         220         230         240         250
GTGIVSAPVP KKLLMMAGID DCYTSARGCT ATLGNFAKAT FDAISKTYSY
       260         270         280         290
LTPDLWKETV FTKSPYQEFT DHLVKTHTRV SVQRTQAPAV ATT
```

Figure 21 UniProt sequences of *rps-2* from *C. elegans* (top) and humans (bottom). The sequences have been slightly shifted in humans but remain relatively the same. The conserved residue is highlighted in green TYR165 in *C. elegans* and TYR169 in humans. The folding structure can be seen in Fig. 5.

3.4 Defining a method to genotype *rps-2* mutant strains using PCR

The most efficient method to easily differentiate between mutant and wild-type strains in vitro is to implement polymerase chain reactions with bespoke primers. We decided to make primers to efficiently distinguish between mutant and wild-type nematodes. To design these primers we used ApE.

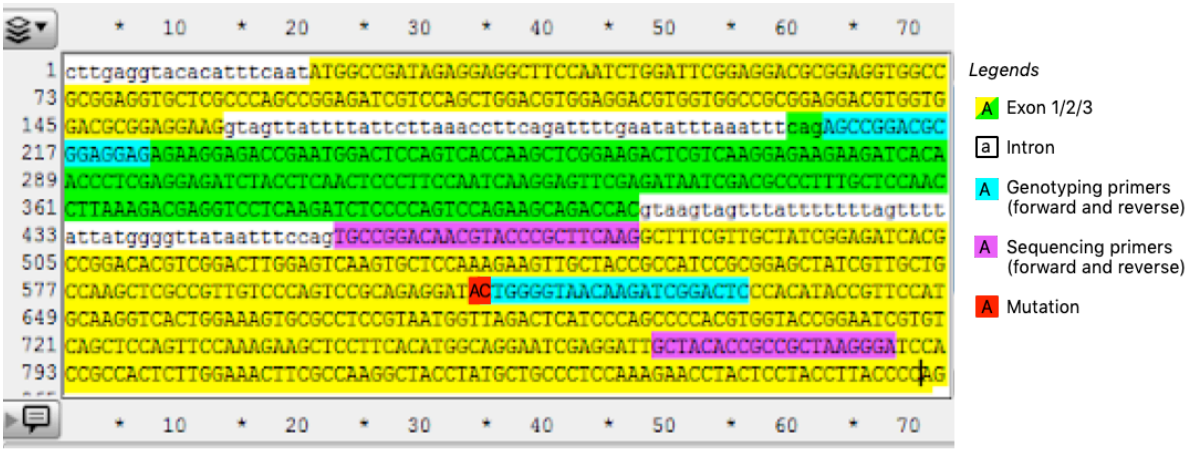

Figure 22 ApE file of *rps-2* Forward genotyping [5' → 3': CAG AGC CGG ACG CGG AGG] and reverse genotyping [5' →3': GAG TCC GAT CTT GTT ACC CCA GT] primers are used to genotype *rps-2* (blue). The 3' end of the genotyping primer [GT] matches with the end of the mutation highlighted in red. Forward sequencing [5' → 3': TGC CGG ACA ACG TAC CCG CTT CAA G] and reverse [5' → 3': GGA TCC CTT AGC GGC GGT GTA GC] primers (pink) and the 3 exons found in *rps-2* (yellow - exon 1, green - exon 2 and yellow - exon 3).

Two different reverse genotyping primers are created that differ only in the last two bases. The reverse primer will only anneal if the sequences match. If the primer anneals, a band will be formed that is 426bp in size.

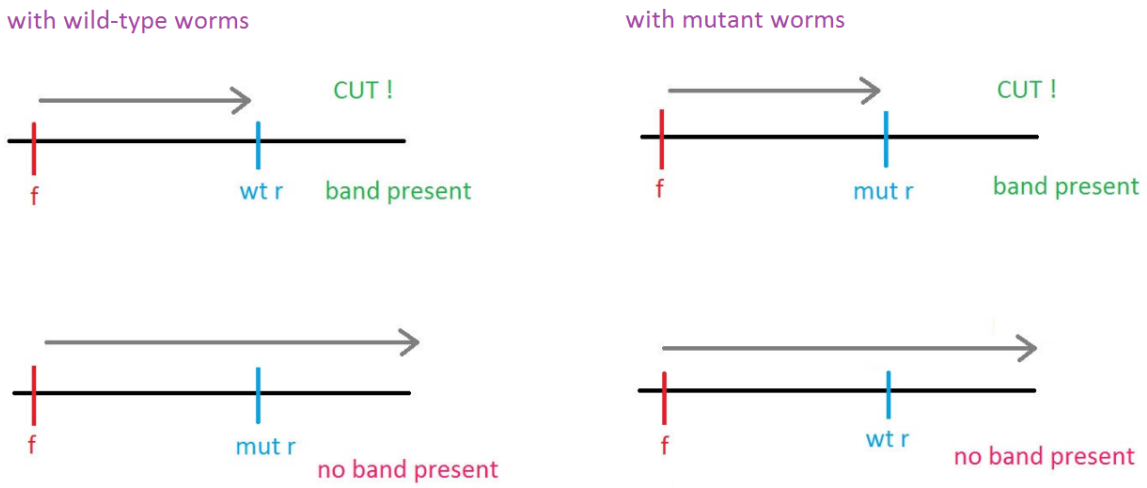

Figure 23 Schematic of customised primers Diagram explaining the presence of bands on a DNA gel depending on the primer used. Top left: when using a wild type reverse primer in the presence of a wild type worm a band will be produced. Bottom left: when using a mutant reverse primer in the presence of a wild type worm the primer will not anneal and therefore the polymerase will not stop and a band will not be made. Top right: when using a mutant reverse primer in the presence of a mutant worm a band will be produced. Bottom right: when using a wild type reverse primer in the presence of a mutant worm the primer will not anneal and therefore the polymerase will not stop and a band will not be made. f = forward primer, wt r = wild type primer, mut r = mutant primer. 'CUT!' represents the action of a restriction enzyme making an incision at the primer when the appropriate reverse primer anneals, as mentioned above the primer will only anneal if the sequences match following this the PCR reaction can continue and bands will be produced.

All primers were made and delivered by Invitrogen, Thermo Fisher Scientific (see Appendix). Upon receiving these primers, PCR experiments were completed. Initially, a gradient PCR was used to find the optimum annealing temperature of 71°C (detailed in the 'Methods' - Chp. 2.3.3). Mutant primers were used as well as wild type primers for two different primer mixes. In the presence of a mutant primer, the mutant strain produced a band at 426bp whilst the wild-type strain produced no band.

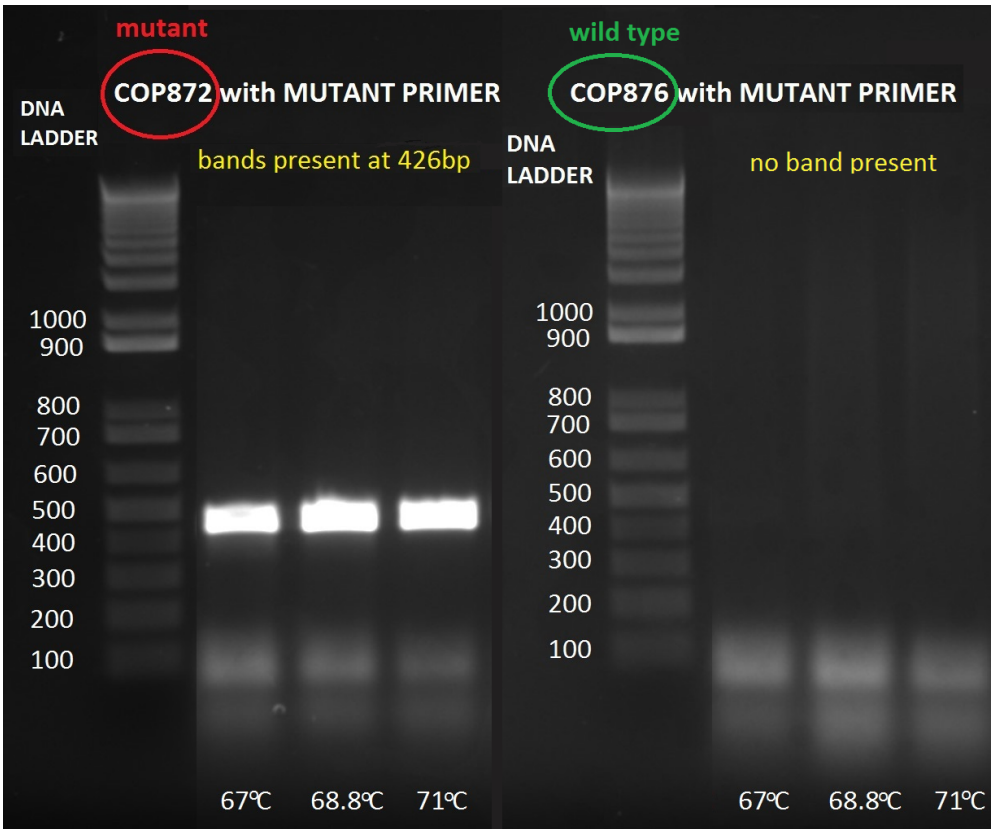

Figure 24 A gradient PCR of DNA gels at temperatures 67 °C, 68.6 °C and 71 °C of (left) COP872 (an identified mutant worm) with a mutant primer that produced a band at 426bp and (right) COP876 (an identified wild type worm) that did not make a band with the custom primer. Background noise is seen around 100bp.

Chromatograms from sequencing had shown that COP872, COP873 and COP875 are mutants however when using the customised genotyping primers a 426bp band should be present in the lane labelled 3 (COP873) but it isn't. This was repeated five times and these results were repeated (Fig. 25)

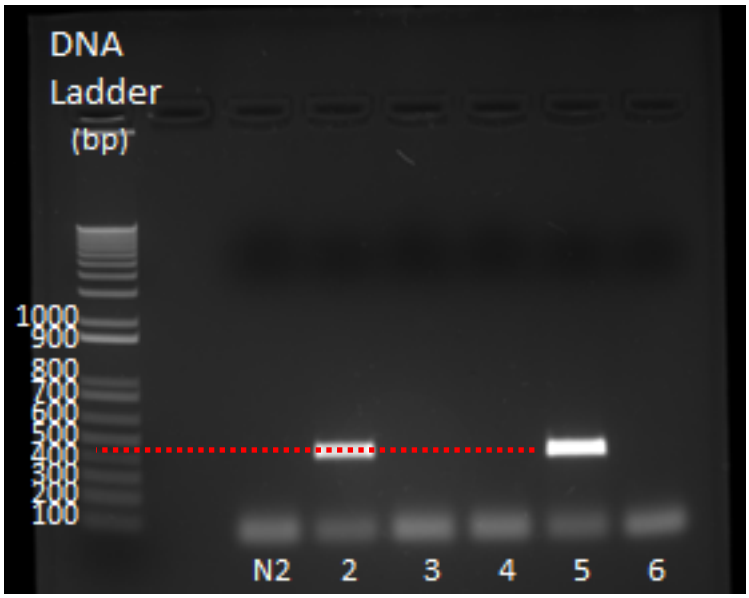

Figure 25 Single worm Genotyping PCR completed at 71°C with the mutant primer. Bands are seen at 426bp (dotted red line) in COP872 and COP875, to show that in the presence of the mutant primer cDNA is formed using DNA from within these worms.

This shows that of the three strains that contain the mutation, COP873 produces a false negative result. The missense mutation is in the COP873 strain but is not shown in PCR reaction. After completing the previously mentioned validation and confirmation experiments, from the two remaining strains, COP872 was selected to outcross for further investigation. This removes the chance of any additional mutations arising during laboratory experimentation since mutagenesis can potentially modify other genes that are not of interest influencing data retrieved (Corsi, 2006).

For the duration of succeeding experiments mentioned in this paper, only the authorised COP872 strain is used. The COP875 strain that was also confirmed to be a mutant was stored at -80 °C.

The COP876 strain was used at multiple times as a "strain control" since it was also produced from Knudra but did not receive the mutation. COP876 should always produce the same results as our N2 wildtype since it also does not have the *rps-2* mutation. If disparities are seen between N2 and COP876, this may indicate anomalies in the CrispR technology Knudra performed, affecting the strain in a divergent manner.

After outcrossing the animals, the single worm PCR was produced from F2 plates (Fig. 26) to identify the mutant *rps-2 -/-* that correlated with the bands seen at 426bp identical to Fig 25.

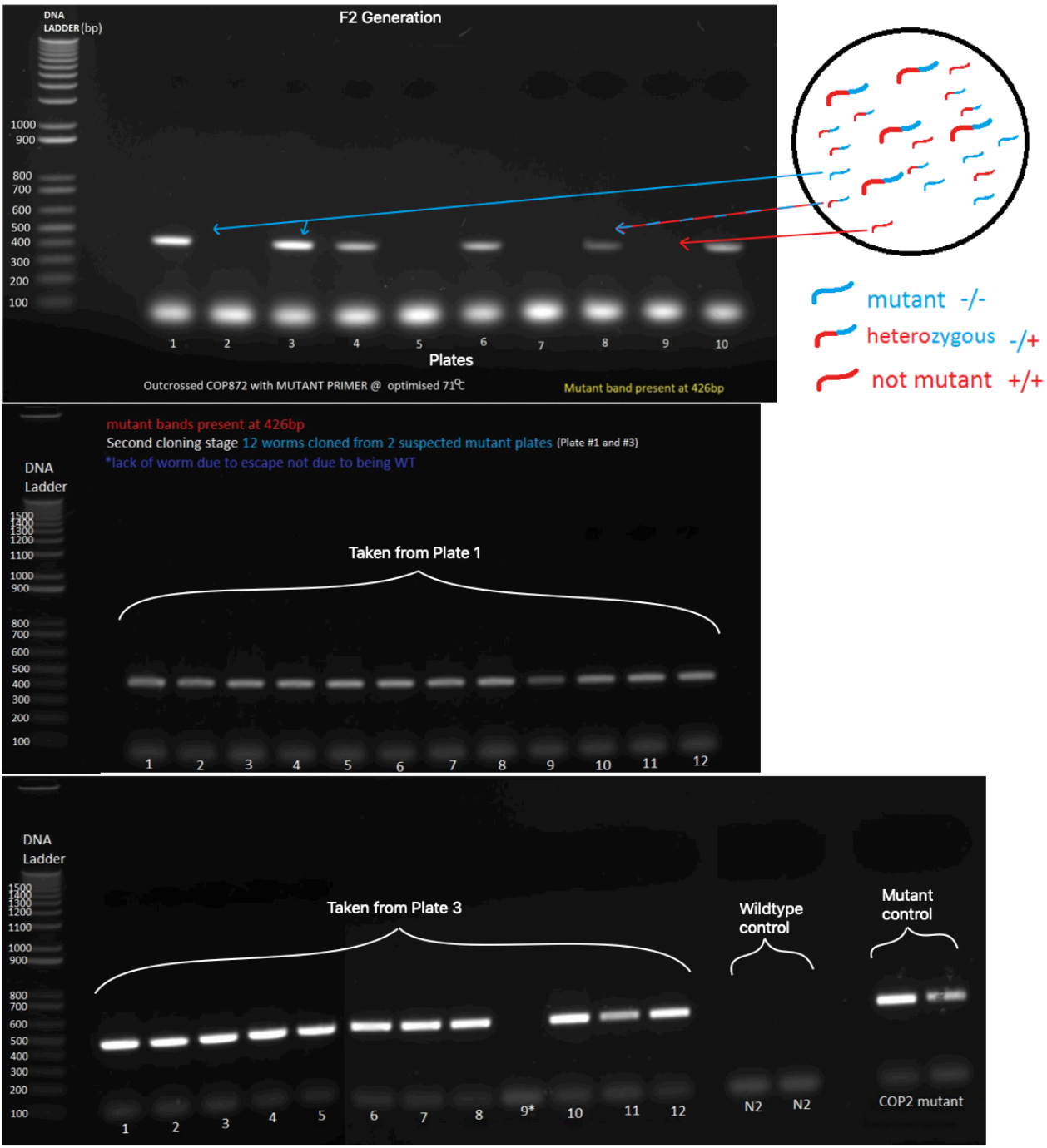

Figure 26 Genotyping PCRs confirmed the new progeny from the F3 generation contained the *rps-2* -/- mutation, all completed at 71°C with the mutant primer

Top: Genotyping PCR from worms in the F2 generation, containing a mixture of genotypes.

Middle: Single worm genotyping PCR from the F3 generation of plate 1 revealed all progeny contains the mutation with 426bp present.

Bottom: Single worm genotyping PCR from the F3 generation of plate 3 revealed all progeny contains the mutation with 426bp present as a bright band. The single worm in plate 9 was lost. A wild type control was used as well as a mutant control obtained from the previous outcross.

Different *rps-2* variants do not present themselves in various phenotypes, therefore, the progeny of each worm in the F2 generation underwent multiple reactions to identify the correct phenotype. Worms on plates 1 and 3 were cloned out since their bands were very prominent and clear on the 1% gel. The progeny was re-plated onto 10 separate plates to produce the F3 generation and then PCR reactions were conducted with these. For the outcross to be deemed successful, 100% of the population had to produce a 426bp band (Fig. 26). This whole process is usually repeated six times to ensure the *rps-2 -/- is* present in our *C. elegans* population.

Chapter 4

Results:

Biochemical investigations of proteins associated with the *rps-2* mutation

We have now produced a genetically compatible group of worms to work with, COP872. To understanding how translational accuracy is affected by the presence of the *rps-2* mutation we looked at the global production of a yolk protein, one of the most abundant proteins in *C. elegans*. Yolk bands are seen in all nematodes at 170kDa, 115kDa and 70kDa (Sharrock, W. J., 1983) and was chosen since it would be able to produce clear bands on an SDS gel.

We also considered how the production of the yolk protein will be altered in the presence of an error inducing drug. Paromomycin was used in previous studies with *S. cerevisiae* however after noticing batch differences in this drug, Nourseothricin sulphate a similar acting aminoglycoside antibiotic was used instead.

Combining the information collected from differences seen in the production of yolk protein under the influence of an error inducing drug in wild type worms vs. mutant should show reveal an increased drop in protein production within the COP872 mutant strain. Both the NTC treatment optimisation and yolk protein quantification assay took place simultaneously.

4.1 Observed increase in yolk protein concentration as nematodes age

Proceeding to look at differences within yolk protein from worms, with and without the mutation, we decided to harvest as much naturally occurring yolk protein from each genetic background. We observed our N2 strain (wild type), the COP876 strain (control) and COP872 (mutant).

In an attempt to harvest the most yolk protein, an aging worm assay was implemented. This revealed the age that would produce the most protein for research. The darker stained the band the more protein is available.

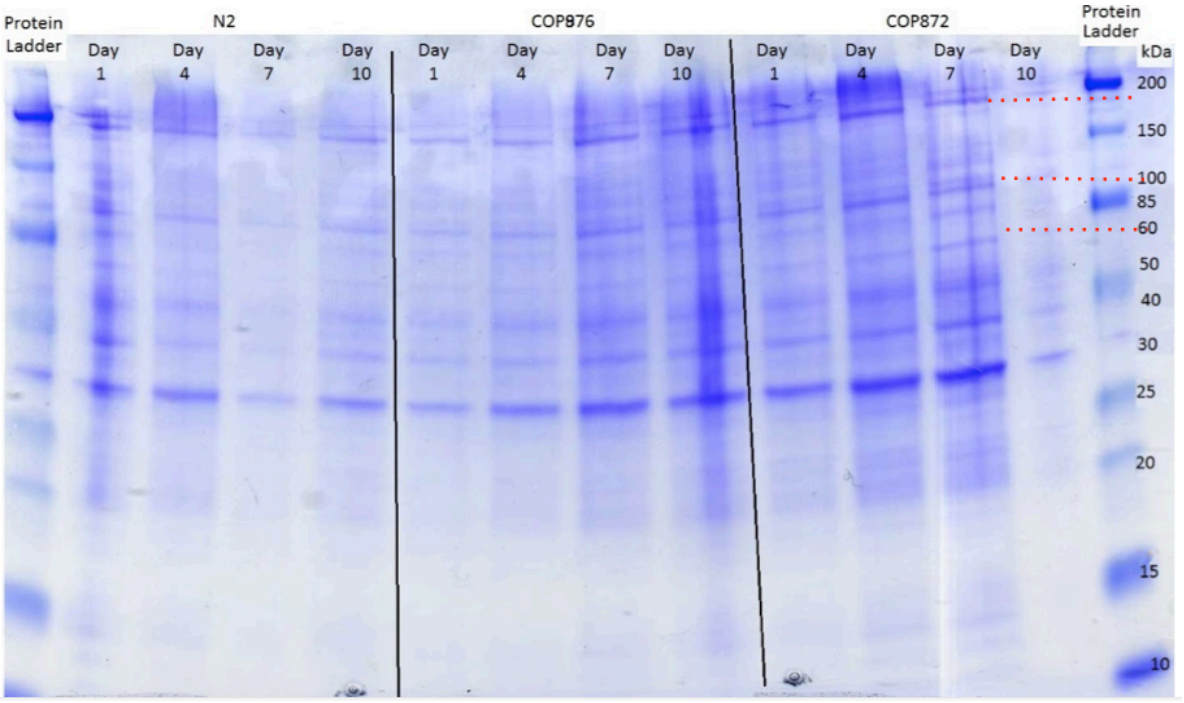

Figure 27 Coomassie stained SDS PAGE gel shows the increase in yolk protein indicated by the prominence of the 170kDa, 115kDa and 70kDa bands. Yolk bands are highlighted with a red dotted line.

Yolk bands gradually become 'darker' in colour as the worms aged, apart from COP872 - day 10, compared to our controls of N2 and COP876. The absence of a band for COP872 was seen constantly during experimental repeats, Fig. 27 is the only gel that produced prominent bands.

4.2 Obtaining the lethal dose of Nourseothricin sulphate (NTC)

To also observe the effect the *rps-2* mutation can have on protein production on a molecular level, the action of NTC was investigated. NTC reduces translational accuracy by inhibiting biosynthesis and inducing miscoding (Krügel, et al., 1993), working similarly to aminoglycoside antibiotics, it inhibits steps of protein synthesis. NTC has a wide field of action against prokaryotic species and has been seen to inhibit growth in eukaryotes such as *Cryptococcus neoformans* and *Saccharomyces cerevisiae*. The suitable NTC concentration to inhibit viability in *S. cerevisiae* studies is 100 µg/ml (Sigma Life Science Data Sheet) where growth is affected at 2 µg/ml. Studies with *S. cerevisiae* formed the initial basis of this research (as outlined in 'Introduction' 1.2.4' Accordingly we decided to consider the effect of NTC on *C. elegans* (Haar, 2017).

We hypothesised that administering NTC would reduce the translational accuracy within the tested nematodes. We would expect the combined effect of the *rps-2* mutation disrupting translation as well as the known effect of NTC would decrease viability. Before using NTC, the optimum dose for wild type *C. elegans* needed to be recognised since yeast concentrations will be completely irrelevant for what works in worms. This ensures we are not using a concentration that is too high to kill the nematodes and simultaneously find a tolerable concentration that is high enough to make a significant difference to the accuracy of translation. This concentration was established by conducting a drug assay titration on wild type worms ('Methods' – 2.4.1).

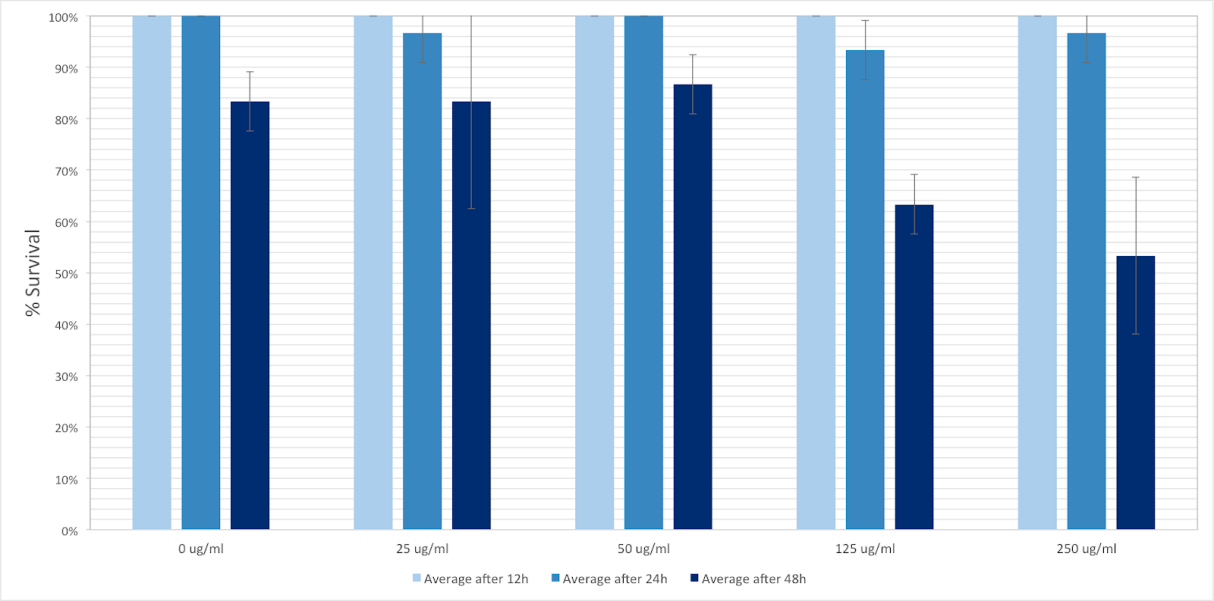

Figure 28 Bar graph to show the average dose of NTC used to have a significant reduction in the survival rate of wild-type worms. The lethal dose was not obtained after 48 h. Results averaged from 3 experiments +/- 1 S.D.

We were able to acknowledge that the concentration of 125 µg/ml proved to be practical to use, as it was seen to have an effect on the survival of *C. elegans*, however, after using R programming and completing ANOVA tests and applied Tukey's test, none of the results produced significant conclusions (See Appendix for data). ANOVA is used to find how different two or more samples are, whilst Tukey HSD is completed *after* ANOVA, to pinpoint what these samples are. As well as not being able to obtain a lethal dose, failing to extract yolk bands from these samples after repeating the experiment five times led to the analysis of another protein found in *C. elegans,* myosin.

4.3 Extraction of myosin-4 may show a difference in its integrity that could have been caused by translational inaccuracies

Observing the bands from the yolk protein in the gel proved to be difficult. After continuous failed attempts to duplicate this experiment and extract yolk proteins, myosin bands were harvested instead. Myosin light chain is approximately 20kDa in weight whilst myosin heavy chain is just over 220 kDa in weight (WormBase ID: WBGene00003369; WBGene00003514). Myosin is recognised to be abundant in nematodes due to their role in muscle contraction, therefore, making it easier to harvest large quantities of protein for research. Before extracting myosin from our COP72 strain, myosin had to be extracted from the wild type strain (‘Methods’–2.5.4).

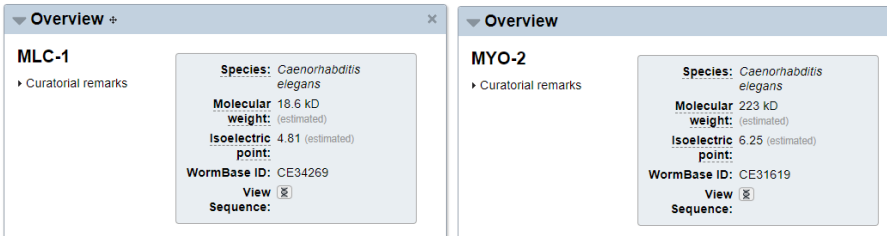

Figure 29 WormBase overview of myosin light and heavy chains Molecular weights of both proteins are outlined. Protein sequences detailed in the ‘Appendix’ [WormBase].

To extract myosin from wild-type worms, a unique protocol is followed (‘Methods’ - Chp. 2.5.2). Nonetheless, only a small amount of myosin was obtained. This is seen as a very faint band on the stained SDS gel (Fig.30). The myosin protein sample was excised with a scalpel, tryptic digested and inspected with mass spectrometry (‘Methods’ – 2.5.2-2.5.4).

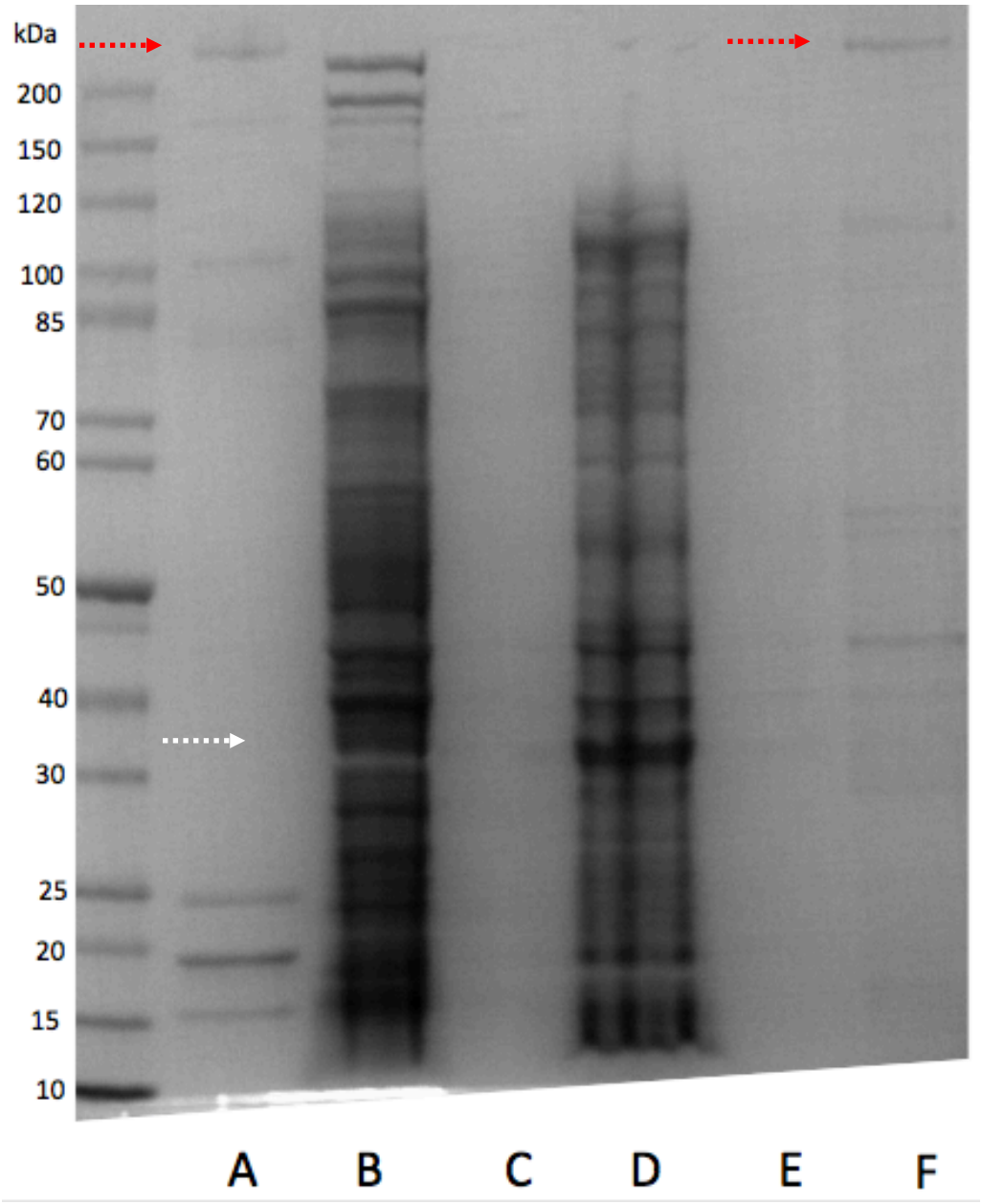

Figure 30 Coomassie stained SDS PAGE gel and stages for myosin extraction. Each stage of the myosin extraction was kept and run on an SDS PAGE to "follow" the protein through the stages. Unlabelled lane – protein ladder,

Lane A - Myosin control

B - Supernatant after lysis

C - Supernatant after lysis and wash with Guba

D - Pellet after washing

E - Supernatant after extracting myosin

F - Sample containing myosin.

Red arrow indicates heavy myosin chains seen in the control and sample at 223kDa. White arrow indicates light myosin chain at 18.3kDa only observed in the control sample.

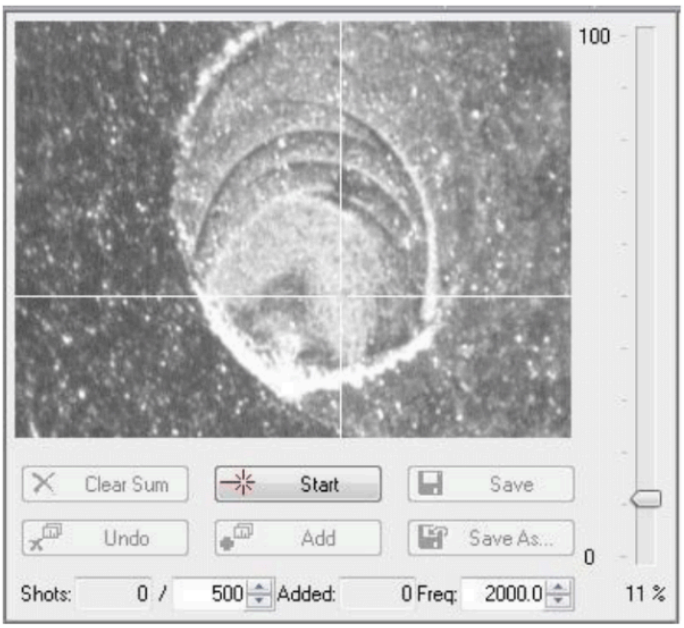

Figure 31 Atypical crystallisation of sample collected, identified as myosin heavy chain orthologue, myosin-4 from *C. elegans*.

The only successful protein sample produced a peptide mass fingerprint that was used to search the UniProt SWISS-PROT database via the MASCOT search engine. The 15 most intense peptide masses were then subject to further analysis by MS/MS and this data searched against the same database. For eukaryotes, a peptide mass fingerprint might not identify the protein, but the MS/MS often will. The HDD of the mass profile was not obtained which could have indicated if the myosin preparation was successful.

The atypical nature of the crystallisation from our sample meant no further investigation could be completed with here, however, more samples obtained through repeating this process are currently awaiting results.

Chapter 5

Results:

Phenotypes associated with the *rps-2* mutation

5.1 Life span assay does not show a significant difference between wild type and *rps-2* mutant strains

Life span assays were completed to monitor the lifespan of the nematodes and detect if the presence of the *rps-2* mutation will have a significant effect on the survival of the organisms. This looks at the global effect of the induced mutation. Trials compared two types of wild type N2 - one wild type with a background from the *Caenorhabditis elegans* Genetics Centre Male (CGCM) stock and the other with a background from the *Caenorhabditis elegans* Genetics Centre Hermaphrodite (CGCH) stock. CGCH nematodes are slightly short-lived in comparison to the CGCM variant line and therefore we should see the numbers of N2 CGCH reduce to zero before the N2 CGCM strain (Gems et al., 2000). This acts as another wild type control during experimentation. Each strain was trialled five times for approximately 20 days at 20°C ('Methods' - Chp. 2.4.3 for full protocol).

A

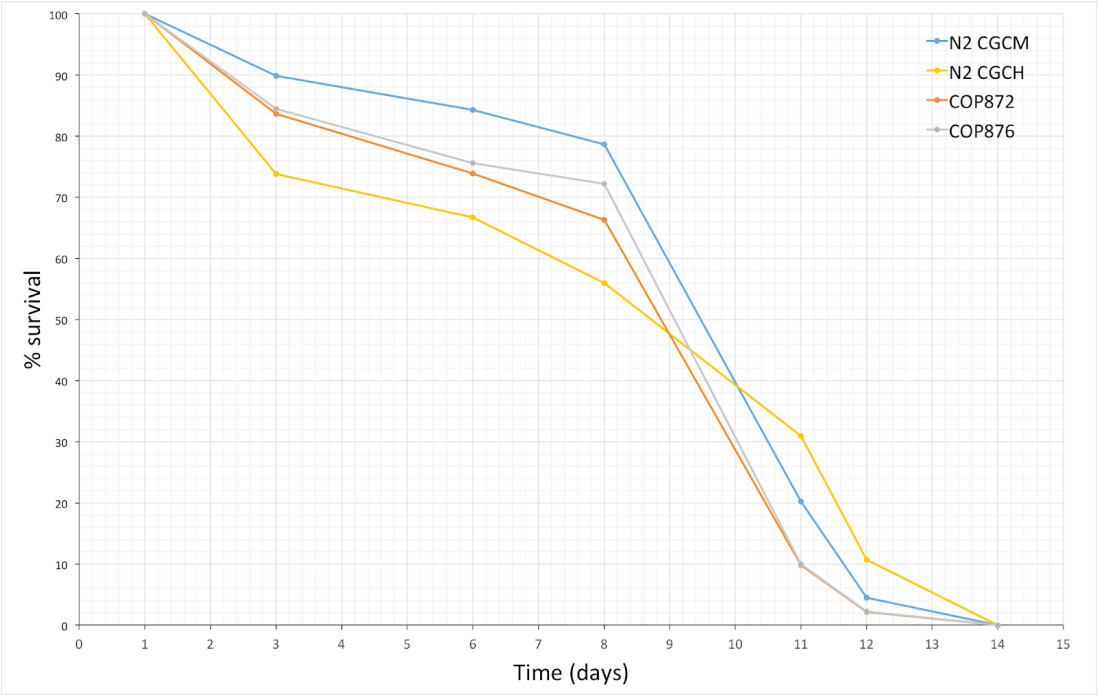

Figure 32 *Legend continued overleaf*

B

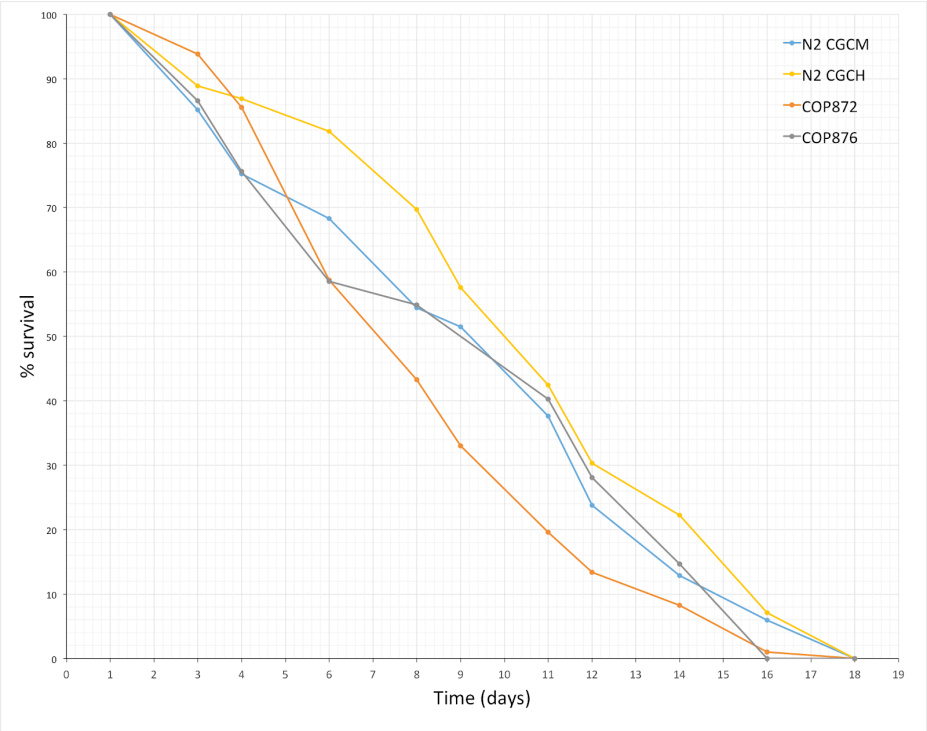

C

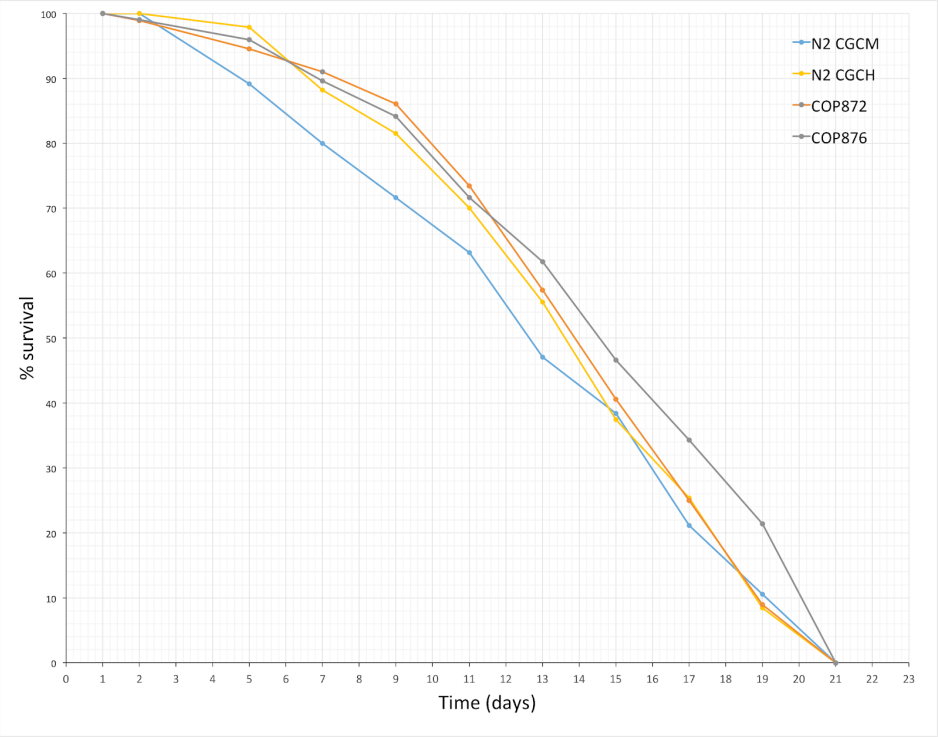

Figure 32 Life span survival curves Three survival curves obtained from trials show inconsistent results between N2 CGCM (blue line), N2 CGCH (yellow), COP872 (orange) and COP876 (grey). Significant result: p value < 0.05

(A) N2 CGCM vs COP872: p = 0.0197

(B) N2 CGCM vs COP872: p = 0.0318, N2 CGCH vs COP872: p = 0.0001

(C) N2 CGCM vs COP876: p = 0.0303, N2 CGCH vs COP876: p = 0.0866.

Statistical analysis were completed using Log-Rank Test via OASIS: Online Application for the Survival Analysis of *Lifespan* Assays Performed in Aging Research. Protocol outlines in 'Methods' – Chp. 2.4.3.

The life span assays completed produced a range of different shaped curves that were interpreted. Whilst (A) and (B) shows 50% survival at approximately 9 days and (C) has 50% survival at approximately 14 days. Data representing N2 CCGH in graphs (A), (B) and (C) are not short-lived compared to N2 CGCM which may reveal an issue with the technique used to count lifespan or laboratory environment.

5.2 Brood size assay does not show a significant difference between wild type and mutant strains

Measuring the fecundity of the variant strains, N2 CGCH, N2 CGCM, COP872 and COP876 is another physiological assay implemented to identify differences caused by the *rps-2* mutation. Testing N2 CGCH was not mandatory here since all animals tested were hermaphrodites, however it is also recognised for the CGCH background to have a slightly lower brood size in comparison to N2 CGCM (Gems et al., 2000). Brood size assays reveal how many live progeny one adult worm can produce. The adult worm was placed at 20^{o}C with an abundance of OP50, ensuring food was not a limiting factor (see 'Methods' - Chp. 2.4.4). Over an average of four days, the adult nematode had laid all eggs onto plates that were periodically counted. It was hypothesised adult worms from the COP872 strain would have a significantly different, presumably lower, progeny size.

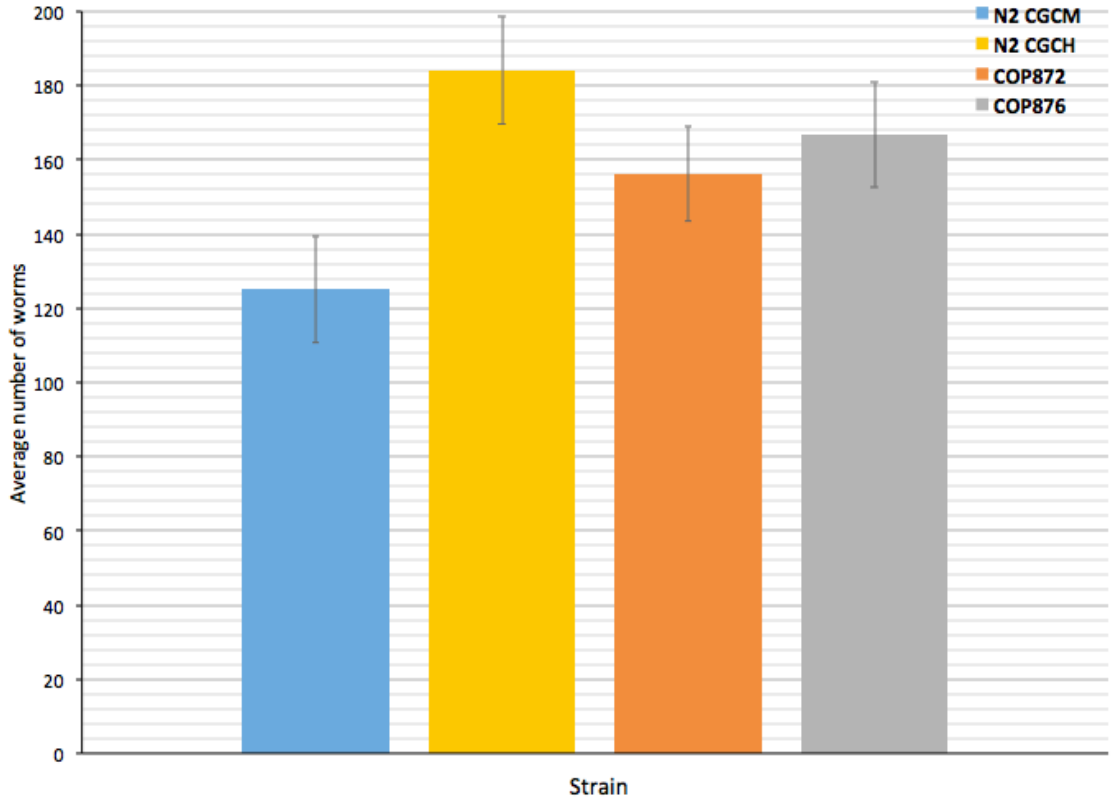

Figure 33 Average brood size assays compiled from five brood size trials. N2 CGCM (control - blue), N2 CGCH (yellow), COP872 (orange) and COP876 (grey) represent the average number of worms hatched. Statistical analysis were completed using a two-tailed T-test comparing how similar all samples are to each other. Significant result: p value < 0.05

None of the results from the five trials showed consistent significance when a two-tailed T-test was carried out indicated below. The overlap in error bars signify there is no significant difference between COP872 and COP876.

N2 CGCM	COP872
0.050721201	
N2 CGCM	COP876
0.272128891	
N2 CGCH	COP872
0.176801716	
N2 CGCH	COP876
0.111347091	
COP872	COP876
0.582768019	

Figure 34 P-values from statistical testing between strains from the brood size assay. All comparisons made were insignificant (> 0.05) shown as a red highlight.

Chapter 6
Discussion

Ageing has always been a fascinating topic. Our imagination fabricates 'fountains of youth' in children's stories, the beauty industry manufactures new anti-ageing serums and creams on a daily basis and there is a global rise in the use of BoTox, the injection that is renowned as "time machine for your face". The anti-ageing sector is worth over $50 billion, but there is still so much that is unknown about the process of ageing. ("Anti-Aging Market..", 2019)

One common factor we see about ageing is its relation to age related diseases. Ageing is seen as a risk factor for many illnesses, such as neurodegenerative diseases - Alzheimer's and Parkinson's. These illnesses are commonly referred to as 'protein misfolding' diseases since we have been able to detect an aggregation of misfolded proteins in the brain, tau protein or Lewy bodies, respectively (Selkoe, 2004). Inherited mutations from mitochondrial DNA has also been associated with the progression of Alzheimer's (Santoro et al., 2010). These findings suggest an issue with the essential steps of protein synthesis – transcription and translation. Literature has recorded that transcriptional errors caused by mutations have significantly increased the viability during the process of ageing (Rodríguez-Rodero et al., 2011, Haar et al., 2017).

This study was set in place to achieve three specific aims to investigate the role of translational accuracy in *C. elegans*. The first aim involved deciphering mechanisms that can be used to study translational accuracy in *C. elegans*. Customisation of genotyping primers that work for both mutant and wildtype nematodes were effective and revealed the mutation can definitely be distinguished at a basic genomic level – through the completion of an agarose PCR gel, worms can quickly be differentiated. This method is commonly seen throughout literature as an approach to type single nucleotide substitutions (Mamotte, C.D.S, 2006). Conservation between human *rps-2* and *C. elegans rps-2* genes were verified using sequence alignments. It has been journaled that *rps-2* is present as therapeutic cancer target (Wang, M. et al., 2009), however, the high conservation between the genes can lead us to deduce that *rps-2* has other indispensable roles that are related to ribosomal function. With a 70% similarity in genes between humans and *C. elegans*, findings made from experiments with the nematode can be reflected and use to form hypotheses directly related to humans. Upon completion of the NTC trial, where 125µg/ml was administered, various concentrations showed no significant difference to viability. It is distinctly understood *C. elegans'* outer cuticle (see 'Introduction' 1.1.1) has the potential to provide a barrier, inhibiting drug penetration, therefore, not having an initial effect on the worm. In addition, and as seen in other studies, the OP50 food source could metabolise the drug and

therefore impairing its uptake by *C. elegans* (Haar et al., 2017). Secondly, mutants were used to complete a number of biochemical investigations. Gel electrophoresis results did display a number of proteins that can be harvested for analysis however yielding a high enough quantity to do so proved to be problematic. Unfortunately, this led to atypical findings from the mass spectrometry read out.

Lastly, phenotypical assays were executed to recognise how the whole organism is affected by the mutation. Prior to experiments, viable and comparable strains were made in the laboratory as a result of outcrossing to ensure the results generated were representative of any conclusions made from lifespan and brood size assays. Both lifespan and brood size assays not only produced insignificant results but known trends were also non-existent. Our N2 CGCH strain did not produce a smaller progeny and it was not seen to be short lived compared to the N2 CGCM strain (Gems et al., 2000). These factors indicate an anomaly within the laboratory environment at the time of experimentation that may have caused abstract numbers to arise e.g. the presence of a fungal infection. Errors within following the protocol may have also occurred during counting stages to hinder the accuracy of results. The phenotypical assays conducted relies on the nematodes being from a genetically uniform background which may not have been the case since only three rounds of the recommended six took place recommended stages, since organisms at generation F_{60} or higher can be considered genetically indistinguishable (Bailey, 1978).
From the information retrieved, various conclusions can be made. The mutations have successfully been incorporated in the desired subjects; however, we have not been able to infer the effect it has had on the nematodes. We cannot rule out the possibility that the presence of the mutation within *rps-2* has no effect on translational accuracy and therefore no effect on its lifespan and brood size. Repeating these assays with a quicker turnaround time will help the reliability of the results. Majority of the assays were implemented over a long space of time allowing other factors to get involved like contamination and miscounting. Developmental assays that monitor the growth of the nematode in wild-type compared mutant strains will also pinpoint if an *rps-2* mutation affects translation during earlier stages of life when protein synthesis is vital.

Another question to ask is if the mutation requires the inactivity of another gene in the protein, to cause an observable effect. Other literature has shown how the mutation of our investigated *rps-2* gene alongside another nearby gene, L148S, in *S. cerevisiae* has caused

an increase in decoding errors reported via dual luciferase system (Haar, T.V.D. et al., 2017). The lack of significant results makes this hard to justify, however, that does provide alternative approaches to understanding *rps-2* to a greater extent. Repeating these experiments and adding another missense mutation homologous to the L148S found in *S. cerevisae* may see a two-fold decrease in the lifespan or brood size. This would allow us to speculate the synergistic action of these genes have doubling effect on translation. There is no known structure for *rps-2* in *C. elegans*. All structures shown in text are from the *RPS2* human homologue. The tertiary folding of the *rps-2* structure can help find the use of the ribosomal protein (Malmström et al., 2010). It was seen in the human structure almost 100 interactions were made with the subunit – none specific to the mutated residue but it forms a starting point for further investigation. The idea that the worms who have experienced *rps-2* mutations digress into a state of dauer and therefore become transcriptionally inactive meaning that translation will not take place, forms another reason for the inability to harvest both yolk proteins and myosin.

In summary, our study has successfully provided methods into confirming genomic mutations within *C. elegans*, although upon finding the mutation, retrieving information about its role emanated in inconclusive results. To strengthen our understanding of *rps-2* the next step should involve mutating a nearby gene and observing if a collaborative effort causes a significant difference to this model organism. Additional physiological assays that were not implemented here can also be put into effect. Developmental assays monitor time spent at each larval stage, it would be hypothesized that translational accuracy is pivotal during early stages of development due to the number of proteins that have to be forged. Low nutrition has been seen to slow down development into larval stages (Uppaluri et al., 2015) and it would be valuable to understand the effect an *rps-2* mutation would also have. This should then answer the question posed – is there a global effect in the presence of our *rps-2* missense mutation? These conclusions should reflect the role *rps-2* has in translational accuracy.

We have seen examples of changes in one gene affecting ageing in nematodes - in the case of transcription factor DAF-16 within *C. elegans* and its human homologue FOXO acting as master regulator, increasing or decreasing lifespan by regulating other genes depending on its presence in the cell. Moving forward, the repetition of experiments initiated in this study will contribute to the study of geroscience - to gradually understand the relationship between ageing and chronic age-related illnesses.

Appendix

Primer Supplementary Material
Provided from Invitrogen by Thermo Fisher Scientific

Sequencing forward primer (5'-3'): 5' to 3' TGC CGG ACA ACG TAC CCG CTT CAA G		Primer length: 25	
Molecular Weight (µg/mole)	7613.0	µg per OD:	28.6
Micromolecular Extension Coeff (OD/µmol)	266.4	nmol per OD:	3.8
Purity	Desalted	OD's	5.70
Tm (1 M Na+)	79	µg's	**162.89**
Tm (50 mM Na+)	58	nmoles	21.4
% GC	60	Coupling Eff.	99%

Sequencing reverse primer (5'-3'): GGA TCC CTT AGC GGC GGT GTA GC		Primer length: 23	
Molecular Weight (µg/mole)	7613.0	µg per OD:	28.6
Micromolecular Extension Coeff (OD/µmol)	266.4	nmol per OD:	3.8
Purity	Desalted	OD's	5.70
Tm (1 M Na+)	79	µg's	**162.89**
Tm (50 mM Na+)	58	nmoles	21.4
% GC	60	Coupling Eff.	99%

Genotyping forward primer (5'-3'): 5' to 3' CAG AGC CGG ACG CGG AGG AG		Primer length: 20	
Molecular Weight (µg/mole)	6243	µg per OD:	27.0
Micromolecular Extension Coeff (OD/µmol)	231.5	nmol per OD:	4.3
Purity	Desalted	OD's	5.0
Tm (1 M Na+)	79	µg's	**134.84**
Tm (50 mM Na+)	57	nmoles	21.6
% GC	75	Coupling Eff.	99%

- Using the nanomole quantity – to reconstitute to a given concentration, convert the nmole figure to µmole, and then divide by the desired concentration in µmole/litre. For example, to make a 100 µmole primer stock solution, assuming 24nmole yield:
  24nmole x 1µmole/1000nmole = 0.024 µmole
  0.024mole/100µmole/litre = 0.00024 L
  0.00024 l x 1000m/L = 0.24ml or 240 µl

FuDR Supplementary Material
Floxuridine (FuDR) is made and frozen. This is then diluted in a falcon tube for use; for 100 plates, 150µl FuDR from the stock is mixed with 19.8ml dH2O. 200µl (10µM) of this solution is added to each 15ml plate that already has a fully grown OP50 "lawn".

Data from R – Significance testing of concentrations in NTC trial

Test 1

```
> aovdata <-aov(V2~V1, data = data)
> aovdata
Call:
   aov(formula = V2 ~ V1, data = data)

Terms:
                       V1 Residuals
Sum of Squares  0.0366667 0.3933333
Deg. of Freedom         3         8

Residual standard error: 0.2217356
Estimated effects may be unbalanced
> summary(aovdata)
            Df Sum Sq Mean Sq F value Pr(>F)
V1           3 0.0367 0.01222   0.249   0.86
Residuals    8 0.3933 0.04917
> tukeydata
  Tukey multiple comparisons of means
    95% family-wise confidence level

Fit: aov(formula = V2 ~ V1, data = data)

$V1
                           diff        lwr       upr
12.5 ug/ml-0 ug/ml    0.06666667 -0.5131074 0.6464408
25 ug/ml-0 ug/ml      0.06666667 -0.5131074 0.6464408
50 ug/ml-0 ug/ml     -0.06666667 -0.6464408 0.5131074
25 ug/ml-12.5 ug/ml   0.00000000 -0.5797741 0.5797741
50 ug/ml-12.5 ug/ml  -0.13333333 -0.7131074 0.4464408
50 ug/ml-25 ug/ml    -0.13333333 -0.7131074 0.4464408
                         p adj
12.5 ug/ml-0 ug/ml   0.9817456
25 ug/ml-0 ug/ml     0.9817456
50 ug/ml-0 ug/ml     0.9817456
25 ug/ml-12.5 ug/ml  1.0000000
50 ug/ml-12.5 ug/ml  0.8798247
50 ug/ml-25 ug/ml    0.8798247
```

P value: 0.86

P adj value of all tests > 0.86 = not significant

Test 2

```
> aovdata <-aov(V2~V1, data = data)
> aovdata
Call:
   aov(formula = V2 ~ V1, data = data)

Terms:
                        V1  Residuals
Sum of Squares  0.17583333 0.07333333
Deg. of Freedom          3          8

Residual standard error: 0.09574271
Estimated effects may be unbalanced
> 
```

```
> summary(aovdata)
            Df  Sum Sq Mean Sq F value Pr(>F)
V1           3 0.17583 0.05861   6.394 0.0161 *
Residuals    8 0.07333 0.00917
---
Signif. codes:
0 '***' 0.001 '**' 0.01 '*' 0.05 '.' 0.1 ' ' 1
> tukeydata <-TukeyHSD(aovdata)
> tukeydata
  Tukey multiple comparisons of means
    95% family-wise confidence level

Fit: aov(formula = V2 ~ V1, data = data)

$V1
                              diff          lwr       upr
125 ug/ml-0 ug/ml    3.333333e-02 -0.21700604 0.2836727
250 ug/ml-0 ug/ml    3.333333e-02 -0.21700604 0.2836727
50 ug/ml-0 ug/ml     3.000000e-01  0.04966063 0.5503394
250 ug/ml-125 ug/ml  5.551115e-17 -0.25033937 0.2503394
50 ug/ml-125 ug/ml   2.666667e-01  0.01632729 0.5170060
50 ug/ml-250 ug/ml   2.666667e-01  0.01632729 0.5170060
                         p adj
125 ug/ml-0 ug/ml    0.9723004
250 ug/ml-0 ug/ml    0.9723004
50 ug/ml-0 ug/ml     0.0207341
250 ug/ml-125 ug/ml  1.0000000
50 ug/ml-125 ug/ml   0.0373114
50 ug/ml-250 ug/ml   0.0373114

>
```

P value: 0.161

P adj value of all tests > 0.161 = not significant

Test 3

```
> aovdata <-aov(V2~V1, data = data)
> aovdata
Call:
   aov(formula = V2 ~ V1, data = data)

Terms:
                        V1 Residuals
Sum of Squares  0.2626667 0.1533333
Deg. of Freedom         4        10

Residual standard error: 0.1238278
Estimated effects may be unbalanced
> 
> summary(aovdata)
            Df Sum Sq Mean Sq F value Pr(>F)
V1           4 0.2627 0.06567   4.283 0.0283 *
Residuals   10 0.1533 0.01533
---
Signif. codes:
0 '***' 0.001 '**' 0.01 '*' 0.05 '.' 0.1 ' ' 1
> tukeydata <- TukeyHSD(aovdata)
> tukeydata
  Tukey multiple comparisons of means
    95% family-wise confidence level

Fit: aov(formula = V2 ~ V1, data = data)

$V1
                              diff           lwr
125 ug/ml-0 ug/ml    -2.000000e-01 -0.5327448848
25 ug/ml-0 ug/ml     -1.110223e-16 -0.3327448848
250 ug/ml-0 ug/ml    -3.000000e-01 -0.6327448848
50 ug/ml-0 ug/ml      3.333333e-02 -0.2994115515
25 ug/ml-125 ug/ml    2.000000e-01 -0.1327448848
250 ug/ml-125 ug/ml -1.000000e-01 -0.4327448848
50 ug/ml-125 ug/ml    2.333333e-01 -0.0994115515
250 ug/ml-25 ug/ml   -3.000000e-01 -0.6327448848
50 ug/ml-25 ug/ml     3.333333e-02 -0.2994115515
50 ug/ml-250 ug/ml    3.333333e-01  0.0005884485
                             upr     p adj
125 ug/ml-0 ug/ml    0.13274488 0.3409933
25 ug/ml-0 ug/ml     0.33274488 1.0000000
250 ug/ml-0 ug/ml    0.03274488 0.0824786
50 ug/ml-0 ug/ml     0.36607822 0.9970057
25 ug/ml-125 ug/ml   0.53274488 0.3409933
250 ug/ml-125 ug/ml  0.23274488 0.8544093
50 ug/ml-125 ug/ml   0.56607822 0.2191626
250 ug/ml-25 ug/ml   0.03274488 0.0824786
50 ug/ml-25 ug/ml    0.36607822 0.9970057
50 ug/ml-250 ug/ml   0.66607822 0.0495503
```

P value: 0.0283

P adj value of all tests > 0.0283 = not significant

SDS PAGE Gels Supplementary Material

The following recipe is for approximately 25 mL of Separating Gel, enough for four 1.0-mm thick mini gels. Novex by life technologies - Thermo Fisher Scientific Inc.

Separating gel	7.5% gel amount	
40% Acrylamide/BIS (37.5:1)	Ready-to-use high-purity (99.9%) solution	4.75 ml
Separating Gel Buffer (1 M Tris-HCl, pH 8.8)	Stock solution: Add 30.3 g Tris to 150 mL water Adjust to pH 8.8 with HCl Bring to 250 mL with water	9.4 ml
10% SDS	Stock solution: 10.0 g SDS Bring to 100 mL with water	250 µl
Catalyst*	Stock solution: 100 mg Ammonium Persulfate in 2 mL of water (Make fresh on the day of use)	625µl
Water		10.05 ml
TEMED*		6.25 µl

Stacking gel solution 4% stacking gel (12.5ml)		
40% Acrylamide/BIS (37.5:1)		1.5 ml
Stacking Gel Buffer (0.375 M Tris HCl, pH 6.8)	11.4 g Tris added to ~150 ml water; adjust to pH 6.8 with HCl Bring to 250 ml with water	4.2 ml
10% SDS	10.0 g SDS Bring to 100 mL with water 250 µl [use from already made stock]	125 µl
Water		5.8 ml
TEMED		50 µl
Catalyst*		1 ml

*Add these last and mix well just before the gel is to be poured.

Primer Supplementary Material

Sequencing Forward Primer	
5’ to 3’ TGC CGG ACA ACG TAC CCG CTT CAA G	
Molecular Weight (µg/µmole):	7613.0
Micromolar Extension Coeff (OD/µmol):	266.4
Purity:	Desalted
Tm (1 M Na+):	79
Tm (50 mM Na+):	58
%GC:	60
Primer length:	25
µg per OD:	28.6
nmoles per OD:	3.8
OD’s:	5.7
µg's	162.89
nmoles	21.4
Genotyping Forward Primer	
5’ to 3’ CAG AGC CGG ACG CGG AGG AG	
Molecular Weight (µg/µmole):	6243
Micromolar Extension Coeff (OD/µmol):	231.5
Purity:	Desalted
Tm (1 M Na+):	79
Tm (50 mM Na+):	57
%GC:	75
Primer length:	20
µg per OD:	27.0
nmoles per OD:	4.3
OD’s:	5.0
µg's	134.84
nmoles	21.6

BLAST sequences Supplementary Information

N2

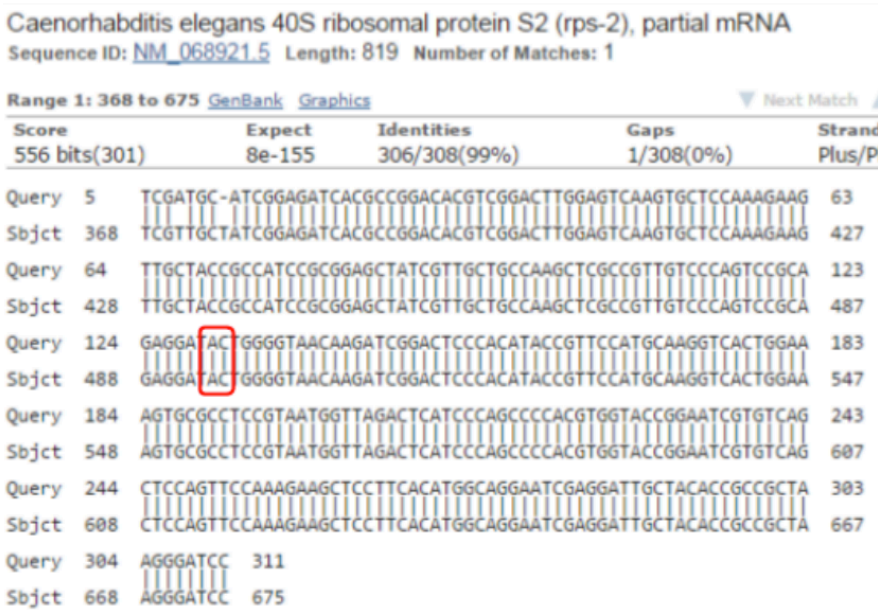

Caenorhabditis elegans 40S ribosomal protein S2 (rps-2), partial mRNA

Sequence ID: NM_068921.5 Length: 819 Number of Matches: 1

Range 1: 368 to 675 GenBank Graphics Next Match

Score	Expect	Identities	Gaps	Strand
556 bits(301)	8e-155	306/308(99%)	1/308(0%)	Plus/P

```
Query  5    TCGATGC-ATCGGAGATCACGCCGGACACGTCGGACTTGGAGTCAAGTGCTCCAAAGAAG  63
            ||||||| ||||||||||||||||||||||||||||||||||||||||||||||||||||
Sbjct  368  TCGTTGCTATCGGAGATCACGCCGGACACGTCGGACTTGGAGTCAAGTGCTCCAAAGAAG  427

Query  64   TTGCTACCGCCATCCGCGGAGCTATCGTTGCTGCCAAGCTCGCCGTTGTCCCAGTCCGCA  123
            ||||||||||||||||||||||||||||||||||||||||||||||||||||||||||||
Sbjct  428  TTGCTACCGCCATCCGCGGAGCTATCGTTGCTGCCAAGCTCGCCGTTGTCCCAGTCCGCA  487

Query  124  GAGGATACTGGGGTAACAAGATCGGACTCCCACATACCGTTCCATGCAAGGTCACTGGAA  183
            |||||||  ||||||||||||||||||||||||||||||||||||||||||||||||||||
Sbjct  488  GAGGATACTGGGGTAACAAGATCGGACTCCCACATACCGTTCCATGCAAGGTCACTGGAA  547

Query  184  AGTGCGCCTCCGTAATGGTTAGACTCATCCCAGCCCCACGTGGTACCGGAATCGTGTCAG  243
            ||||||||||||||||||||||||||||||||||||||||||||||||||||||||||||
Sbjct  548  AGTGCGCCTCCGTAATGGTTAGACTCATCCCAGCCCCACGTGGTACCGGAATCGTGTCAG  607

Query  244  CTCCAGTTCCAAAGAAGCTCCTTCACATGGCAGGAATCGAGGATTGCTACACCGCCGCTA  303
            ||||||||||||||||||||||||||||||||||||||||||||||||||||||||||||
Sbjct  608  CTCCAGTTCCAAAGAAGCTCCTTCACATGGCAGGAATCGAGGATTGCTACACCGCCGCTA  667

Query  304  AGGGATCC  311
            ||||||||
Sbjct  668  AGGGATCC  675
```

COP872

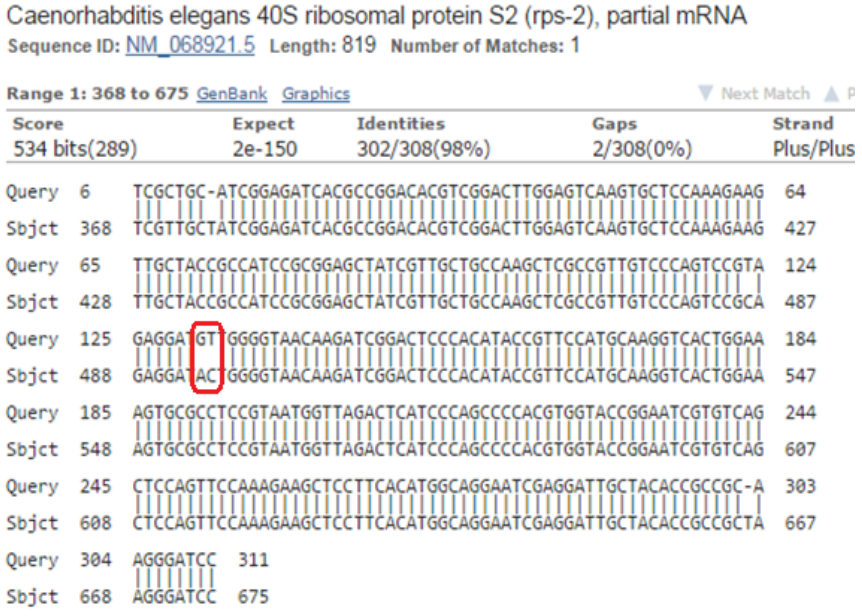

Caenorhabditis elegans 40S ribosomal protein S2 (rps-2), partial mRNA

Sequence ID: NM_068921.5 Length: 819 Number of Matches: 1

Range 1: 368 to 675 GenBank Graphics Next Match

Score	Expect	Identities	Gaps	Strand
534 bits(289)	2e-150	302/308(98%)	2/308(0%)	Plus/Plus

```
Query  6    TCGCTGC-ATCGGAGATCACGCCGGACACGTCGGACTTGGAGTCAAGTGCTCCAAAGAAG  64
            ||| ||| ||||||||||||||||||||||||||||||||||||||||||||||||||||
Sbjct  368  TCGTTGCTATCGGAGATCACGCCGGACACGTCGGACTTGGAGTCAAGTGCTCCAAAGAAG  427

Query  65   TTGCTACCGCCATCCGCGGAGCTATCGTTGCTGCCAAGCTCGCCGTTGTCCCAGTCCGTA  124
            ||||||||||||||||||||||||||||||||||||||||||||||||||||||||||| |
Sbjct  428  TTGCTACCGCCATCCGCGGAGCTATCGTTGCTGCCAAGCTCGCCGTTGTCCCAGTCCGCA  487

Query  125  GAGGATGTTGGGGTAACAAGATCGGACTCCCACATACCGTTCCATGCAAGGTCACTGGAA  184
            |||||| ||||||||||||||||||||||||||||||||||||||||||||||||||||||
Sbjct  488  GAGGATACTGGGGTAACAAGATCGGACTCCCACATACCGTTCCATGCAAGGTCACTGGAA  547

Query  185  AGTGCGCCTCCGTAATGGTTAGACTCATCCCAGCCCCACGTGGTACCGGAATCGTGTCAG  244
            ||||||||||||||||||||||||||||||||||||||||||||||||||||||||||||
Sbjct  548  AGTGCGCCTCCGTAATGGTTAGACTCATCCCAGCCCCACGTGGTACCGGAATCGTGTCAG  607

Query  245  CTCCAGTTCCAAAGAAGCTCCTTCACATGGCAGGAATCGAGGATTGCTACACCGCCGC-A  303
            ||||||||||||||||||||||||||||||||||||||||||||||||||||||||||| |
Sbjct  608  CTCCAGTTCCAAAGAAGCTCCTTCACATGGCAGGAATCGAGGATTGCTACACCGCCGCTA  667

Query  304  AGGGATCC  311
            ||||||||
Sbjct  668  AGGGATCC  675
```

COP873

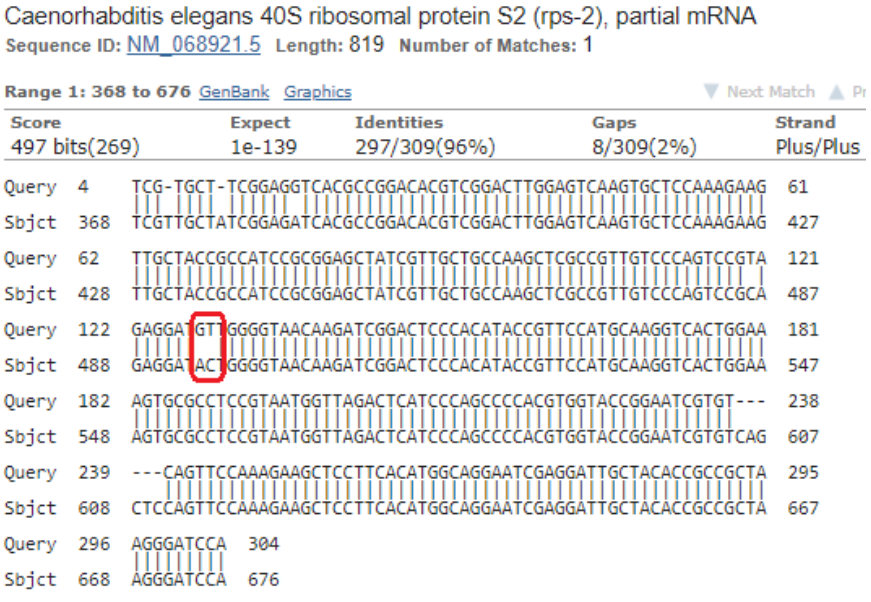

Caenorhabditis elegans 40S ribosomal protein S2 (rps-2), partial mRNA

Sequence ID: NM_068921.5 Length: 819 Number of Matches: 1

Range 1: 368 to 676 GenBank Graphics Next Match

Score	Expect	Identities	Gaps	Strand
497 bits(269)	1e-139	297/309(96%)	8/309(2%)	Plus/Plus

```
Query  4    TCG-TGCT-TCGGAGGTCACGCCGGACACGTCGGACTTGGAGTCAAGTGCTCCAAAGAAG  61
            ||| |||| |||||| ||||||||||||||||||||||||||||||||||||||||||||
Sbjct  368  TCGTTGCTATCGGAGATCACGCCGGACACGTCGGACTTGGAGTCAAGTGCTCCAAAGAAG  427

Query  62   TTGCTACCGCCATCCGCGGAGCTATCGTTGCTGCCAAGCTCGCCGTTGTCCCAGTCCGTA  121
            ||||||||||||||||||||||||||||||||||||||||||||||||||||||||||| |
Sbjct  428  TTGCTACCGCCATCCGCGGAGCTATCGTTGCTGCCAAGCTCGCCGTTGTCCCAGTCCGCA  487

Query  122  GAGGATGTTGGGGTAACAAGATCGGACTCCCACATACCGTTCCATGCAAGGTCACTGGAA  181
            ||||| ||||||||||||||||||||||||||||||||||||||||||||||||||||||
Sbjct  488  GAGGATACTGGGGTAACAAGATCGGACTCCCACATACCGTTCCATGCAAGGTCACTGGAA  547

Query  182  AGTGCGCCTCCGTAATGGTTAGACTCATCCCAGCCCCACGTGGTACCGGAATCGTGT---  238
            ||||||||||||||||||||||||||||||||||||||||||||||||||||||||   
Sbjct  548  AGTGCGCCTCCGTAATGGTTAGACTCATCCCAGCCCCACGTGGTACCGGAATCGTGTCAG  607

Query  239  ---CAGTTCCAAAGAAGCTCCTTCACATGGCAGGAATCGAGGATTGCTACACCGCCGCTA  295
               ||||||||||||||||||||||||||||||||||||||||||||||||||||||||||
Sbjct  608  CTCCAGTTCCAAAGAAGCTCCTTCACATGGCAGGAATCGAGGATTGCTACACCGCCGCTA  667

Query  296  AGGGATCCA  304
            |||||||||
Sbjct  668  AGGGATCCA  676
```

Caenorhabditis elegans 40S ribosomal protein S2 (rps-2), partial mRNA

Sequence ID: NM_068921.5 Length: 819 Number of Matches: 1

Range 1: 404 to 676 GenBank Graphics Next Match Pr

Score	Expect	Identities	Gaps	Strand
472 bits(255)	6e-132	270/277(97%)	4/277(1%)	Plus/Plus

```
Query  44   TTGGAAGTCNAAGTGCTCCCAAAGAAGTTGCTACCGCCATCCGCGGAAGCTATCGTTGCT  103
            ||||  ||||  |||||||  ||||||||||||||||||||||||||||| ||||||||||||
Sbjct  404  TTGG-AGTC-AAGTGCT-CCAAAGAAGTTGCTACCGCCATCCGCGG-AGCTATCGTTGCT  459

Query  104  GCCAAGCTCGCCGTTGTCCCAGTCCGCAGAGGATACTGGGGTAACAAGATCGGACTCCCA  163
            ||||||||||||||||||||||||||||||||||||||||||||||||||||||||||||
Sbjct  460  GCCAAGCTCGCCGTTGTCCCAGTCCGCAGAGGATACTGGGGTAACAAGATCGGACTCCCA  519

Query  164  CATACCGTTCCATGCAAGGTCACTGGAAAGTGCGCCTCCGTAATGGTTAGACTCATCCCA  223
            ||||||||||||||||||||||||||||||||||||||||||||||||||||||||||||
Sbjct  520  CATACCGTTCCATGCAAGGTCACTGGAAAGTGCGCCTCCGTAATGGTTAGACTCATCCCA  579

Query  224  GCCCCACGTGGTACCGGAATCGTGTCAGCTCCAGTTCCAAAGAAGCTCCTTCACATGGCA  283
            ||||||||||||||||||||||||||||||||||||||||||||||||||||||||||||
Sbjct  580  GCCCCACGTGGTACCGGAATCGTGTCAGCTCCAGTTCCAAAGAAGCTCCTTCACATGGCA  639

Query  284  GGAATCGAGGATTGCTACACCGCCNTAAAGGGATCCA  320
            ||||||||||||||||||||||||  ||||||||||
Sbjct  640  GGAATCGAGGATTGCTACACCGCCGCTAAGGGATCCA  676
```

COP874

Caenorhabditis elegans 40S ribosomal protein S2 (rps-2), partial mRNA

Sequence ID: NM_068921.5 Length: 819 Number of Matches: 1

Range 1: 373 to 676 GenBank Graphics Next Match

Score	Expect	Identities	Gaps	Stran
523 bits(283)	2e-147	298/305(98%)	3/305(0%)	Plus/

```
Query  9    GCT-TCGGANATCACGCCGGACACGTCGGACTTGGAGTCAAGTGCTCCAAAGAAGTTGCT  67
            ||| ||||| ||||||||||||||||||||||||||||||||||||||||||||||||||||
Sbjct  373  GCTATCGGAGATCACGCCGGACACGTCGGACTTGGAGTCAAGTGCTCCAAAGAAGTTGCT  432

Query  68   ACCGCCATCCGCGGAGCTATCGTTGCTGCCAAGCTCGCCGTTGTCCCAGTCCGCAGAGGA  127
            ||||||||||||||||||||||||||||||||||||||||||||||||||||| ||||||
Sbjct  433  ACCGCCATCCGCGGAGCTATCGTTGCTGCCAAGCTCGCCGTTGTCCCAGTCCGCAGAGGA  492

Query  128  TGTTGGGGTAACAAGATCGGACTCCCACATACCGTTCCATGCAAGGTCACTGGAAAGTGC  187
            |||||||||||||||||||||||||||||||||||||||||||||||||||||||||||||
Sbjct  493  TACTGGGGTAACAAGATCGGACTCCCACATACCGTTCCATGCAAGGTCACTGGAAAGTGC  552

Query  188  GCCTCCGTAATGGTTAGACTCATCCCAGCCCCACGTGGTACCGGAATCGTGTCAGCTCCA  247
            ||||||||||||||||||||||||||||||||||||||||||||||||||||||||||||
Sbjct  553  GCCTCCGTAATGGTTAGACTCATCCCAGCCCCACGTGGTACCGGAATCGTGTCAGCTCCA  612

Query  248  GTTCCAAAGAAGCTCCTTCACATGGCAGGAATCGAGGATTGCTACACCGCC-CTAAAGGG  306
            |||||||||||||||||||||||||||||||||||||||||||||||||| |||| |||
Sbjct  613  GTTCCAAAGAAGCTCCTTCACATGGCAGGAATCGAGGATTGCTACACCGCCGCTAA-GGG  671

Query  307  ATCCA  311
            |||||
Sbjct  672  ATCCA  676
```

COP875

Caenorhabditis elegans 40S ribosomal protein S2 (rps-2), partial mRNA

Sequence ID: NM_068921.5 Length: 819 Number of Matches: 1

Range 1: 377 to 675 GenBank Graphics Next Match

Score	Expect	Identities	Gaps	Strand
547 bits(296)	2e-154	299/300(99%)	1/300(0%)	Plus/Plu

```
Query  14   TCGGAGATCACGCCGGACACGTCGGACTTGGAGTCAAGTGCTCCAAAGAAGTTGCTACCG  73
            ||||||||||||||||||||||||||||||||||||||||||||||||||||||||||||
Sbjct  377  TCGGAGATCACGCCGGACACGTCGGACTTGGAGTCAAGTGCTCCAAAGAAGTTGCTACCG  436

Query  74   CCATCCGCGGAGCTATCGTTGCTGCCAAGCTCGCCGTTGTCCCAGTCCGCAGAGGATACT  133
            ||||||||||||||||||||||||||||||||||||||||||||||||||||||||||||
Sbjct  437  CCATCCGCGGAGCTATCGTTGCTGCCAAGCTCGCCGTTGTCCCAGTCCGCAGAGGATACT  496

Query  134  GGGGTAACAAGATCGGACTCCCACATACCGTTCCATGCAAGGTCACTGGAAAGTGCGCCT  193
            ||||||||||||||||||||||||||||||||||||||||||||||||||||||||||||
Sbjct  497  GGGGTAACAAGATCGGACTCCCACATACCGTTCCATGCAAGGTCACTGGAAAGTGCGCCT  556

Query  194  CCGTAATGGTTAGACTCATCCCAGCCCCACGTGGTACCGGAATCGTGTCAGCTCCAGTTC  253
            ||||||||||||||||||||||||||||||||||||||||||||||||||||||||||||
Sbjct  557  CCGTAATGGTTAGACTCATCCCAGCCCCACGTGGTACCGGAATCGTGTCAGCTCCAGTTC  616

Query  254  CAAAGAAGCTCCTTCACATGGCAGGAATCGAGGATTGCTACACCGCCGCTAAAGGGATCC  313
            |||||||||||||||||||||||||||||||||||||||||||||||||| |||||||||
Sbjct  617  CAAAGAAGCTCCTTCACATGGCAGGAATCGAGGATTGCTACACCGCCGCTAA-GGGATCC  675
```

COP876

Knudra Sequence Supplementary Information

N2 base sequence

CGGTTCGAGCATCGGAGATCACGCCGGACACGTCGGACTTGGAGTCAAGTGCTCCAAAGAAGTTGCTACC
GCCATCCGCGGAGCTATCGTTGCTGCCAAGCTCGCCGTTGTCCCAGTCCGCAGAGGATACTGGGGTAACAA
GATCGGACTCCCACATACCGTTCCATGCAAGGTCACTGGAAAGTGCGCCTCCGTAATGGTTAGACTCATCC
CAGCCCCACGTGGTACCGGAATCGTGTCAGCTCCAGTTCCAAAGAAGCTCCTTCACATGGCAGGAATCGAG
GATTGCTACACCGCTAAGGGATCC

COP872 base sequence

GGGCATCGCTGCATCGGAGATCACGCCGGACACGTCGGACTTGGAGTCAAGTGCTCCAAAGAAGTTGCTA
CCGCCATCCGCGGAGCTATCGTTGCTGCCAAGCTCGCCGTTGTCCCAGTCCGTAGAGGATGTTGGGGTAAC
AAGATCGGACTCCCACATACCGTTCCATGCAAGGTCACTGGAAAGTGCGCCTCCGTAATGGTTAGACTCAT
CCCAGCCCCACGTGGTACCGGAATCGTGTCAGCTCCAGTTCCAAAGAAGCTCCTTCACATGGCAGGAATCG
AGGATTGCTACACCGCCGCAAGGGATCCCA

COP873 base sequence

GCATCGTGCTTCGGAGGTCACGCCGGACACGTCGGACTTGGAGTCAAGTGCTCCAAAGAAGTTGCTACCG
CCATCCGCGGAGCTATCGTTGCTGCCAAGCTCGCCGTTGTCCCAGTCCGTAGAGGATGTTGGGGTAACAAG
ATCGGACTCCCACATACCGTTCCATGCAAGGTCACTGGAAAGTGCGCCTCCGTAATGGTTAGACTCATCCC
AGCCCCACGTGGTACCGGAATCGTGTCAGTTCCAAAGAAGCTCCTTCACATGGCAGGAATCGAGGATTGCT
ACACCGCCGCTAAGGGATCCATCAT

COP874 base sequence

GGNTNNNNGNNNTCGGNNNANNCGCCGGANNCGTCCGGTAANTTTGGAAGTCNAAGTGCTCCCAAAGA
AGTTGCTACCGCCATCCGCGGAAGCTATCGTTGCTGCCAAGCTCGCCGTTGTCCCAGTCCGCAGAGGATAC
TGGGGTAACAAGATCGGACTCCCACATACCGTTCCATGCAAGGTCACTGGAAAGTGCGCCTCCGTAATGGT
TAGACTCATCCCAGCCCCACGTGGTACCGGAATCGTGTCAGCTCCAGTTCCAAAGAAGCTCCTTCACATGG
CAGGAATCGAGGATTGCTACACCGCCNTAAAGGGATCCA

COP875 base sequence

GNNNNNNNGCTTCGGANATCACGCCGGACACGTCGGACTTGGAGTCAAGTGCTCCAAAGAAGTTGCTAC
CGCCATCCGCGGAGCTATCGTTGCTGCCAAGCTCGCCGTTGTCCCAGTCCGTAGAGGATGTTGGGGTAACA
AGATCGGACTCCCACATACCGTTCCATGCAAGGTCACTGGAAAGTGCGCCTCCGTAATGGTTAGACTCATC
CCAGCCCCACGTGGTACCGGAATCGTGTCAGCTCCAGTTCCAAAGAAGCTCCTTCACATGGCAGGAATCGA
GGATTGCTACACCGCCCTAAAGGGATCCAAA

COP876 base sequence

GGAATGGAGCATCGGATATCACGCCGGACACGTCGGACTTGGAGTCAAGTGCTCCAAAGAAGTTGCTACC
GCCATCCGCGGAGCTATCGTTGCTGCCAAGCTCGCCGTTGTCCCAGTCCGCAGAGGATACTGGGGTAACAA
GATCGGACTCCCACATACCGTTCCATGCAAGGGCAAGGTCACTGGAAAGTGCGCCTCCGTAATGGTTAGAC
TCATCCCAGCCCCACGTGGTACCGGAATCGTGTCAGCTCCAGTTCCAAAGAAGCTCCTTCACATGGCAGGA
ATCGAGGATTGCTACACCGCCGCTAAGGGATCCATCCATTGGATTTACCTACTA

No mutation Mutation

Myosin regulatory light chain 1 protein sequence

MSKAAKKKSSKKRSGSEAAQFDQKTIQEFKEAFGIMDQNKDGIIDKSDLKDLYASMGQIAPDSQIDAMIKEASGPINFTVFL
TLFGERLTGTDPEATIIGAFAMFDKKDCGKIKEDDLIKILQNKRGEPLDEDEVKAMYKGKPPIEGGEVDYKAFAHLITTGAQD
ELASA

Myosin-2 protein sequence

MDYENDPGWKYLRRSREEMLQDQSRAYDSKKNVWIPDSEDGYIEGVITKTAGDNVTVSIGQGAEKTVKKDVVQEMNPPK
FEKTEDMSNLTFLNDASVLYNLKARYAAMLIYTYSGLFCVVINPYKRLPIYTDSVARMFMGKRRTEMPPHLFAVSDEAYRN
MLQNHENQSMLITGESGAGKTENTKKVISYFAAVGAAQQETFGAKKAATEEDKNKKKVTLEDQIVQTNPVLEAFGNAKTV
RNNNSSRFGKFIRIHFSKQGRVASCDIEHYLLEKSRVIRQAPGERCYHIFYQVFSDYLPNLKKDLLLNKPVKDYWFIAQAELIID
GINDKEEHQLTDEAFDILKFTPTEKMECYRLVAAMMHMGNMKFKQRPREEQAEPDGTDDAERAAKCFGIDSEEFLKALTR
PRVKVGNEWVNKGQNIEQVNWAVGAMAKGLYSRIFNWLVKKCNQTLDQKGISRDHFIGVLDIAGFEIFDFNSFEQLWIN
FVNEKLQQFFNHHMFVLEQEEYAREGIQWTFIDFGLDLQACIELIEKPLGIIAMLDEECIVPKATDLTLAQKLIDQHLGKHPNF
EKPKPPKGKQAEAHFAMRHYAGTVRYNCLNWLEKNKDPLNDTVVTVMKASKEHALIVEVWQDYTTQEEAAAAAAKGTA
GAKKKGKSGSFMTVSMLYRESLNKLMTMLHSTHPHFIRCIIPNEKKASGVIDAGLVLNQLTCNGVLEGIRICRKGFPNRTLHP
DFVQRYALLAADESIIGKTDAKKGSALMLARLVKEKKLEEENFRVGLTKVFFKAGIVAHLEDLRDQSLAQLITGLQAQIRWYY
QTIERKRRVEKITALKIIQRNIRSWAELRTWVWFKLYGKVKPLVNSGKIEAQYEKLQETVATLKDTVVQEEEKKRQLQEGAER
LNKETADLLAQLEASKGSTREVEERMTAMNEQKVALEGKLADASKKLEVEEARAVEINKQKKLVEAECADLKKNCQDVDLS
LRKVEAEKNAKEHQIRALQDEMRQQDENISKLNKERKNQEEQNKKLTEDLQAAEEQNLAANKLKAKLMQSLEDSEQTME
REKRNRADMDKNKRKAEGELKIAQETLEELNKSKSDAENALRRKETELHTLGMKLEDEQAAVAKLQKGIQQDEARVKDLH
DQLADEKDARQRADRSRADQQAEYDELTEQLEDQARATAAQIELGKKKDAELTKLRRDLEESGLKFGEQLTVLKKKGSDAI
QELSDQIEQLQKQKGRIEKEKGHMQREFDESSAALDQEAKLRADQERIAKGYEVRLLELRLKADEQSRQLQDFVSSKGRLNS
ENSDLARQVEELEAKIQAANRLKLQFSNELDHAKRQAEEESRERQNLSNLSKNLARELEQLKESIEDEVAGKNEASRQLSKAS
VELDQWRTKFETEGLIGADEFDEVKKRQNQKTSEIQDALDACNAKIVALENARSRLTAEADANRLEAEHHAQAVSSLEKKQ
KAFDKVIDEWKKKVDDLYLELDGAQRDARQLSGEAHKLRGQHDTLADQVEGLRRENKSLSDETRDLTESLSEGGRATHALS
KNLRRLEMEKEELQRGLDEAEAALESEESKALRCQIEVSQIRAEIEKRIAEKEEEFENHRKVHQQTIDSIQATLDSETKAKSELF
RVKKKLEADINELEIALDHANKANEDAQKNIRRYLDQIRELQQTVDEEQKRREEFREHLLAAERKLAVAKQEQEELIVKLEALE
RARRVVESSVKEHQEHNNELNSQNVALAAAKSQLDNEIALLNSDIAEAHTELSASEDRGRRAASDAAKLAEDLRHEQEQSQ
QLERFKKQLESAVKDLQERADAAEAAVMKGGAKAIQKAEQRLKAFQSDLETESRRAGEASKTLARADRKVREFEFQVAEDK
KNYDKLQELVEKLTAKLKLQKKQLEEAEEQANSHLSKYRTVQLSLETAEERADSAEQCLVRIRSRTRANAEQK

Data from Lifespan – Significance testing N2, COP87

Test Result: Log-Rank Test

Condition	Statistics		
	Chi^2	P-value	Bonferroni P-value
N2 CGCM *v.s.* N2 CGCH	0.11	0.7400	1.0000
N2 CGCM *v.s.* COP872	5.44	0.0197	0.0590
N2 CGCM *v.s.* COP876	3.24	0.0719	0.2157
N2 CGCH *v.s.* N2 CGCM	0.11	0.7400	1.0000
N2 CGCH *v.s.* COP872	1.77	0.1831	0.5492
N2 CGCH *v.s.* COP876	0.88	0.3491	1.0000
COP872 *v.s.* N2 CGCM	5.44	0.0197	0.0590
COP872 *v.s.* N2 CGCH	1.77	0.1831	0.5492
COP872 *v.s.* COP876	0.37	0.5440	1.0000
COP876 *v.s.* N2 CGCM	3.24	0.0719	0.2157
COP876 *v.s.* N2 CGCH	0.88	0.3491	1.0000
COP876 *v.s.* COP872	0.37	0.5440	1.0000

Trial A

Thermo Fisher PCR Purifcation Kit Supplementary Information

https://www.thermofisher.com/document-connect/document-connect.html?url=https://assets.thermofisher.com/TFS-Assets/LSG/manuals/MAN0012662_GeneJET_PCR_Purification_UG.pdf&title=User%20Guide:%20GeneJET%20PCR%20Purification%20Kit

References

Altun, Z. F. and Hall, D.H. (2011) Nervous system, general description. In WormAtlas.

Anti Aging Market is Determined to Reach US$ 271.0 Billion by 2024. (2019). Accessed at: https://www.marketwatch.com/press-release/anti-aging-market-is-determined-to-reach-us-2710-billion-by-2024-2019-03-04

Aparna C. H., Madhavi Latha N., Supriya P., Gowrisankar D. (2015) A Review On Matrix Assisted Laser Desorption/Ionisation Mass Spectroscopy. Asian Journal of Pharmaaceutical and Clinical Research 8(5) pp.28-33

Ashkenazy, H. ConSurf (2016) An improved methodology to estimate and visualize evolutionary conservation in macromolecules. Nucleic Acids Res. 44, W344–50

Bailey, D. W. (1978) Sources of subline divergence and their relative importance for sublines of six major inbred strains of mice. In Origins of Inbred Mice, Morse, H. C., ed. (Academic Press, New York), pp. 423-438.

Ben-Shem, A., Garreau, de, Melnikov, S., Jenner, L., Yusupova, G. and Yusupov, M. (2011) 'The structure of the eukaryotic ribosome at 3.0 Å resolution', Science (New York). 334(6062), pp. 1524-9

Bidou, L., Rousset, J.-P. and Namy, O. (2010) 'Translational errors: From yeast to new therapeutic targets', FEMS Yeast Research, 10(8), pp. 1070–1082.

Brenner, S. (1974). The genetics of Caenorhabditis elegans. Genetics 77, 71–94.

Charmpilas, N., Daskalaki, I., Papandreou, M., & Tavernarakis, N. (2015). Protein synthesis as an integral quality control mechanism during ageing. Ageing Research Reviews, 23, pp. 75-89.

Corsi A. K., Wightman B., and Chalfie M. A Transparent window into biology: A primer on Caenorhabditis elegans (2015), WormBook, ed. The *C. elegans* Research Community, WormBook, http://www.wormbook.org.

Corsi, A. K. (2006). A Biochemist's Guide to *C. elegans*. Analytical Biochemistry, 359(1), pp. 1–17.

Dillin A, Hsu A, Arantes-Oliveira N, Lehrer-Graiwer J, Hsin H, Fraser A, Kamath R, Ahringer J, Kenyon C (2002) Rates of behavior and aging specified by mitochondrial function during development. Science 298(5602):pp. 2398–2401.

Doudna, J. and Charpentier, E. (2014) 'Genome editing. The new frontier of genome engineering with CRISPR-Cas9', Science (New York, N.Y.)., 346(6213).,

Drummond, D. A., & Wilke, C. O. (2009). The evolutionary consequences of erroneous protein synthesis. Nature reviews. Genetics, 10(10), 715-24.

Félix M-A, Ashe A, Piffaretti J, (2011) ;Natural and Experimental Infection of Caenorhabditis Nematodes by Novel Viruses Related to Nodaviruses. Hodgkin J, ed. PLoS Biology. 9(1):e1000586.

Ferreira-Cerca, S. (2005). Roles of Eukaryotic Ribosomal Proteins in Maturation and Transport of Pre-18S rRNA and Ribosome Function. Molecular Cell, 20(2), pp.263–275.

Fields, S., Johnston, M. (2005). "Cell biology. Whither model organism research?". Science. 307 (5717): pp. 1885–6

Fielenbach, N. and Antebi, A. (2008) '*C. Elegans* dauer formation and the molecular basis of plasticity', 22(16)9

Frank, J., Agrawal, R. K., (1998) The movement of tRNA through the ribosome Biophysical Journal 74 pp. 589-594

Friedman, D. B., & Johnson, T. E. (1988). A Mutation in the Age-1 Gene in Caenorhabditis Elegans Lengthens Life and Reduces Hermaphrodite Fertility. Genetics, 118(1), pp. 75–86.

Frolova L, Le Goff X, Rasmussen H. H. (1994) A highly conserved eukaryotic protein family possessing properties of polypeptide chain release factor. Nature 372: 701–703.[7] Stroustrup, N., Ulmschneider, B.E.,

Gems, D. & Riddle, D.L. (2000) Defining wild-type life span in Caenorhabditis elegans. J. Gerontol. 55A: B215-B219

Gems, D., & Partridge, L. (2013). Genetics of Longevity in Model Organisms: Debates and Paradigm Shifts. Annual Review Of Physiology, 75(1), pp. 621-644.

Gomes AC, Miranda I, Silva RM, Moura GR, Thomas B, Akoulitchev A, Santos MAS. (2007). A genetic code alteration generates a proteome of high diversity in the human pathogen Candida albicans. Genome Biol. 8, R206

Green and, R., & Noller, H. (1997). RIBOSOMES AND TRANSLATION. Annual Review Of Biochemistry, 66(1), pp. 679-716.

Guo, H. H., Choe, J., & Loeb, L. A. (2004). Protein tolerance to random amino acid change. Proceedings of the National Academy of Sciences of the United States of America, 101(25), 9205–9210.

Haar, T.V.D., Leadsham, J. E., Sauvadet, A., Tarrant, D., Adam, I. S., Saromi, K., Laun, P., Rinnerthaler, M., Breitenbach-Koller, H., Breitenbach, M., Tuite, M. F., Gourlay, C. W (2017). The control of translational accuracy is a determinant of healthy ageing in yeast. Open Biology, 7(1), p.160291.

Henderson, D., Huebner, C., Markowitz, M., Taube, N., Harvanek, Z. M., Jakob, U., & Knoefler, D. (2017). Do developmental temperatures affect redox level and lifespan in *C. elegans* through upregulation of peroxiredoxin?. Redox biology, 14, 386-390.

Hopkins, C. (2016) *C. Elegans* CRISPR genome editing review. Available at: http://www.knudra.com/technology/celeganscrispr].

Jan A. Pechenik. (2005) Biology of the Invertebrates. New York: McGraw Hill

Jouffe C., Cretenet G., Symul L., Martin E., Atger F., Naef F., Gachon F. (2013) The circadian clock coordinates ribosome biogenesis 2013;11(1)

Kapur, M & Ackerman, S. L, (2018) 'mRNA Translation Gone Awry: Translation Fidelity and Neurological Disease' Trends in Genetics, 34(3) pp. 218-231

Kenmochi, N., Kawaguchi, T., Rozen, S., Davis, E., Goodman, N., Hudson, T. J. , Tanaka, T., Page, D. C. (1998). "A map of 75 human ribosomal protein genes". Genome Res. 8 (5): pp.509–23

Kenyon, C., Chang, J., Gensch, E., Rudner, A., & Tabtiang, R. (1993). A *C. elegans* mutant that lives twice as long as wild type. Nature, 366(6454), pp. 461-464.

Kimble, J. and Hirsh, D. (1979) The postembryonic cell lineages of the hermaphrodite and male gonads in Caenorhabditis elegans. Dev. Biol. 70: 396-417.

Kirstein-Miles, J., Scior, A., Deuerling, E., & Morimoto, R. I. (2013). The nascent polypeptide-associated complex is a key regulator of proteostasis. The EMBO journal, 32(10), 1451–1468. doi:10.1038/emboj.2013.87

Krügel, H., Fiedler, G., Smith, C., & Baumberg, S., (1993) Sequence and transcriptional analysis of the nourseothricin acetyltransferase-encoding gene nat1 from Streptomyces noursei. Gene, 127(1), pp.127–131

Lai, C.-H., Chou, C.-Y., Ch'ang, L.-Y., Liu, C.-S. and Lin, W. (2000) 'Identification of novel human genes Evolutionarily conserved in Caenorhabditis elegans by comparative Proteomics', 10(5).

Mali, P., Yang, L., Esvelt, K., Aach, J., Guell, M., DiCarlo, J., Norville, J. and Church, G. (2013) 'RNA-guided human genome engineering via Cas9', Science (New York, N.Y.)., 339(6121), pp. 823–6.

Malmström L., Goodlett D.R. (2010) Protein Structure Modeling. In: Fenyö D. (eds) Computational Biology. Methods in Molecular Biology (Methods and Protocols), vol 673. Humana Press, Totowa, NJ

Mamotte, C.D.S, (2006). Genotyping of single nucleotide substitutions. The Clinical biochemist. Reviews, 27(1), 63-75.

McCulloch D, Gems D (2003) Body size, insulin/IGF signaling and aging in the nematode Caenorhabditis elegans. Experimental Gerontology 38 pp. 129–136

Meyer-Schuman, R., & Antonellis, A. (2017). Emerging mechanisms of aminoacyl-tRNA synthetase mutations in recessive and dominant human disease. Human molecular genetics, 26(R2), R114-R127.

Moore, P. B., Steitz, T. A. (2002) The involvement of RNA in ribosome function. Nature; 418:229-35; PMID:12110899;

Orgel L. E. (1970). The maintenance of the accuracy of protein synthesis and its relevance to ageing: a correction. Proceedings of the National Academy of Sciences of the United States of America, 67(3),

Pestova, T. V., & Kolupaeva, V. G. (2002). The roles of individual eukaryotic translation initiation factors in ribosomal scanning and initiation codon selection. Genes & development, 16(22), pp. 2906–2922.

Pestova, T. V., Lorsch, J. R. , Hellen, C. U. T. (2007) The mechanism of translation initiation in eukaryotes. In: Mathews M, Sonenberg N, Hershey JWB, editors. Translational Control in Biology and Medicine. Cold Spring Harbor, NY: Cold Spring Harbor Laboratory Press;. pp. 87–128.

Pestova, T.V., Kolupaeva, V.G., Lomakin, I.B., Pilipenko, E.V., Shatsky, I.N., Agol, V.I. and Hellen, C.U.T. (2001) 'Molecular mechanisms of translation initiation in eukaryotes', Proceedings of the National Academy of Sciences, 98(13), pp. 7029–7036.

Porta-de-la-Riva M, Fontrodona L, Villanueva A, Cerón J. Basic Caenorhabditis elegans (2012) ;Methods: Synchronization and Observation. Journal of Visualized Experiments : JoVE. (64):4019

Ramakrishnan V. (2002) Ribosome structure and the mechanism of translation. Cell; (108):557- 72; PMID:11909526;

Riddle, D. L. , Blumenthal, T., Meyer, B. J., et al., editors. (1997) *C. elegans* II 2nd Edition, Cold Spring Harbor (NY): Cold Spring Harbor Laboratory Press;].

Rodnina MV, Beringer M, Wintermeyer W. How ribosomes make peptide bonds. Trends Biochem Sci (2007); 32:20-6; PMID:17157507; http://dx.doi. org/10.1016/j.tibs.2006.11.007

Rodríguez-Rodero, S., Fernández-Morera, J. L., Menéndez-Torre, E., Calvanese, V., Fernández, A. F., & Fraga, M. F. (2011). Aging genetics and aging. Aging and disease, 2(3), 186-95.

RPS2 ribosomal protein S2 [Homo sapiens (human)] - Gene - NCBI. (2019). Accessed at: https://www.ncbi.nlm.nih.gov/gene/6187

Russell, D., & Cassada, R. C. (1975). The dauerlarva, a post-embryonic developmental variant of the nematode Caenorhabditis elegans. Dev Biol, 46, 326-42.

Santoro, A., Balbi, V., Balducci, E., Pirazzini, C., Rosini, F., Tavano, F., … Franceschi, C. (2010). Evidence for sub-haplogroup h5 of mitochondrial DNA as a risk factor for late onset Alzheimer's disease. PloS one, 5(8), e12037.

Schafer, W. R. (2005), Egg-laying WormBook, ed. The *C. elegans* Research Community, WormBook, doi/10.1895/wormbook.1.38.1, http://www.wormbook.org.

Scheper, G.C., Knaap, M.S.V.D. & Proud, C.G., (2007). Translation matters: protein synthesis defects in inherited disease. Nature Reviews Genetics, 8(9), pp.711–723.

Schmeing, T. M., Voorhees, R. M. , Kelley, A. C., Gao, Y. G. , Murphy, F. V., Weir JR, Ramakrishnan V. (2009) The crystal structure of the ribosome bound to EF-Tu and aminoacyl-tRNA. Science; 326: pp. 688- 94;

Selkoe, D. J. (2004) Cell biology of protein misfolding: the examples of Alzheimer's and Parkinson's diseases. Nat Cell Biol 6:1054–61.10.1038/ncb1104-1054

Sharrock, W. J., (1983) Yolk proteins of Caenorhabditis elegans, Developmental Biology 96(1) pg182-188

Sources of sublime divergence and their relative importance for sublines of six major inbred strains of mice. In Origins of Inbred Mice, Morse, H. C., ed. (Academic Press, New York), pp. 423-438.

Stroustrup, N., Ulmschneider, B.E., Nash, Z.M., López-Moyado, I.F., Apfeld, J. and Fontana, W. (2013) 'The Caenorhabditis elegans Lifespan machine', Nature Methods, 10(7), pp. 665–670.

Sulston, J. and Hodgkin, J. (1988) Methods. In The nematode *C. elegans* (ed. W.B. Wood). pp v 587-606. Cold Spring Harbor Laboratory Press, Cold Spring Harbor, New York.

Uppaluri, S., & Brangwynne, C. P. (2015). A size threshold governs Caenorhabditis elegans developmental progression. Proceedings. Biological sciences, 282(1813), 20151283.

Villa, N. and Fraser, C.S. (2014) 'Mechanism of translation in eukaryotes — UC Davis'

Von Ehrenstein, G. and Schierenberg, E. (1980). Cell lineages and development of Caenorhabditis elegans and other nematodes. In Nematodes as biological models Vol. I, Behavioral and developmental models Chapter 1. pp 2-68. Academic Press, New York

Wang, M., Hu, Y., & Stearns, M. E. (2009). RPS2: a novel therapeutic target in prostate cancer. Journal of experimental & clinical cancer research: CR, 28(1), 6

Wilson, D. N., & Doudna Cate, J. H. (2012). The Structure and Function of the Eukaryotic Ribosome. Cold Spring Harbor Perspectives in Biology, 4(5), a011536.

Wolkow, C.A. and Hall, D.H. (2015). Introduction to the Dauer Larva, Overview. In WormAtlas.

Zarkower, D. Somatic sex determination (2006), WormBook, ed. The *C. elegans* Research Community, WormBook, http://www.wormbook.org.